Study on Effects of Submicron Glass Fiber Modification on Mechanical Properties of Vinyl Ester Resin and Short Carbon Fiber Reinforced Vinyl Ester Composite

NGUYEN THI THANH NHAN

2020

Study on Effects of Submicron Glass Fiber Modification on Mechanical Properties of Vinyl Ester Resin and Short Carbon Fiber Reinforced Vinyl Ester Composite

Doctoral Thesis

By

NGUYEN THI THANH NHAN

Supervised by Prof. Kazuya OKUBO

Assoc. Prof. Kiyotaka OBUNAI

Doshisha University

2020

Thesis contents

Chapter 1. Background

1. 1. Introduction

Carbon fiber reinforced polymer (CFRP) is composite material constituted from carbon fiber (CF) and polymer matrix. While CF provides strength and stiffness, resin matrix offers toughness, protects and binds fibers together to form desired shape. Also called graphite fiber or carbon graphite, carbon fiber consists of very thin strands of the element carbon. These fibers are twice as stiff as and five times as strong as steel (per unit of weight). They also are highly chemically resistant and highly-temperature tolerant with low thermal expansion [1-3]. Polymer matrix was utilized for CFRP can be classified into two main groups: thermosetting and thermoplastic. Thermoset composite matrices include polyesters, vinyl esters, epoxies, cyanate esters, bismaleimide, polyimides and phenolics. Among them, epoxy, unsaturated polyester, vinyl ester is the most popularly used [4]. The high crosslinking in cured -resin may lead to number of outstanding superior features mainly such as high glass transition temperature, high specific structure and strength, high creep resistance, good dimensional stability at high temperature, and good solvent resistance. The good wettability between fiber and matrix, lower price compared to thermoplastic, in conjunction with the ease of processing, are main reasons of extensively employing thermosetting polymers as in encapsulating constituent, tooling compounds, electronic substrate, and packaging [5-7]. Though thermoplastic composites offer the potential for short processing times, but their inherent characteristics have prevented them from replacing thermoset composites in the aerospace industry, because of high processing temperatures (200–400 ^{0}C), the lack of tack and boardiness of the prepreg results in expensive manual handling operations. Thermoforming of thermoplastics composite has proven to be much more difficult than CFRP thermosetting matrix due to the tendency of the fibers to wrinkle and buckle if not maintained under tension during the forming operation [8]. CFRPs are strong and light, and have usage in aerospace as well as in sail boats, and notably in modern bicycles and motor cycles, where high strength-to-weight ratios are required. They are also used in laptops, tripods, fishing rods, racquet frames, stringed instrument bodies and golf clubs. Since sustaining high damping, carbon fiber–epoxy composite materials can dissipate any vibration of the composite structure that is induced, they are used for manufacturing high-speed

transmission shafts, machine-tool spindles, and robot arms. Being interested thanks to light weight and high strength compared to other traditional materials such as iron and steel, the demand for CFRP increases continually and yearly. In 2012, the global demand was 65000 tonnes but reached 74000 tonnes just after one year and enlarged nearly double in 2015, followed by 128.000 tonnes in 2018 [2,3,9]. The market size of polymer composite is 12300 million dollars in 2019 and it will go up to 24300 million dollars in 2025 [10]. The example of the tremendous increase of global demand of carbon fiber polymer composite for automobile manufacturing is shown in the Figure. 1-1 [11].

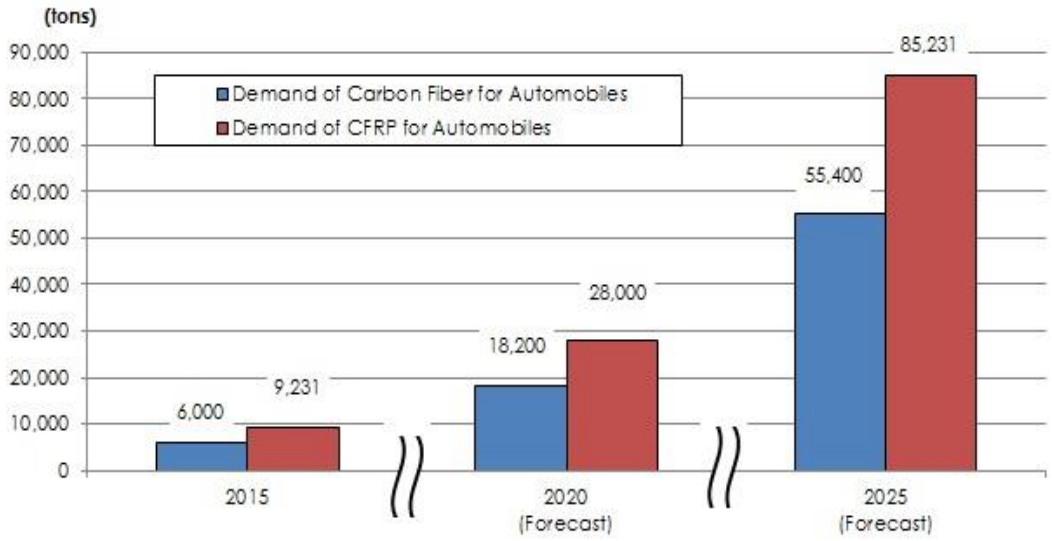

Fig 1-1. Forecast of global demand of Carbon Fiber/CFRP for automobile manufacturing [11].

1.2. Short carbon fiber composite

Continuous fibers exhibit the highest strength when they are oriented uni-directionally, but the composite exhibits low strength in the direction perpendicular to the fiber orientation. Compared to other types of reinforcement, the continuous fiber reinforced composites offer the best combination of strength and stiffness, increased strength with increased temperature being among some of the benefits [12]. Examples of continuous reinforcements include unidirectional, woven cloth, and helical winding while those of discontinuous reinforcements are chopped fibers and random mat (see Fig. 1-2). Depending on type and quantity of reinforcement, mechanical property as well as manufacturing, cost of composite increase significantly [13]. As be well known, CFRP has widely applied in automotive structures because of having lightweight compared to

other materials such as metals and alloys. However, under force of regulations for reducing CO_2 emission (i.e EURO 6), from 2020, a high tax will be applied to vehicles exceed 95 mg/ km of CO2 emission, car manufactures have to find many solutions to decrease weight. There are several alternatives, include: utilizing lighter materials, increasing of functionality of components and innovating of car system designs. The employment of new lightweight material such as high-tensile steel, aluminium alloy, and composites is the most direct and effective means of weight reduction. Among above methods, applications of CFRP to mass production automotive bodies have been widely adopted, particularly in German cars, such as BMW and Audi. Their technology is mainly based on so-called high-pressure resin transfer molding (HP-RTM) using carbon fiber textiles and fast-curing epoxy resins. However, several drawbacks are existed in this technology, including difficulties in much higher rate of production, carbon textile wastes intrinsic to cutting, and the slow adhesion process currently required to join surrounding components. This fact leads to the increase of applications of discontinuous fiber, with the outbreak of research about using carbon fiber in thermoplastic composite in Japan for automobile [14, 15].

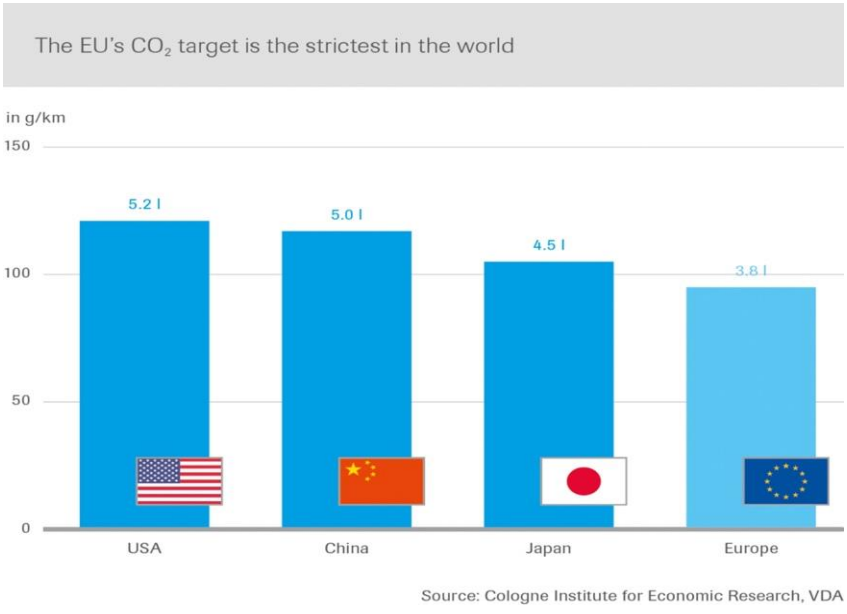

Fig 1-2. The target of CO_2 emission in 2020 in some countries and EU [16].

Short-fiber-reinforced polymer composites are very attractive because of their ease of fabrication using conventional techniques such as extrusion and injection moulding processes is more efficient and inexpensive to produce large-scale composite parts less

expensiveness while still having superior mechanical properties There are many micromechanics models used in previous studies for short fibre composites, such as Hirsch's model, Halpin–Tsai model, Cox's shear-lag model, Nairn modified shear-lag model, Mendels, et al. stress transfer model and so on. Some models have good agreement with experimental results but some of them need to further modify to get a good match [16-18]. Various models for predicting the fiber orientation states are available, which are based on the theory of Folgar and Tucker. They have been successfully applied to predict fiber orientation and are already implemented in commercial software packages for flow simulation [19]. The mechanical performance of a discontinuous fiber composite is a function of length, diameter and orientation of the fiber [20]. Optimal mechanical properties in composite materials are strongly related to the efficiency of load transfer, achieved only if the fiber length is greater than the critical fiber length (l_c – see Fig. 1-3), which is determined by a balance between the tensile strength of the fiber (σ_f), and the maximum sustainable interfacial shear stress, and is given by the equation as bellows:

$$\tau_{max} = \frac{\sigma_f . d}{2 . l_c} \quad (1\text{-}1)$$

where d is the fiber diameter, τ_{max} is identified with the interfacial shear strength (IFSS) [21]. Therefore, the critical fiber length is dependent on fiber strength, fiber diameter as well as interfacial shear strength (IFSS) between fiber and matrix. Modification fiber surface or/and matrix can lead to the increase of IFSS value, consequently, decrease critical fiber length [22,23]. The degree of fiber orientation in short-fiber composites also plays an important role in determining many properties of these materials. The fibers in short fiber composites are rarely oriented in a single direction, which is necessary to obtain the maximum reinforcement effects. During the processing of short-fiber composites, the initial random distribution of fiber turns into rotation during shear flow and re-alignment during elongational flow. This change relates to the geometrical properties of the fibers, the viscoelastic properties of the matrix, and the change in shape produced by the processing where polymer melt undergoes both elongation and shear flow [24, 25]. Fiber orientation distributions can be predicted by solving for the velocity field during flow, and by using a model of orientation dynamics. Current practice is to use the second-order orientation tensor (or moment tensor) A as the primary variable to represent local fiber orientation. This quantity captures both the principal directions of

orientation and the extent of alignment about those directions. Governing equations for the evolution of A can be developed from the basic solution for single-fiber motion, and the resulting equations can be solved numerically for complex flow fields. The results of the orientation model can then be used to predict the mechanical properties and structural performance of the finished part [26].

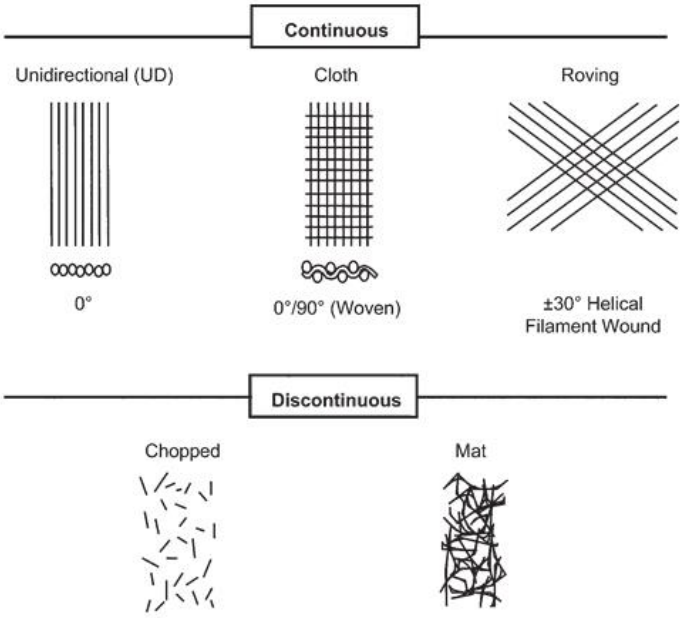

Fig.1- 3. Typical reinforcement types [13].

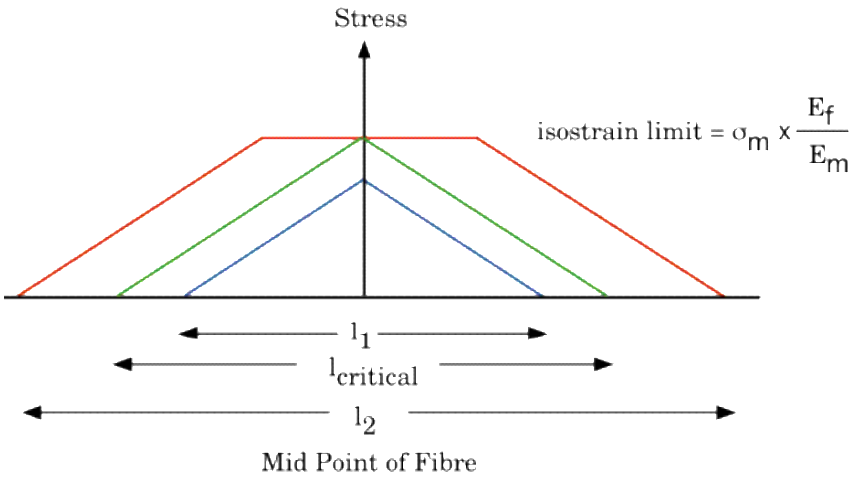

Fig. 1- 4. The relationship between fiber length and shear tress concentration on fiber surface [13].

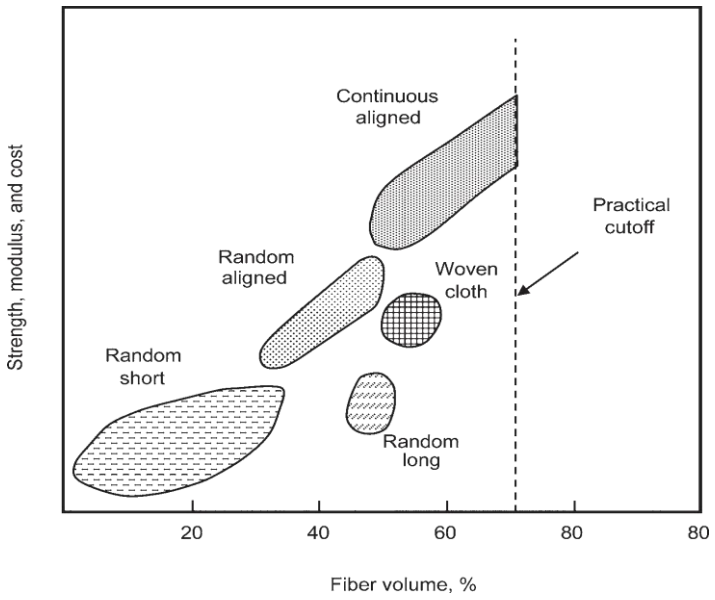

Fig. 1- 5. The effect of reinforcement type and concentration to composite performance [13].

Because of their heterogeneous architecture, anisotropic behavior and damage development, short fiber reinforcement composites SFRC structure design is very complicated compared to homogeneous materials such as metals. The huge variation of microstructures induces a significant dispersion of the mechanical properties, especially under fatigue loading where the prediction of initiation and kinetics of damage, their effect on the residual mechanical behaviour and on the lifetime of the materials can present a very significant challenge [27]. Studies on microstructural examinations of fatigue damage processes in short fiber composites revealed matrix/fiber interfaces, matrix/filler interfaces, and fiber ends, where high stress concentration exists, as the origins of crack initiation. Initiated microcracks could propagate along matrix/fiber interfaces and eventually advance into the matrix regions leading to the final failure of the composite. Stress concentrations near discontinuous fibers are related to fiber volume fraction, distance between fiber ends, and the matrix/fiber modulus ratio, and, therefore, the applied stress fields can be related to local stress fields [28]. For the tensile test, four fracture mechanisms appearing i.e., matrix deformation and fracture, fiber/matrix debonding, fiber pull-out, and fiber fracture. The occurrence and extent of each of the mechanisms depended on the properties of the composite components and the morphology and spatial location of the fibers [29]. By observing the crack initiation and propagation of SCFRPs during bending tests, Lin et al. [30] stated that the fiber-bridging

effect was effective to maintain the composite integrity resulting in a non-catastrophic fracture behaviour.

1.3. Modification methods and their effect on mechanical properties of CFRP

As mentioned above, CFRP has two major constituents are matrix and fiber. To improve mechanical properties of this system, modification is proposed throughout modifying each phase to promote the interfacial strength between them as well as mechanical performance of composite. The interphase is a transition region formed by the fiber surface and the matrix. Under loading condition, the stress will be transferred from matrix to fiber via this region. Therefore, the improvement of interface directly leads to overall increment of composite performance.

a. Modification of carbon fiber surface

Beside inherent excellent characteristics of strength and stiffness, carbon fiber also has lower density compared to glass fiber, owns good electrical conductivity as well as thermal conductivity [31]. However, carbon fibers exhibit a low adhesion to the polymer matrix, because they are smooth and chemically inert. This has a negative effect on the mechanical properties of fiber-reinforced composites. In order to enhance the adhesion between the carbon fibers and polymer matrix, various methods of carbon fiber modification are applied: plasma treatment, thermal, chemical and electrochemical oxidation, the deposition of more active forms of carbon, or grafting of the carbon fiber surface with polymers [32]. Kim. et al classifies treatment methods of carbon fiber surface into two oxidative and non-oxidative treatments. According to oxidative medium, oxidative treatments are further divided into dry oxidization and wet oxidization [33]. The wet oxidization uses liquid oxidizing agents, such as nitric acid, hydrogen peroxide, supercritical water, and potassium persulfate etc. While the dry oxidization treatment is carried out in atmosphere of gas. The gas can be some oxygen containing gases such as oxygen, ozone, carbon dioxide and air etc. The non-oxidative treatments do not change the chemical structure of fiber surface itself, but could introduce some additional reactive species close to the fiber surface. This method will not influence the mechanical properties of carbon fiber and generally can effectively improve the interfacial properties. Coating/sizing and surface grafting lie on this method. The coating/sizing forms the extremely thin layer on the surface of fiber to protect fiber from damage during fiber handling and re-processing as well as composite manufacturing and increase wettability

of fiber to matrix and further increase of the interfacial adhesion. The surface grafting is one of the most effective methods to activate and/or functionalize carbon fiber surface. The grafted materials can be multifunctional polymer chains, and covalently bonded carbon nanotubes [34]. Pittmanjr et al. used long-chain tetraethylenepentamine (TEPA) to graft onto nitric acid oxidized ex-PAN carbon fiber surface, resulting in a dramatic increase of the amount of amine groups on fiber surface and consequently, improving the wettability of fiber to matrix of epoxy matrix. The effectiveness of this treatment is dependent on the concentration of oxidative medium, treatment time and temperature as well as fiber itself. [35, 36].

b. Modification of matrix

Modification of matrix not only improves the interfacial shear strength between fiber and resin but also has effect on fracture toughness of matrix. For the polyolefin resins such as polyethylene (PE), polypropylene (PP) having inert nature, graft-polymers i.e maleic anhydride modified polypropylene (PP-g-MAH) with two ends of polar and non-polar often added into matrix to improve fiber/matrix adhesion. The level of improvement has been shown to depend on the concentration of MAHgPP and on the type of fibre used, in particular on its chemical reactivity [37]. In that case, coupling agent MAPP plays in role as a chemical bridge between the fibers and the matrix to increase the interfacial shear strength [38]. With thermosetting polymers, Pegoretti, A., et al claimed about the improvement IFSS of 40% with the dispersion of 5% of graphite nanoplatelets into matrix epoxy based on glass fiber composite induced the increase of tensile modulus, tensile strength and Izod impact strength of composite [39]. Shao also reported about the enlargement of IFSS between epoxy resin and carbon fiber with the addition of 0.3 wt% and 0.8 wt% micro – fibrillated cellulose (MFC) fiber up to 16.6% and 40%, respectively [3]. The toughness of matrix is one of the key factor to mechanical performance of composite such as fatigue, interlaminar fracture toughness or impact resistance ability. High toughness provides high ability to resist the initiation and propagation of matrix crack, reduce the stress concentration at defects, interface or CF breakage areas. Thermosetting polymers are brittle, low impact resistance and fracture toughness resulted from the highly cross-linked network structures, compared to the metallic materials, restrict wide application of this material. Several methods have been studied to improve the fracture toughness of composites, such as modifying thermosets

with ductile thermoplastics and rubber (soft polymer type toughening agents) or hard toughening agents (i.e. carbon nanotubes, nanoclays and silica) to enhance the toughness of the epoxy matrix system [3, 40]. In the seventies of last century carboxy-terminated nitrile butadienes (CTBNs) were introduced as tougheners. They are immiscible with epoxies but become miscible after a pre-reaction with an excess of epoxy resin. Rubber toughening has several drawbacks like lowering the modulus and reducing the glass transition temperature, due to incomplete phase separation of the elastomeric phase may result in plasticizing of the matrix. Another issue is the relatively high viscosity of epoxy resins containing reactive liquid rubbers, which can be critical for infusion processes. In the period of years 2002 to 2003, surface modified silica nanoparticles became available in industrial quantities. With incorporation of silica nanoparticle, properties like strength, modulus, toughness and especially fatigue performance of cured bulk epoxy resins can be improved [41]. Several toughening mechanisms have been suggested to explain the complex behaviour of polymers with nanofillers as follows:

- Crack deflection: Crack deflection is defined as the twist and tilt of the crack front between microstructural elements which leads to an increase of fracture toughness at the crack tip [42].
- Crack pinning/bowing: The crack propagates through resin, the crack front bows out between the filler particles and remains pinned at the particles.
- Crack bridging: Sigl et al. proposed that a rigid or ductile particle plays two roles: The first is as a bridging particle that applies compressive traction in the crack wake and the second is the ductile particle deforms plastically in the material surrounding the crack tip, which provides additional crack shielding. Sigl et al. also pointed out that the shielding resulting from yielded particles is negligible, and that the particle bridging provides most of the improvements in toughness.
- Particle de-bonding: Debonding is the loss of adhesion between filler (particle or fiber) and matrix, due to the action of different stressors, such as hygrothermal aging, fatigue, or external stress. Particle debonding is a major dissipation mechanism that contributes itself and triggers other mechanisms such as matrix shear bands or plastic void growth.
- Microcracking or crazing of the matrix: As mentioned above, microcracks caused by the presence of rubber particles. These microcracks cause tensile yielding and,

thus, a large tensile deformation. Voids result when the microcracks open, and these voids permit large strains. Debonding or microcracking effectively lowers the modulus in the frontal zone around the crack tip, and thus effectively reduces the stress intensity there.

- Deformation of the matrix: Occur in the vicinity of the crack tip, because of cavitation and multiple but localized shear yielding, dissipates fracture failure and further improve toughness of resin [43-47].

These mechanisms can occur at the same time with one or more are dominant depending upon the nature of particles and matrix.

1.4. Object of this research

This study focuses on investigating effect of submicron glass fiber addition on mechanical properties of vinyl ester resin as well as short carbon fiber reinforced VE composite. To determine clearly this objective, the thesis was divided into five chapters as follows:

Chapter 1 shows the background acknowledge about carbon fiber polymer composite with two minor sections exhibit more detailed about short carbon fiber composite as well as modification methods of fiber and matrix and their effects on mechanical performance of CFRP, which is also main subject of this investigation.

Chapter 2 is about modifying of vinyl ester resin with the addition of submicron glass fiber. To clarify the dispersed statement of sGF in matrix, the SEM picture of post mixed-resin was observed. The change of mechanical and dynamic properties of resin was discovered throughout experimental methods such as bending test, impact resistance, tension-tension fatigue test and dynamic mechanical analysis. Besides, toughened effect of glass fiber modifier also determined by the Mode I fracture toughness test.

Chapter 3 indicates effect of sGF modification on short carbon fiber composite at different lengths of reinforcement. Due to the increment of viscosity could bring more void bubbles into mixed-system and difficulty to processing by the addition of glass fiber, the composite fabrication method as well as void content in composites considered and confirmed. Static strengths i.e. flexural strength, impact resistance ability, tensile strength as well as fatigue life of un-modified and modified composites were accessed at different content of the modifier and at different length of carbon fiber. Micro-mechanisms of interaction fiber-resin and damage during test also were examined by means of

fragmentation test, micro-droplet test, digital image correlation and scanning electron microscope observation.

Due to the significant increase of fracture toughness of modified resin in chapter 2, the impact resistance and impact tolerance of composite was also expected to improve. The chapter 4 evaluates fracture statement of samples, the compression and the compression after impact strength of unmodified and modified composites to assess the mentioned aims.

Chapter 5 shows and concludes some highlight results of this research as well as some proposals for next further studies.

References

[1] Fekete, J.R., Hall, J.N. 2017. Design of auto body: Materials perspective. In *Automotive Steels Design, Metallurgy, Processing and Applications* Radhakanta Rana and Shiv Brat Singh (eds)1, pp. 1-18. Publisher: Woodhead Publishing.

[2] Palanikumar, K. 2012. Analyzing surface quality in machined composites. In: H. Hocheng (ed). *Machining Technology for Composite Materials* Volume I (6), pp.154-182. Publisher: Woodhead Publishing.

[3] Shao, Y, 2014. Study on the effects of matrix properties on the mechanical properties of carbon fiber reinforced plastic composite. PhD Thesis, Doshisha University, Kyoto, Japan.

[4] Campbell F.C. Thermoset Resins: The Glue That Holds the Strings Together. In: Campbell F.C (Ed), Manufacturing Processes for Advanced Composites, 2004, Volume 3, pp. 63-101. Publisher: Elsevier Science. https://doi.org/10.1016/B978-1-85617-415-2.X5000-X.

[5] Abdul KhalilH.P.S, et al. 2017. Nanofibrillated cellulose reinforcement in thermoset polymer composites. In: Mohammad Jawaid, Sami Boufi and Abdul Khalil H.P.S. (Eds), Cellulose-Reinforced Nanofibre Composites, Volume 1, pp. 1-24. Publisher: Woodhead Publishing.

[6] Alkateb. M, Sapuan. S.M., Leman, Z., Ishak, M.R., Jawaid, M. 2018. Energy absorption of natural fiber reeinforced thermoset polymer composites materials for automobile crashworthiness: A review. In: Khan, A., et al (Eds). Thermoset composites:

Preparation, properties and applications, Volume 1, pp. 1 – 32. Publisher: Materials Research Forum LLC, Millersville, USA.

[7] Deborah D.L. Chung. 2017. Polymer-Matrix Composites: Structure and Processing. In: Deborah D.L. Chung (Ed), Carbon Composites, 2nd Edition, Volume 3, Pages 161-217, Publisher: Butterworth-Heinemann. https://doi.org/10.1016/C2014-0-02567-1.

[8] Campbell, F.C. 2004. Thermoplastic Composites: An Unfulfilled Promise. In: Campbell, F.C (Ed), Manufacturing Processes for Advanced Composites, Volume 10, Pages 357-397. Publisher: Elsevier Science. https://doi.org/10.1016/B978-1-85617-415-2.X5000-X

[9] Witten. E, Mathes. V, Sauer. M, Kühnel. M. 2018. Composites Market Report 2018. https://www.avk-tv.de/files/20181115_avk_ccev_market_report_2018_final.pdf

[10]. CFRP Market 2019 by Size, Share, Trends, Development, Revenue, Demand and Forecast to 2025. 2019. https://www.marketwatch.com/press-release/cfrp-market-2019-by-size-share-trends-development-revenue-demand-and-forecast-to-2025-2019-08-19. Published: Aug 19, 2019 3:34 a.m. ET

[11] Forecast of Global Demand of CFRP for Automobile Manufacturing: Key Research Findings 2016. Press Release 2016, September, 11st. Yano Research Institute Ltd. https://www.yanoresearch.com/en/press-release/show/press_id/1610.

[12] Kapranos, P., et al. 2014. Advanced Casting Methodologies: Inert Environment Vacuum Casting and Solidification, Die Casting, Compocasting, and Roll Casting. In: Hashmi, S., et al (Eds), *Comprehensive Materials Processing*, Volume 5, Pages 3-37. Publisher: Elsevier

[13] Campbell, F.C. 2010. Introduction to Composite Material. *Structural Composite Materials*, 1, 1-29.

[14] Ishikawa, T., et al. 2018. Overview of automotive structural composites technology developments in Japan. *Composite Sciences and Technology*, 155, pp. 221- 246

[15] Wan, Y., Takahashi, J. 2014. Deconsolidation behavior of carbon fiber reinforced thermoplastics. Journal of Reinforced Plastics and Composites, Vol. 33(17) 1613–1624

[16] Verban de Automobilindustrie. *CO_2 regulation of passenger cars and light commercial vehicles in Europe.* https://www.vda.de/en/topics/environment-and-climate/co2-regulation-for-passenger-cars-and-light-commercial-vehicles/co2-regulation-of-passenger-cars-and-light-commercial-vehicles-in-europe.html

[17] Rezaei, F., Yunus, R., Ibrahim, N.A., Mahdi, E.S. 2008. Development of Short-Carbon-Fiber-Reinforced Polypropylene Composite for Car Bonnet, *Polymer-Plastics Technology and Engineering*, 47:4, 351-357, doi: 10.1080/03602550801897323

[18] Capela, C., Oliveira, S.E., Ferreiraa, J.A.M. Fatigue behavior of short carbon fiber reinforced epoxy composites. Composites Part B: Engineering Volume 164, 1 May 2019, Pages 191-197.

[19] Das, O., Kim, N.K., Bhattacharyya, D. The mechanics of biocomposites. In: Ambrosio, L (Ed), *Biomedical Composites*, 2nd Edition, 2017, Volume 16, pp. 375-411. Publisher: Woodhead Publishing. https://doi.org/10.1016/C2015-0-02024-X

[20] Van Hattum, F.W.J., Bernardo, C.A. A Model to Predict The Strength of Short Fiber Composites. *Polymer Composites*, 1999, Vol. 20 (4), pp. 524 – 533.

[21] Mortazavian, S., Ali, F. Fatigue behavior and modeling of short fiber reinforced polymer composites: a literature review. Int J Fatig, 70 (2015), pp. 297-321

[22] ReeD, R.P., BergG, J.C. 2006. Measuring effective interfacial shear strength in carbon fiber bundle polymeric composites. J. Adhesion Sci. Technol., 20(16), pp. 1929–1936.

[23] Monetfe, L., Anderson, M.P., Grest, G.S. Meaning of the Critical Length Concept in Composites: Study of Matrix Viscosity and Strain Rate on the Average Fiber Fragmentation Length in Short-Fiber Polymer Composites. Polymer Composites, 1993, Vol. 14 (2) pp. 101 – 115.

[24] Miwa, M., Endo, I. Critical fibre length and tensile strength for carbon fibre-epoxy composites. *Journal of Materials Science* 29 (1994) 1174-1178.

[25] Dufresne, A. Cellulose-Based Composites and Nanocomposites. In: Ebnesajjad, S (Ed) *Handbook of Biopolymers and Biodegradable Plastics* 2013, Volume 8, pp.153-169. Publisher: William Andrew. https://doi.org/10.1016/C2011-0-07342-8

[26] Gonzalez, L. M., Cumbrera , F. L., Sanchez-Baijo, F., Pajares, A. Measurement of orientation in short-fiber composites. Acta metall, mater. Vol. 42, No, 3, pp. 689-694, 1994

[27] TuckerIII, C.L. Modeling: Scaling Analysis. In: K.H. Jürgen Buschow, K.H, et al (Eds), *Encyclopedia of Materials: Science and Technology*, 2001, pp. 5726-5733. Publisher: Pergamon.

[28] Laribi, M.A. Fast fatigue life prediction of short fiber reinforced composites using a new hybrid damage approach: Application to SMC. *Composites Part B* 139 (2018) pp. 155–162.

[29] Hour, K.Y., Sehitoglu, H. Damage Development in a Short Fiber Reinforced Composite. *Journal of Composite Materials*, Vol. 27, No. 8/1993, pp 782 – 805.

[30] Wang, K., et al. In-situ 3D fracture propagation of short carbon fiber reinforced polymer composites. *Composites Science and Technology*, Volume 182, 29 September 2019, 107788.

[31] Lin, T., Jia, D., He, P., Wang, M. In situ crack growth observation and fracture behavior of short carbonfiber reinforced geopolymer matrix composites, *Mater. Sci.Eng. A* 527 (9) (2010) 2404–2407https://doi.org/10.1016/j.msea.2009.12.004.

[32] Tiwari, S., Bijwe, J. Surface Treatment of Carbon Fibers - A Review. *2nd International Conference on Innovations in Automation and Mechatronics Engineering, ICIAME 2014*. Procedia Technology 14 (2014), pp. 505-512.

[33] Chukov, D.I. Surface modification of carbon fibers and its effect on the fiber–matrix interaction of UHMWPE based composites. *Journal of Alloys and Compounds* Volume 586, Supplement 1, 15 February 2014, pp. S459-S463.

[34] Kim, J., Ma, Y. Engineered Interfaces in Fiber Reinforced Composites, Book, Elsevier Science Ltd, 1998.

[35] Zhang, W. Modification of carbon fiber / epoxy matrix interphase in a composite material: Design of a self-healing interphase by introducing thermally reversible Diels-Alder adducts. Doctoral Thesis. Institut National des Sciences Appliquées de Lyon (INSA Lyon) University. 2014.

[36] Reactivities of amine functions grafted to carbon fiber surfaces by tetraethylenepentamine. Designing interfacial bonding, *Carbon,* 1997, Vol. 35(7), pp. 929- 943.

[37] Tiwari, S., Bijiwe, J. 2014. Surface Treatment of Carbon Fibers - A Review. *Procedia Technology* (14), pp. 505-512.

[38] Jannerfeldt, G., et al. Matrix Modification for Improved Reinforcement Effectiveness in Polypropylene/Glass Fibre Composites. *Applied Composite Materials* 8: pp. 327–341, 2001.

[39] Yi, S., et al. Effects of Matrix Modification on the Mechanical Properties of Wood–Polypropylene Composites. *Polymers* 2017,9, 712; doi:10.3390/polym9120712.

[40] Pegoretti, A., et al. 2016. Improving fiber/matrix interfacial strength through graphene and graphene-oxide nano platelets. *IOP Conf. Ser.: Mater. Sci. Eng.* 139 012004. doi:10.1088/1757-899X/139/1/012004.

[41] Bae, J.S., et al. 2018. Novel thermoplastic toughening agents in epoxy matrix for vacuum infusion process manufactured composites. *Carbon letters Vol. 25, pp. 43-49.* DOI: http://dx.doi.org/10.5714/CL.2018.25.043.

[42] Sprenger, S., Kothmann, M.H., Altstaedt, V. Carbon fiber-reinforced composites using an epoxy resin matrix modified with reactive liquid rubber and silica nanoparticles. *Composites Science and Technology* 105 (2014), pp. 86–95.

[43] Rodel, J. 1992. Interaction Between Crack Deflection and Crack Bridging. *Journal of the European Ceramic Society* 10, pp. 143-150

[44] Zhang H, Tang LC, Zhang Z, Friedrich K, Sprenger S. 2008. Fracture behaviours of in situ nanoparticle-filled epoxy at different temperatures. *Polymer* 49, pp. 3816–3825.

[45] Zhao, Q., Hoa, S.V. 2007. Toughening mechanism of epoxy resin with micro/nano particles. *Journal of Composite Materials* 41(2), pp. 201- 219.

[46] Wypych,G. 2018. Mechanisms of adhesion loss. In: Wypych, G (Ed), *Handbook of Adhesion Promoters*. Publisher: ChemTec Publishing, Volume 3, pp. 45-53.

[47] Lauke, B. 2013. Effect of particle size distribution on debonding energy and crack resistance of polymer composites. *Computational Materials Science*, 77, pp. 53-60.

[48] Chen, T.K., Shy, H.J. 1991. Effects of matrix ductility on rubber/matrix interfacially modified epoxy resins. *Polymer*, 33(8), pp. 1656-1663.

Chapter 2

Modifying vinyl ester by submicron glass fiber and its effect on mechanical properties of resin

2.1. Introduction

Vinyl ester resins are typically formulated from styrene and a condensation product of methacrylic acid with an epoxy. Because the reactive double bonds are at the ends of relatively long chains, their cross-link density tends to be lower than the standard polyester resins. Therefore, it may also be regarded as fill the gap between epoxy resin and polyester resin in the both sides of mechanical property as well as effective economy [1-4]. Thanks to good toughness, excellent resistance, good mechanical properties outstanding heat performance, and flexible processibility compared to unsaturated polyester, VE is being increasingly used in solvent storage tanks, sewer pipes, ship and boat construction, coating, automobile structural parts, swimming-pool [5,6]. Similar to other thermosets, pure vinyl ester resin is inherently brittle due to their highly cross-linked structure. One approach to increase its performance is to modify with fillers at micro/nano scale [7-12]. There is a large number of studies conducted to investigate properties of vinyl ester resin reinforced by micro/nano particles. Vahid Arabli et al studied in curing kinetics, modeling, mechanical properties and thermal stability in graphene oxide/vinyl ester resin nanocomposite [13]. They claimed that with a low content of graphene oxide (0.3%), the matrix became stiffer while the glass transition temperature shifted to a higher value. Dipa Ray used fly ash had a particle size distribution in the range of 76 to 152 μm to fill in VE matrix [14]. Auad et al. modified vinyl ester resin of different molecular weights by rubber. The research group claimed that the addition of elastomers produces toughening of the networks, but at the same time a reduction of their mechanical properties such as flexural modulus and compression yield stress [15]. S. Grishchuk et al investigated about structure and properties of vinyl ester resins modified with organophilic synthetic layered silicates bearing non- and co-reactive intercalants. They found that fracture toughness (Kc) and energy (Gc) were markedly improved with increasing organophilic synthetic layered silicates amount [16]. However, along with restriction of loading content in polymer, the size of nano fillers are close to the molecular

scale, leading to detrimental effects on properties of filled system because of intercalating of nano particles and base material [17] Therefore, submicron particles have been considered as filled-gap material between nano and micro filler in recent years. In spite of that, in best authors's knowledge, there was still very few literatures about using micro-nano filler for polymer matrix [18-20]. In this study, the submicron glass fiber (sGF) with diameter in the range of micro-nano scale used to reinforce vinyl ester resin at low content to facilitate using experimental data for further research of carbon fiber composite after that. Mechanical properties were characterized to access effects of sGF on submicron composite (sMC) system.

2.2. Materials and Experiments

2.2.1. Materials

The general vinyl ester resin (VE) supplied by DIC Corporation, gel time of 60 minutes. The hardener and promoter (DIC Corp) were Percure AH (acetyl acetone peroxide) and RP-330 (general cobalt accelerator) used at the weight ratio of 1% and 0.2%, respectively against weight of VE. The submicron glass fiber (sGF) was from Nippon Muki Co., Ltd, Japan with diameter in the range of 0.4 to 2.4 µm and length of 20 to 200 µm and minority of length reaches 1 mm (Fig. 2-1). All materials used without any further treatment.

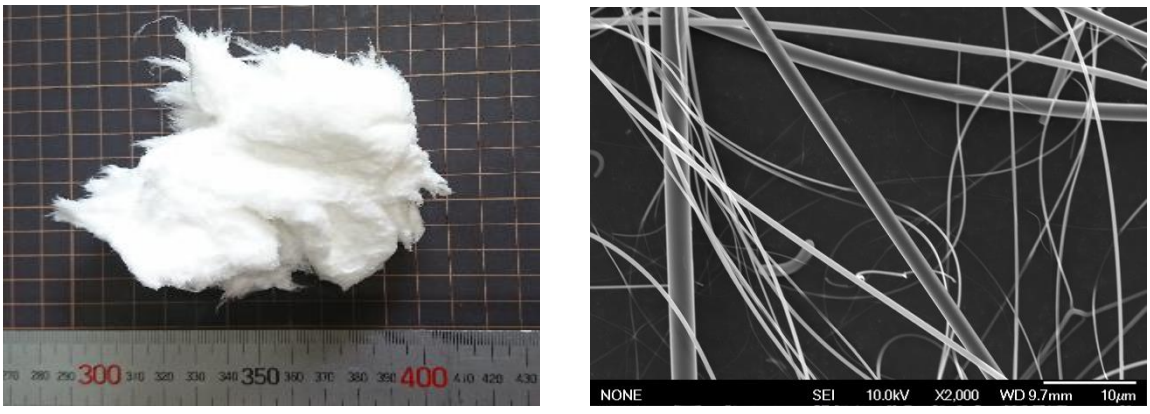

(a) (b)

(Source:Nippon Muki Co., Ltd)

Fig. 2-1. Submicron glass fiber as in using condition (a) and under observation by scanning electron microscope (b).

2.2.2. Preparation of sub-micron composite

After eliminating absorbed moisture in the dry oven for 12 hours at 60 ^{0}C, sGF was put into the stainless steel cup of the homogenizer and mixed with resin at speed of 5000 rpm for 30 minutes followed by adding hardener and promoter and mixed again by the plastic bar. The mixture was applied vacuum pressure to remove air bubbles trapped in resin during mixing until no bubbles remained on the surface of resin cup when observed by naked-eyes. To limit styrene evaporated, the vacuum time and vacuum pressure were controlled. The mixture of resin and glass fiber was gently poured into the mould, silently kept for 15 minutes to facilitate bubbles escaped, followed by casting process in the dry oven for 3 hours at 80 ^{0}C and post-cured at 100 ^{0}C with the same time. The plate of sMC after that was cut into coupon specimens by the diamond cutter. The plate of neat resin also prepared in the same mould with the same processing conditions.

2.2.3. Izod resistance test

The impact resistance test of neat resin and sMC was performed using the pendulum testing device according to the standard ASTM D4812 for unnotched sample and D256 for notched-sample. The test was conducted when the hammer (with the mass of 2.106 kg) impacted onto the edge of specimen for both of the notched and the un-notched. At least 10 specimens (the dimension of 65 mm x10 mm x 4 mm) were used for each sample group.

2.2.4. Three point bending test

The three point bending test was carried out on the Autograph 100 kN tester (Shimadu Corp) at the speed of 2 mm/min, the support length of 60 mm following the standard ASTM D790. At least five specimens were prepared for each condition. The yield strength as well as Young modulus were calculated by determining 0.2% offset yield stress from stress-strain graph achieved on computer during the test. The dimension of samples was 100 mm x 10 mm x 2.5 mm.

The figure 2-2 shows an impact equipment (left) and a geometry of bending test (right).

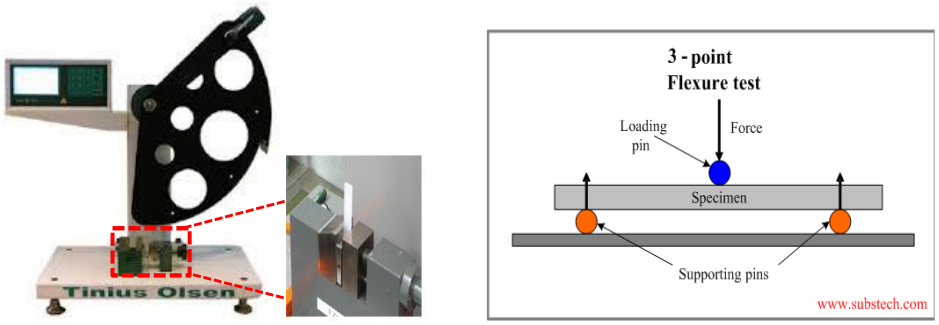

Pendulum impact tester

Fig. 2-2. The pendulum impact tester (left) and the geometry of the three point bending test (right).

2.2.5. Dynamic mechanical analysis

Dynamic mechanical analysis was performed on the DMA 7100 analyzer (Hitachi) using the tensile mode (see Fig. 2-3). In this study, samples were cut into small pieces with dimensions of 40x10x1 mm^3 and the gage length of 20 mm. The digital Vernier calliper was used to measure the dimension of the specimens before testing. The test conditions included the oscillation frequency of 1Hz, the range of temperature from 40 °C to 180 °C and the ramping speed of 3 °C/min.

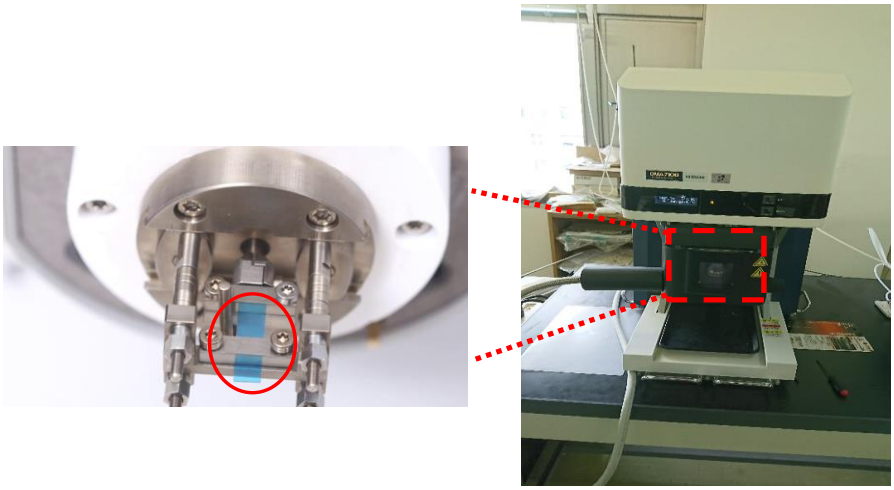

Fig. 2-3. The DMA tester in Nara Industrial Promotion Center which was used for testing.

2.2.6. Preparation of plain strain fracture toughness sample

To characterize the toughness of neat VE and sMC in terms of the critical-stress-intensity factor (K_{Ic}), the Single Edge Notch Bending (SENB) geometry samples were prepared. The SENB was cut from the casted resin plate with the sharp-notch was created by tapping the edge of specimen to a round-cutting saw and the natural crack was

generated by tapping on a fresh razor blade placed in the notch. The dimensions of specimens of 45x40x5 mm^3 and notch length of 5 mm were prepared (see Fig. 2-4). A geometry and a testing method was illustrated in the Fig. 2-4.

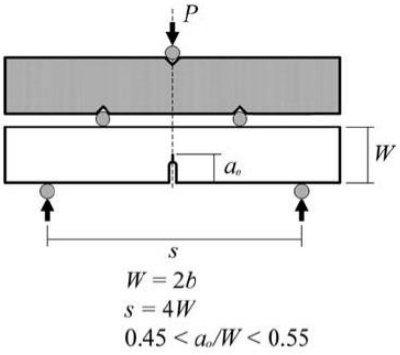

Fig. 2-4. The illustration of SENB sample for the fracture toughness test.

2.2.7. Scanning electron microscope (SEM) observation

Dispersed statement of sGF inside matrix after mixing as well as fracture surfaces of specimens after tests were observed by SEM equipment JSM 7001FD. Prior to SEM observation, all specimens were subjected to sputter coating of a thin layer of gold to avoid electrical charging.

2.2.8. Preparation of Compact tension sample

The compact tension (CT) sample was drawn up by pouring resin into silicone molds followed by the processing of curing and post-curing in dry oven. For the sake of understanding resistance against crack propagation in matrix, a cyclic tension load was applied on samples at maximum load of 150 N, load ratio of 0.2 and frequency of applied load was 1 Hz. The geometry of CT sample was shown as in the Fig.2-5.

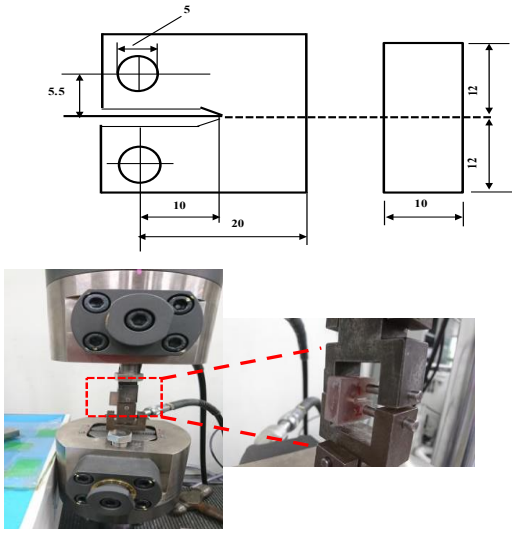

Fig. 2-5. The geometry of CT-specimen according to ASTM D5045 and the Servo Pulser 100 kN tester (Shimazdu).

2.3. Results and Discussion

2.3.1. Dispersion of sGF in resin

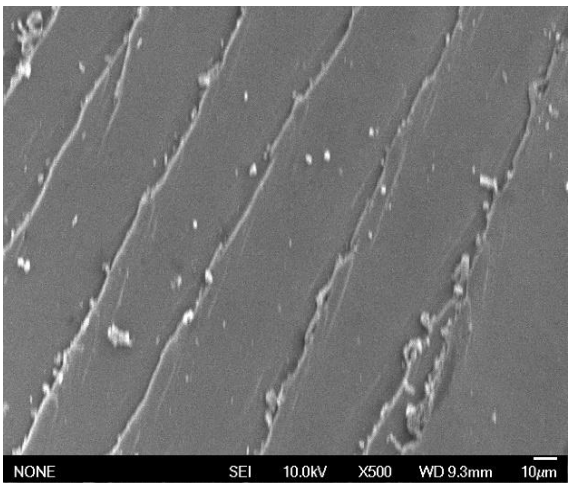

(a) neat resin

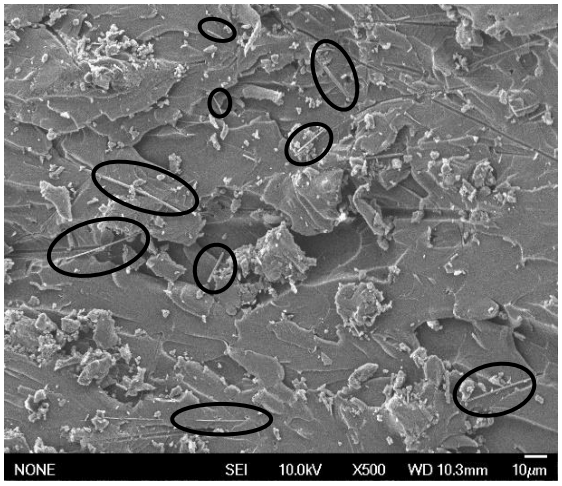

(b) 0.6 wt% sGF modification

Fig. 2-6. SEM images of fracture surface after fracture toughness test of (a) neat resin and (b) 0.6 wt% sGF composite show the good dispersion of glass fiber in matrix.

Compared to neat resin matrix, it can be seen that the submicron glass fiber was well-dispersed inside VE matrix of composite (Fig.2-6 a-b). The length as well as the diameter of glass fiber after mixing was pretty different. To identify the length of sGF after mixing process, the mixture of resin and modifier was diluted in acetone then removed all the excess resin through a filter paper by applying the vacuum. The images of collected sGF after filtrating were taken by SEM equipment to measure the length of individual 300 fibers. The result was used to build the histogram plot of fiber length distribution of glass fiber.

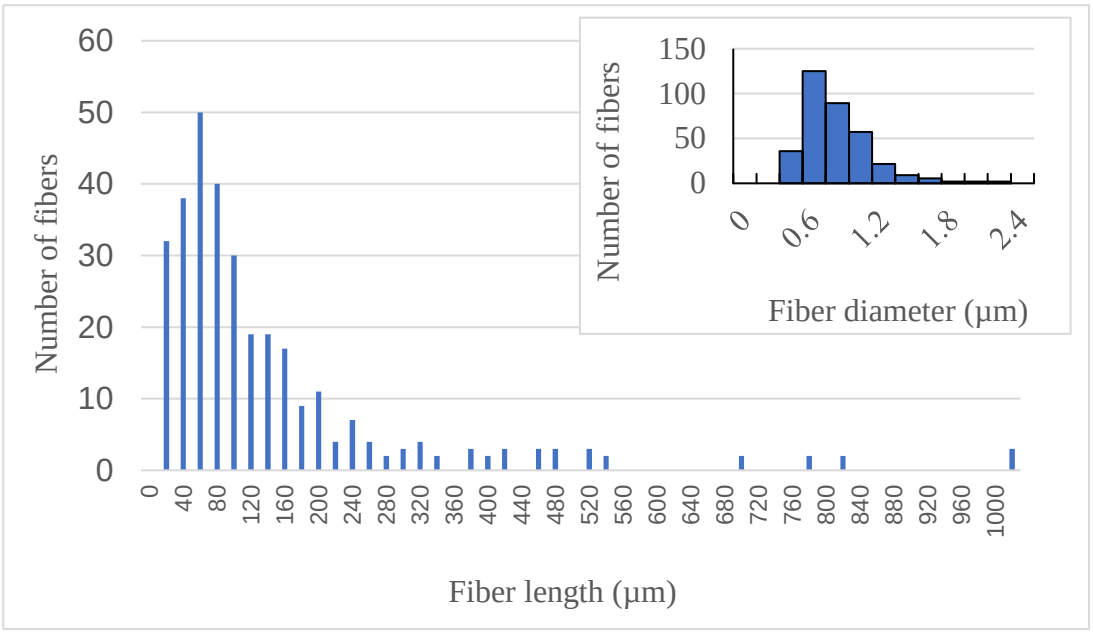

Fig. 2-7. The length distribution of submicron glass fiber after mixing in vinyl ester resin (the small upper graph shows the fiber diameter distribution of sGF – source from Nippon Muki Co., Ltd).

Fig. 2-7 shows the majority of fiber has the length in a range of 20 to 200 µm however the minority of them has the length is longer until around 1 mm. Therefore, the aspect ratio of sGF is in a wide range from 16 to 400 with a maximum probability are from 100 to 150 as shown in the Fig. 2-8.

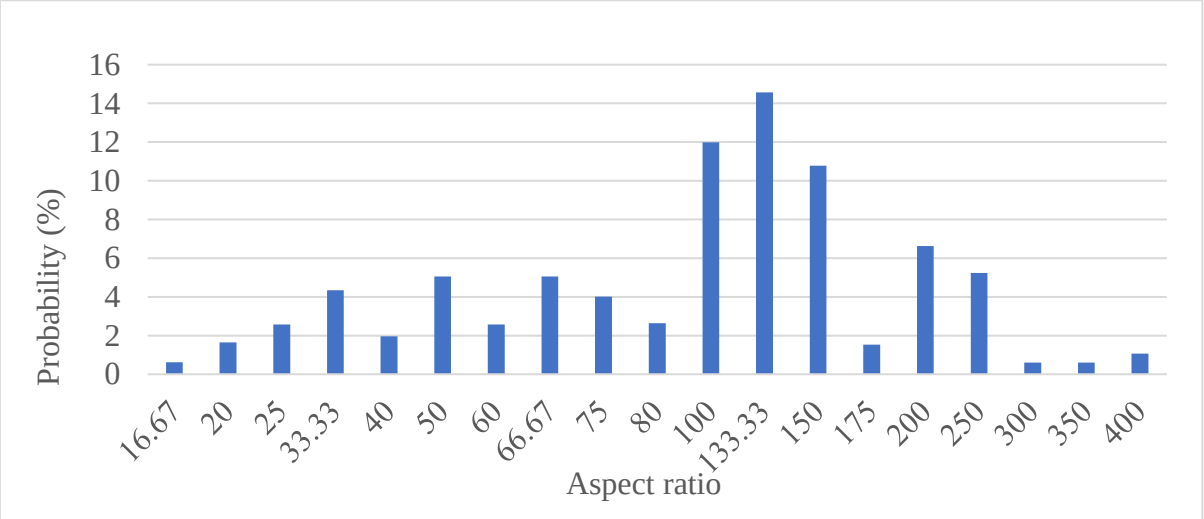

Fig. 2-8 The aspect ratio of glass fiber after mixing in resin.

2.3.2. Izod impact resistance

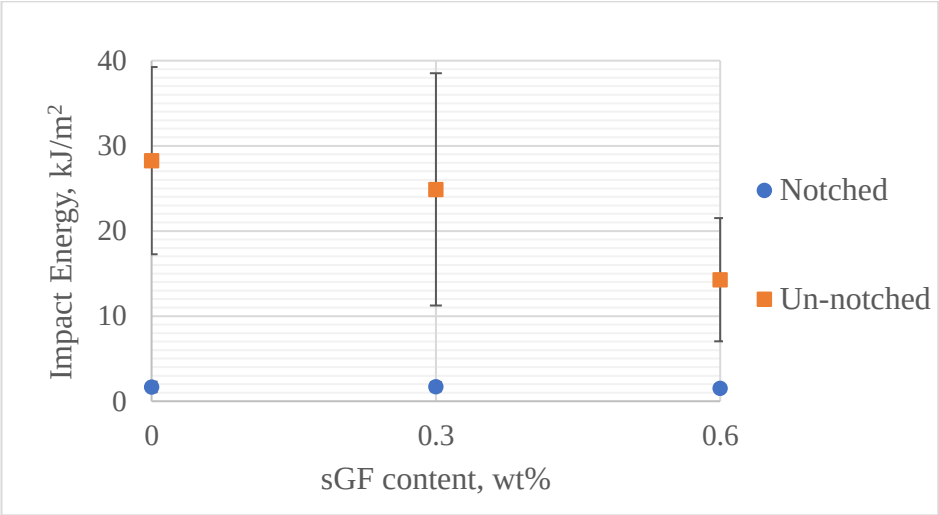

Fig. 2-9. Izod impact resistance of sMC with respect to sGF contents

The Izod impact resistance of sMC decreased with the addition of sGF in un-notched samples (see Fig.2-9). This hints at low adhesion between fiber and resin. As mentioned by Armitt, C.D [21], stresses concentrate around filler particulates which causes un-homogeneousness of filled system and then plays a role as flaws deteriorate the impact resistance of material. In the case of sGF, because of the large change of the aspect ratio, the larger length the larger stress concentration. These results also are good agreement with that of DMA in later section while the energy dissipation ability degrades by adding of sGF. Whereas, the notched impact resistance was the same with all contents of sGF. Consequently, the ratio of the notched to the un-notched values decreases in the order of decreasing of sGF content in sMC: 0.6 wt%>0.3 wt%>0.0 wt%. In the other words, this indicates increasing the content of sGF in sMC, material becomes more sensitive to scratches or sharp features in the part design that may act like notches.

2.3.3. Flexural properties

Fig. 2-10 shows bending properties of sMC at different contents of sGF reinforcement. In general, there was no significant change in bending strength, yield strength as well as Young modulus when comparing those of neat resin with sMC. The flexural strength of resin was approximately 130 MPa. This value was similar with that noticed by the supplier. The tress-strain curves also point out the linear elastic behaviour of sMC under flexural load was almost the same regardless the concentration of glass fiber (see Fig. 2-11). Normally, the fillers with high aspect ratio such as glass fiber and

carbon fiber have high effectiveness in elevating flexural modulus as well as yield strength [21], but there was not the similar observation in this case. It might be caused by the low content of sGF used in VE matrix. On the other hand, adding glass fiber at 0.3 wt% and 0.6 wt % did not show any effect on bending property of vinyl ester resin.

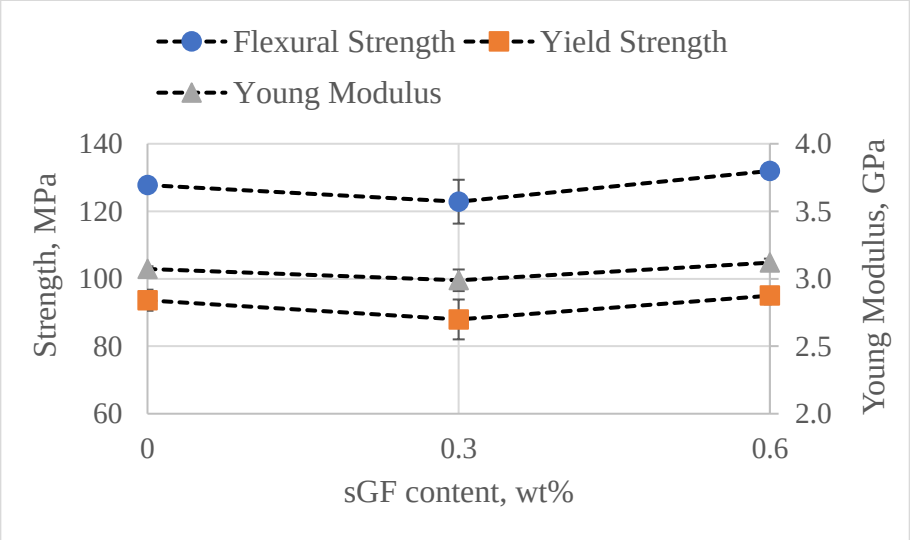

Fig. 2-10. Bending properties of sMC with respect to sGF contents.

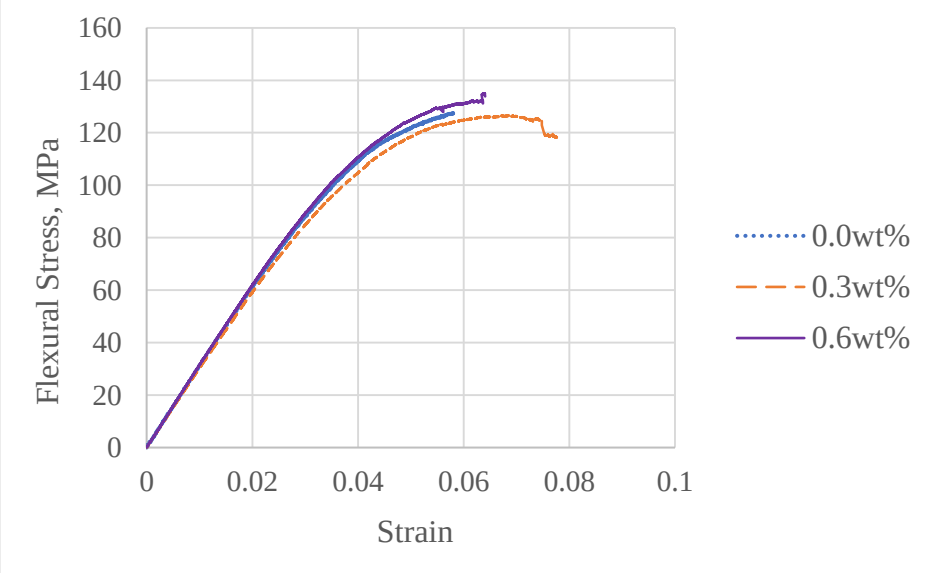

Fig. 2-11. Typical stress-strain curves of sMC with respect to sGF contents.

2.3.4. Dynamic mechanical property

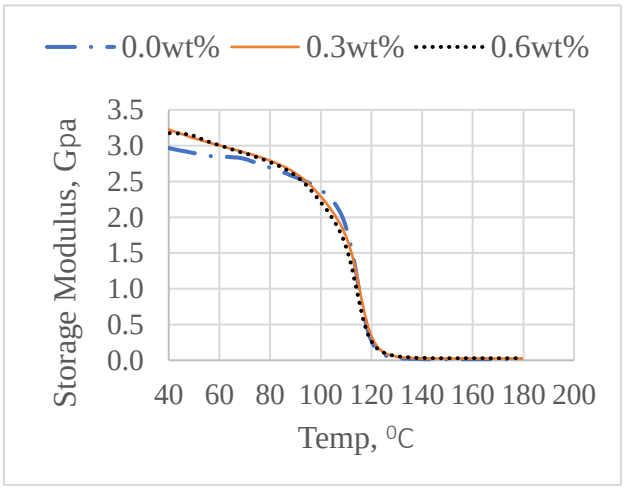

(a)

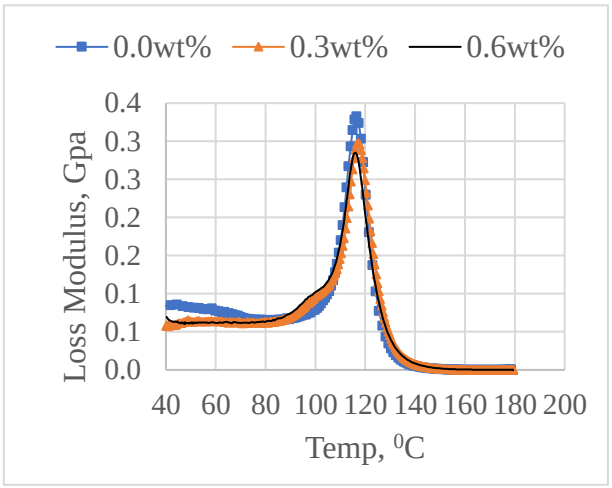

(b)

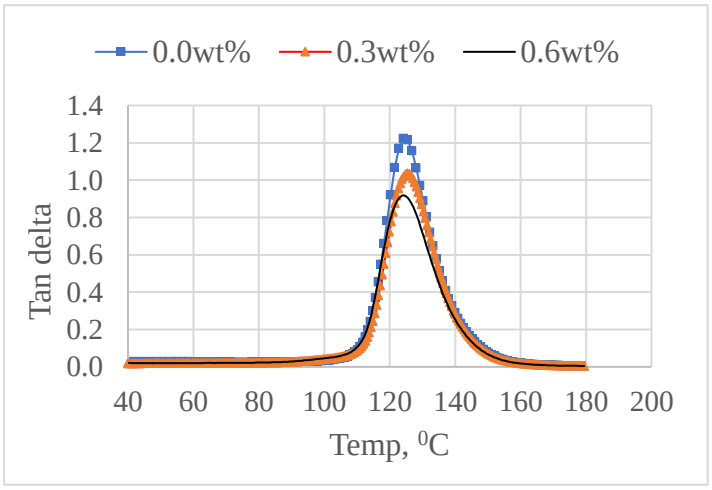

(c)

Fig. 2-12. DMA results of sMC with respect to the different contents of sGF (a) Storage Modulus, (b) Loss Modulus and (c) Tan delta

As can be seen from the peak of the loss modulus curve as well as that of tan delta, the glass transition temperature (T_g) of resin was unchanged regardless the presence of sGF (Fig. 2-12 –b and c). This indicates that the cross-link density of polymer is not affected by sGF addition. In the other words, the adhesion between glass fiber and vinyl ester resin is poor. However, the storage modulus of sMC in Fig. 2-12-a was slightly higher than that of neat resin in a range far below T_g (from 40 to 85 ^{0}C). The damping characteristic of resin (inferred from tan delta magnitude) also decreased with the increase of sGF content. It might be filler particulates absorb polymer chains into its surface,

decrease distance between resin molecules, restrict mobility of matrix molecular chains result in increasing of the elastic behaviour and brittleness, reducing damping of modified matrix in low-temperature range (below 85^0C). These results is good agreement with those of un-notch impact test.

2.3.5. Fracture toughness

The critical stress intensity factor of sMC was improved 26 and 61% corresponding to 0.3 and 0.6 wt% glass fiber used in comparison with that of neat VE, as can be seen in Fig. 2-13. The SEM observation revealed that the fractured surface of neat VE was smooth and glassy with micro-flow lines while that of sMC became rougher with lots of tortuous micro cracks. The existence of sGF (inside the black circles at Fig. 2-14) was also clearly observed at fractured surface of sMC. These results suggest that the fracture toughness of matrix is effectively improved by mechanical bridging of added sGF at crack fronts. Cracks encounter glass fibers on the way of developing, might change their directions or pin or stop propagating. These events might delay crack propagation as well as absorb crack propagation energy and help to increase K_{Ic} value of modified resin.

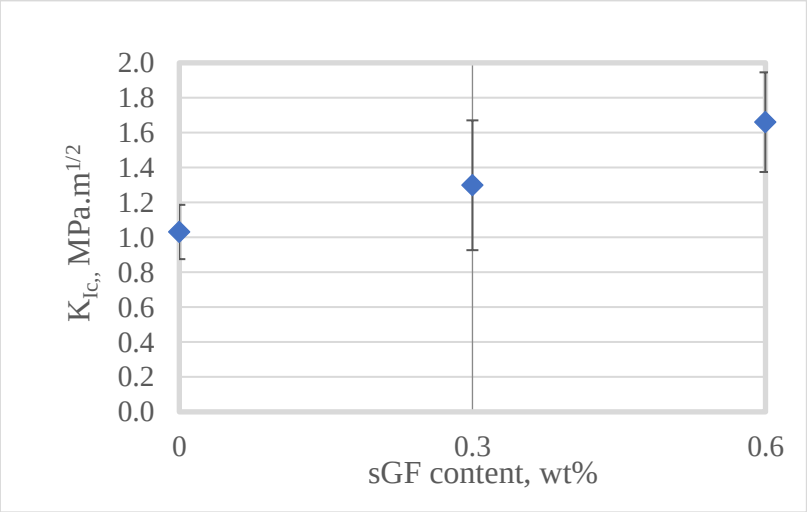

Fig. 2-13. The fracture toughness of resin with respect to sGF content.

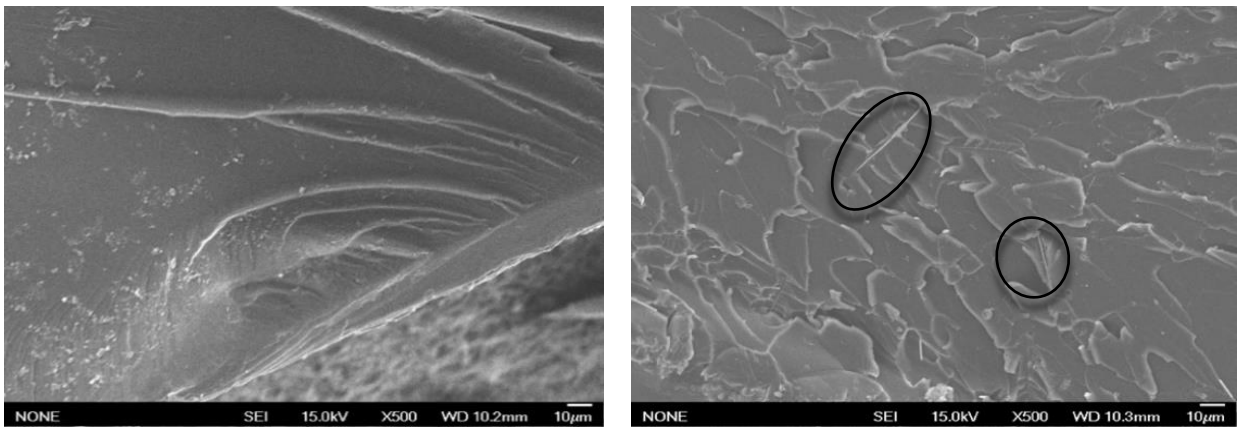

a) un-modified b) 0.6 wt% sGF

Fig. 2-14. Fractured surface SEM images of (a) neat resin and (b) sMC with 0.6wt% glass fiber after fracture toughness test.

In some cases, strong interfacial adhesion occurring between filler and the matrix resin system is vital for optimal enhancement of mechanical performance. Using appropriate filler, the values for the stiffness, tensile strength as well as the fracture toughness will be substantially increased [22]. However, as pointed out in previous discussions, the low adhesion between glass fiber and VE resin might be the main cause of the moderate improvement of fracture toughness in this research.

2.3.6. Resistance against crack propagation

The fatigue life of sMC under cyclic loading condition significantly improved compared to that of neat resin (see Fig. 2-15). The increase in the number of failure cycle was proportional to the content of glass fiber in sMC. At the content of 0.6 wt% of glass fiber, some specimens had the fatigue life extended over 1,500 cycles while the average value of unmodified resin was only 2,00 cycles.

In order to better understand the extending mechanism of sGF in composite, the fracture surfaces of specimens at the zones ahead of the crack tip were observed using SEM images (Fig. 2-16). In the case of neat resin, fracture surface showed the brittle behavior with micro crack lines like river marks appeared nearly parallel along with the increasing of testing cycle. Whereas, it was not found the parallel lines of micro cracks in fracture surface of sMC. The manner was the same with that of sMC in fracture toughness test: the fracture surface became rougher, cracks were tortuous and overlapped.

From parallel cracks in neat VE become indiscriminative cracks in sMC, this change can be explained by deflection and overlapping of cracks thanks to existence of glass fibers in the following discussion. Besides, the de-bonding of sGF caused the considerable deformation of matrix because of forming of fish-bone shapes as can be seen in the Fig. 2-16e.

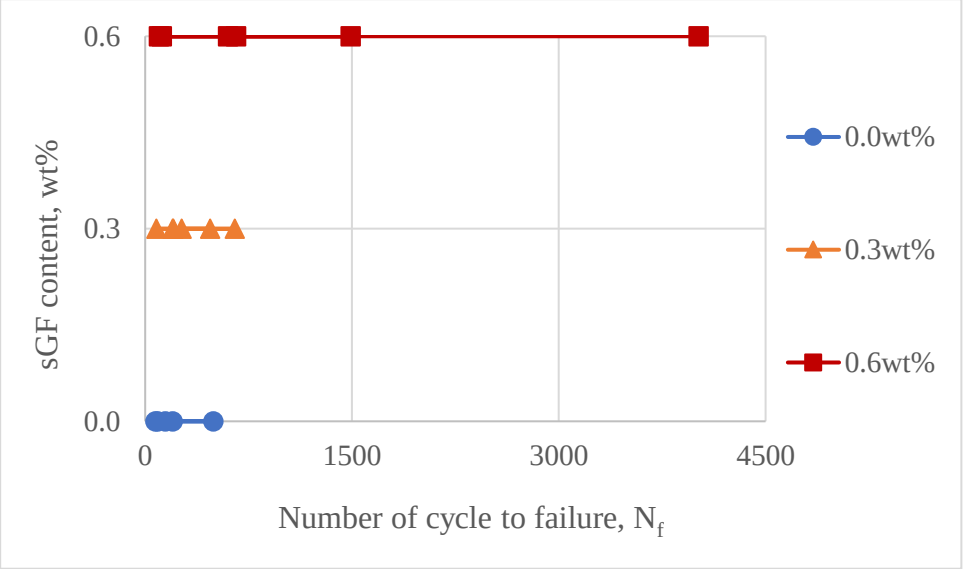

Fig. 2-15. The number of cycle to failure of neat resin and sMC specimens under tension-tension loading condition.

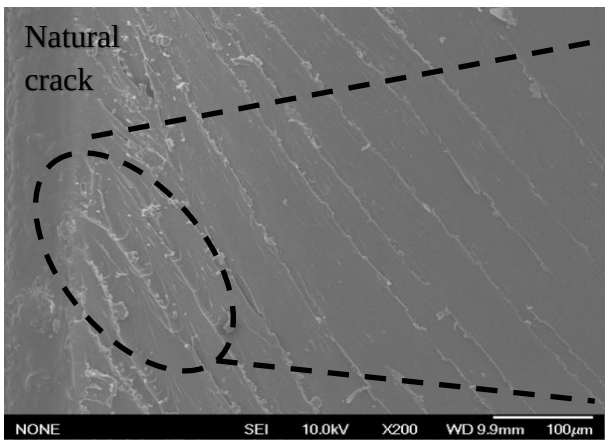

(a)

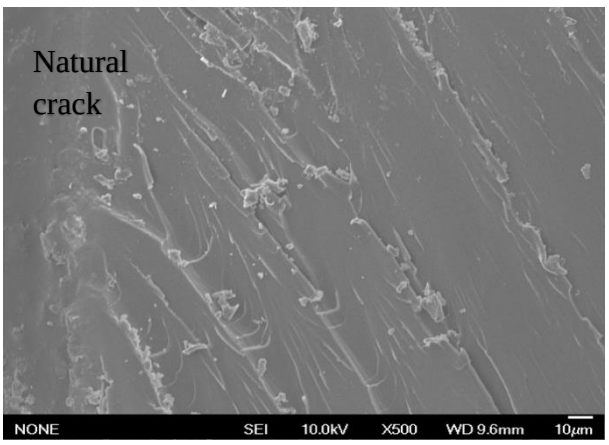

(b)

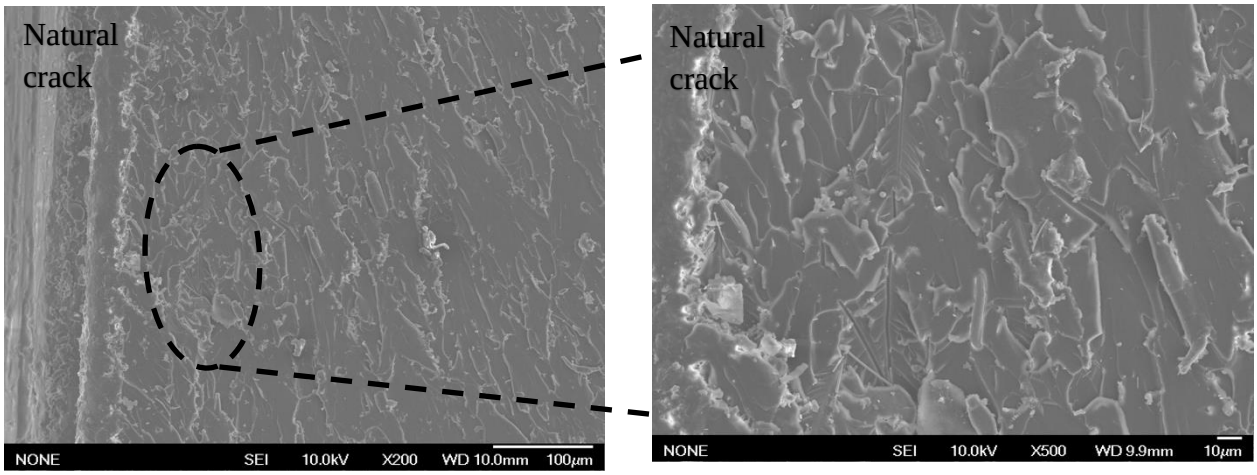

(c) (d)

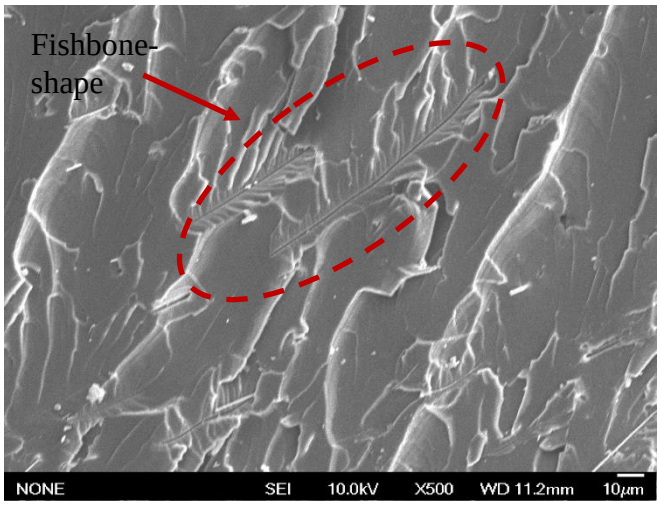

(e)

Fig. 2-16. The SEM images of fracture surface of specimens under tension-tension load after test: (a-b) neat VE, (c-d) sMC at 0.6% sGF, (e) sMC at 0.3% sGF with fishbone-shape observed clearly.

Along with SEM images, the fracture surface of specimens also was used to observe the propagation of striations under the fatigue load by the lazer microscope (see Fig. 2-17). With sMCs, the evidence of crack deflection is obviously detected at branched-off positions of crack growth lines (blue circles). As mentioned by Petit, J. [23], the striation spacing notifies observer the crack growth rate during a cycle. Fig. 2-18 shows the striation spacing on the fracture surface of neat VE and sMCs, increasing the glass fiber content in matrix decreases the distance between adjacent striations and therefore,

declines the crack growth rate. In other words, the enlargement of number of cycle to failure in sMCs is due to the delay of crack propagation owning to reinforcing effect of sGF. These results indicate that glass fiber plays important role in improving the fatigue life of resin by deflecting micro-crack lines, delaying the propagation of cracks as well as partly dissipating crack growth energy for de-bonding fibers from matrix.

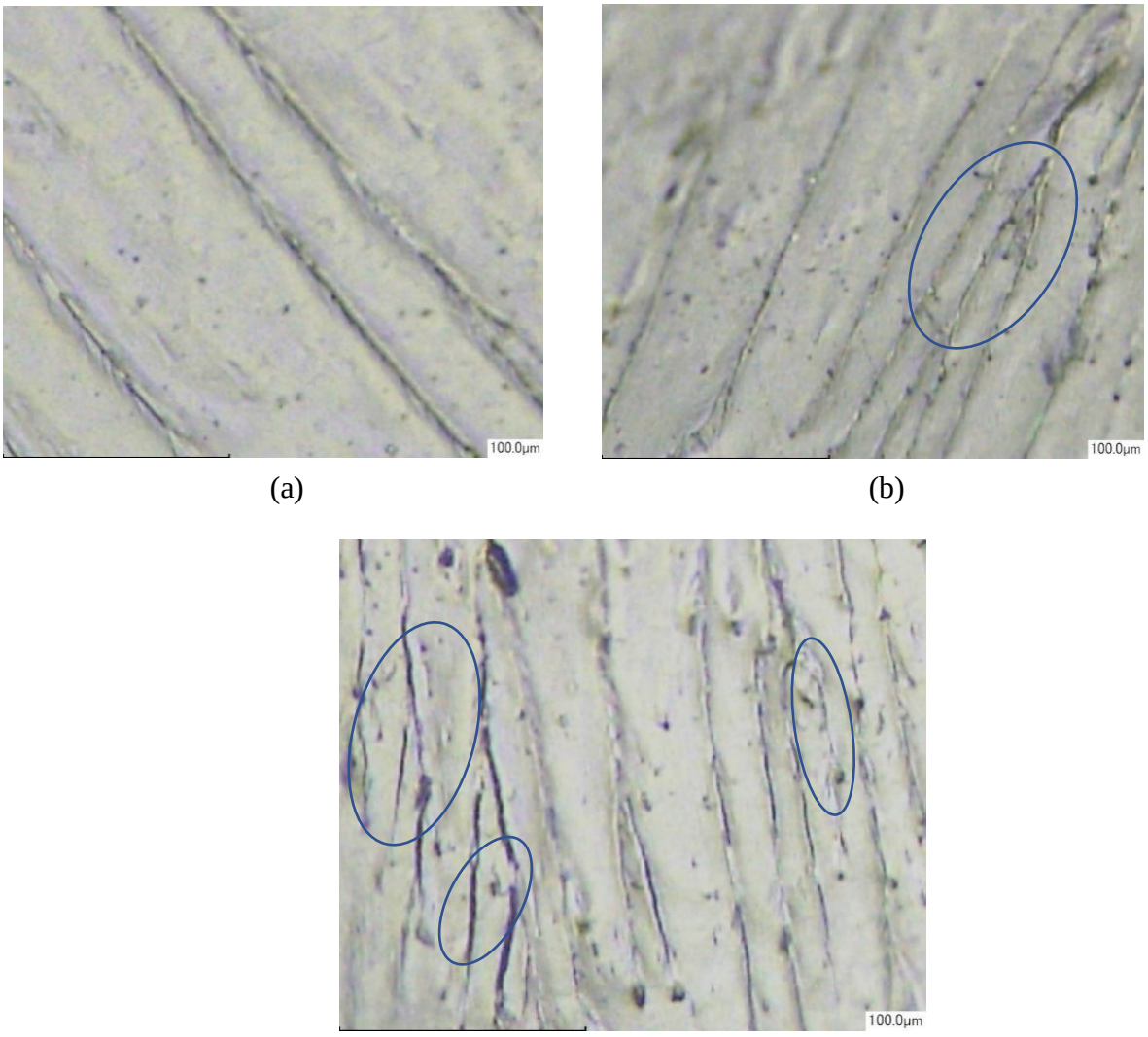

(a) (b)

(c)

Fig. 2-17. Lazer microscope images of fracture surface of (a) neat VE, (b) sMC at 0.3 wt% and (c) sMC at 0.6 wt% of sGF.

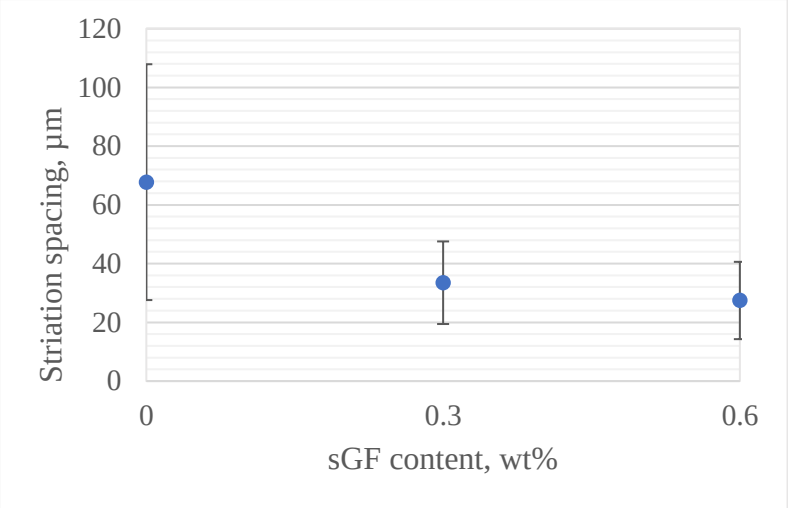

Fig. 2-18. Striation spacing of sMCs with respect to different contents of sGF.

2.4. Conclusions

The sGF was used as reinforcement in VE matrix at low content to investigate its effect on mechanical properties of sMC. Some results can be shown briefly as follows:

1. Submicron glass fiber was well-dispersed in resin by conventional mixing technique. The length of glass fiber after mixing were pretty varied leads to a huge variation of aspect ratio in VE matrix.
2. Impact resistance of un-notched sMC was decreased with the increase of sGF content in matrix while notched -impact resistance as well as flexural properties were almost unchanged compared to those of neat resin. Dynamic mechanical analysis indicated the slight increase of elastic behavior and the decrease of damping property in sMC. However, the Mode I fracture toughness improved significantly from 26 to 61% while the content of sGF lifted from 0.3 to 0.6 wt% in composite. Crack growth rate of notch specimens of sMC under tensile cyclic load also considerably degraded. The observation of SEM and lazer microscope shows evidence of improving fatigue life of sMC is due to deflecting micro-cracks and delaying the propagation of cracks as well as partly dissipating crack growth energy for de-bonding fibers from matrix.

References

[1] RaoP, B.S., Madec, J., Marechal, E. (1986). Synthesis of vinyl ester resins. Evidence of secondary reactions by13C NMR. *Polymer Bulletin*, 16(2–3), pp 153–157

[2] Mullins, M.J., Liu, D., Sue, H-J. (2017). Mechanical Properties of Thermosets. In: Q. Guo (ed). *Thermosets (2nd Edition)*, pp. 35–67. Elsevier (Imprint).

[3] Hodgkin, J. (2001). Thermosets: Epoxies and Polyesters. In: K.H. Jürgen Buschow et al. (eds). *Encyclopedia of Materials: Science and Technology (Second Edition)*, pp. 9215-9221. Elsevier Ltd.

[4] Varma, I.K., Gupta, V.B. 2000. Thermosetting Resin - Properties. In: A. Kelly and C. Zweben (eds). *Comprehensive Composite Materials*, pp.1-56. Pergamon (Imprint).

[5] Kandola, B.K., Ebdon, J.R., Zhou, C. 2018. Development of vinyl ester resins with improved flame retardant properties for structural marine applications. *Reactive and Functional Polymers*, pp.111-122.

[6] Jaswal, S., Gaur, B. 2014. New trends in vinyl ester resins. *Reviews in Chemical Engineering*, 30(6), pp. 567-581.

[7] Ku, K., Prajapati, M., Trada, M. 2012. Fracture Toughness of Vinyl Ester Composites Reinforced with Sawdust and Postcured in Microwaves. *International Journal of Microwave Science and Technology*, vol. 2012, Article ID 152726, 8 pages. https://doi.org/10.1155/2012/152726.

[8] Koro De La CaBa (2005). Properties of a Vinyl Ester Resin Modified with a Liquid Polymer. *High Performance Polymers* 17(4), pp.605-616. DOI: 10.1177/0954008305053206

[9] Ullett, J.S., Chartoff, R.P. 1995. Toughening of Unsaturated Polyester and Vinyl Ester Resins with Liquid Rubbers. *Polymer Engineering and Science*, 35(13), pp.1086-1097.

[10] Orozco, R. 1999. *Effects of toughened matrix resins on composite materials for wind turbine blades.* PhD Thesis, Montana State University, Bozeman, Montana.

[11] Marra, F., et al. 2016. Electromagnetic and Dynamic Mechanical Properties of Epoxy and Vinyl ester - Based Composites Filled with Graphene Nanoplatelets. *Polymers*, 8(8), 272. doi:10.3390/polym8080272

[12] Burchill, P.J., Simpson, G.J. 1997. Improved interlaminar fracture toughness for vinyl ester resin - fiber glass composites. In: Eleventh international conference on composite materials, Gold Coast, Queensland, Australia 14th-18th July. Proceedings Volume 2, Fatigue, fracture and ceramic matrix composites.

[13] Arabli, V., Aghili, A. 2016. Graphene oxide/vinyl ester resin nanocomposite: the effect of graphene oxide, curing kinetics, modeling, mechanical properties and thermal stability. *RSC Adv*, 6, pp. 22331-22340. DOI: 10.1039/C5RA23731A

[14] Ray, D., et al. 2006. Static and Dynamic Mechanical Properties of Vinylester Resin Matrix Composites Filled with Fly Ash. *Macromolecular Materials and Engineering*, 291(7), pp.784-792

[15] Auad, M.L., Proia, M., Borrajo, J., Aranguren, M.I. 2002. Rubber modified vinyl ester resins of different molecular weights. *Journal of Materials Science*, 37, pp. 4117 – 4126

[16] Grishchuk, S., Castella, N., Apostolov, A., Kocsis, J. 2011. Structure and properties of vinyl ester resins modified with organophilic synthetic layered silicates bearing non- and co-reactive intercalants. *Journal of Composite Materials*, 46(8), pp. 941–947.

[17] Li, Y. 2007. *The Development of Sub-Micron Filler Enhanced Polymer Composites* (Doctoral dissertation, Nottingham Trent University, Nottingham, UK). Retrieved from http://irep.ntu.ac.uk/id/eprint/192/1/194139_Yalan_thesis_final.pdf

[18] Jeongwoong, ANN. 1996. Micro-Composites of Poly(styrene) and Nylon 3 by In-Situ Polymerization. *Polymer Journal*, 28(6), pp. 496-500.

[19] Bogomolova, O.Y. 2017. Effect of adhesion between submicron filler particles and a polymeric matrix on the structure and mechanical properties of epoxy resin based compositions. *Mechanics of Composite Materials*, 53(1), pp. 117-122.

[20] Marquis, D.M., Guillaume, E., Chivas-Joly, C. 2011. Properties of Nanofillers in Polymer, Nanocomposites and Polymers with Analytical Methods, Dr. John Cuppoletti (Ed.), ISBN: 978-953-307-352-1, InTech, Available from: http://www.intechopen.com/books/nanocomposites-and-polymers-with-analyticalmethods/properties-of-nanofillers-in-polymer.

[21] Armitt, C.D. 2011. Functional Fillers for Plastics. In: Myer Kutz (eds), *Applied Plastics Engineering Handbook Processing and Materials*, pp. 455-468. Elsevier Inc. DOI: https://doi.org/10.1016/C2010-0-67336-6.

[22] Domun, N., Hadavinia, H., Zhang,T., Sainsbury, T., Liaghata, G.H., Vahida, S. 2015. Improving the fracture toughness and the strength of epoxy using nanomaterials – a review of the current status. *Nanoscale*, 2015 (7), 10294-10329.

[23] Petit, J. 2001. Fatigue Crack Propagation: Effect of Environment. In: K.H. Jürgen Buschow et al (eds), *Encyclopedia of Materials: Science and Technology*, pp. 2892-2896. https://doi.org/10.1016/B0-08-043152-6/00515-5.

Chapter 3

Effect of submicron glass fiber modification and carbon fiber length on mechanical properties of short carbon fiber reinforced polymer composite

3.1. Introduction

Fiber reinforced composites were developed for several decades and widely used in many industrial applications such as automotive, electronic, marine industries. Composites materials are classified by the type of matrix, type of reinforced fiber, and morphology of reinforcement, so on. Among them, short carbon fiber reinforced polymer composites recently are gathering an attention because of their ease of fabrication, economic benefits and also its superior mechanical properties [1-6]. They can fill the mechanical property gap between the continuous-fiber laminates used as primary structures by the aircraft and aerospace industry and the unreinforced polymers used in partial-load-bearing applications [7]. When considering the CF composites applied for industrial applications, by using the thermoset matrices such as vinyl ester is attractive because of its thermal stability. Vinyl esters are unsaturated esters of epoxy resins. They therefore offer similar mechanical and in-service properties to those of the epoxy resins and equivalent processing techniques to those of the polyesters but more flexible and has higher fracture toughness than a cured polyester. Generally, they have good wettability, strong resistance with acid and alkalis, room temperature cure, low absorption of moisture, and good mechanical properties [8-11]. Moreover, carbon fibers are the strongest fibers currently available to reinforce polymeric matrices. Not any do high performance grade carbon fibers display tensile strength exceeding 6 GPa and tensile modulus exceeding 600 GPa, low-density (1.8 -2.0 g/cm^3) but also possess the highest specific stiffness and strength [12,13]. Therefore, the combination of carbon fiber and vinyl ester attracted much attention of researchers and considered as potential materials in industry and aviation [14]. One of the disadvantage of CF composites is the mechanical properties of short carbon fiber composites still be much lower in comparison to that of long fiber composites. Cracks easily occur either or both ends of fiber since (finite) short carbon fiber used. Therefore, it is difficult to make the most of excellent performance of carbon

fiber [2,15,16]. Some researchers reported that the modifying matrix by nano or micro-scale filler often to be employed to improve the fracture toughness of matrix, the adhesion fiber/matrix and delay the initiation and propagation of cracks therefore elevating mechanical properties of composites [17-19]. Takagaki et al. reported that a very little addition of nano-fibers, MFC (Micro Fibrillated Cellulose) less than 0.8 wt.% to epoxy matrix of carbon fabric composites extended their fatigue life ten times longer than that of unmodified case [20]. Xu et al. studied the effect of nano-clay modification of epoxy matrix on the mechanical properties of CF/ EP composites. They showed that the mode-I interlaminar fracture toughness increased by 85% for 4 phr nano-clay, and the flexural strength increased by 38% for 2 phr nanoclay [21]. However, the nano filler shows high agglomerating because of its high specific surface energy, so that the filler has usually dispersed in liquid such as water. Therefore, eliminating the water from nano filler and well dispersed in matrix resin without agglomerating is difficult. Based on these considerations, the sub-micro range inorganic filler was selected for not only avoiding the agglomerating, but also bring advantage of utilizing modern polymer processing technologies [22, 23]. In this study, the CF composites made from 1, 3, and 25 mm length of carbon fiber and vinyl ester resin modified by sub-micron glass fiber was prepared to investigate the effect of sub-micron glass fiber and fiber length on the mechanical properties of composites.

3.2. Material and Processing

3.2.1. Material and modification method of resin

The resin, modifier as well as modification method were the same with those applied in processing vinyl composite in the chapter 2. The carbon fiber (Yoshino Limited, Japan) was used as the reinforcement at 1,3, 25 mm in length. The density of fiber is 1.8 g/cm^3.

3.2.2. Fabrication of composite

Processing method plays an important role in determining cost production of components as well as mechanical performance of final products [24, 25]. In this research, submicron glass fiber was added into resin and mixed by the homogenizer at 0.3 and 0.6 wt% compared to resin. The viscosity of resin become higher with higher content of modifier but still be suitable for using the VARTM (Vacuum Assisted Resin Transfer Molding). This method reduces the cost and design difficulties associated with large

metal tools [26] and expected to remove air bubbles during infusing resin into mold. The diagram of VARTM as follows:

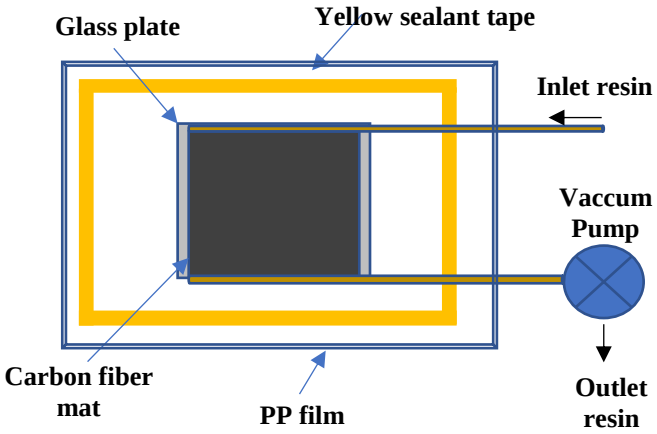

Fig. 3-1. Schema of vacuum system VARTM.

Two PP films were firmly stuck together by the yellow sealant tape to make a vacuum bag. Two glass plates were used to make a closed – mold with the mat – form fiber inside. Under the attraction force of vacuum pressure, resin was led into the mold and impregnated to over volume of fiber mat. The sample after that was kept at room-temperature for 1 day following by post-curing step at 100 ^{0}C in 3 hours. To confirm distribution of sGF, sample was cut from the composite plate and burned in the muffle furnace at 550 ^{0}C for 5 hours. The SEM pictures of samples after ignition are shown in the Fig. 3-2.

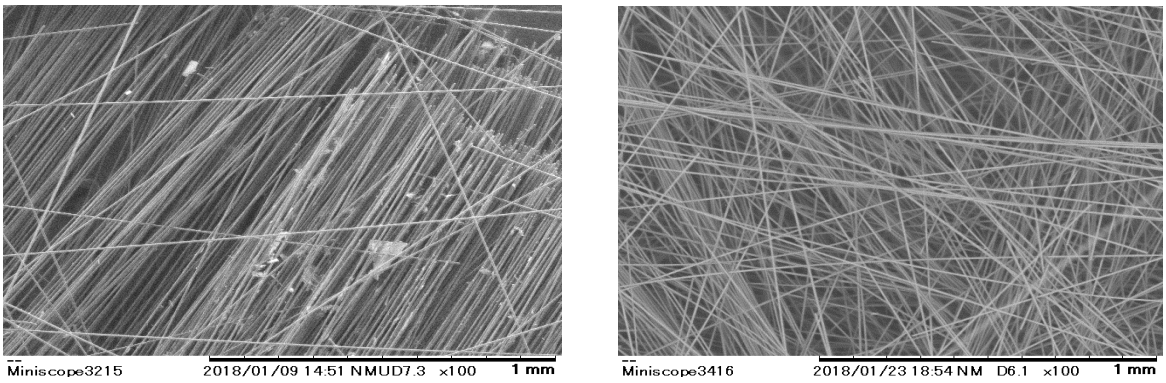

(a) The top layer of sample (b) The middle layer of sample

Fig. 3-2. The sample after burning in the muffle furnace.

Glass fiber was agglomerated on the top layer of sample while there was no fiber observed in the middle layers. Therefore, VARTM is not suitable to infuse sGF modified

vinyl ester resin into fiber. To overcome this deficiency, another method was carried -out as follows:

A thin aluminium plate covered by a non-stick film was put on the scale. At the beginning, a thin layer of resin was spread out on the surface of the film followed by a layer of the carbon fiber. The weight of resin and fiber was controlled to achieve the desired ratio of fiber/matrix. The process was repeated time to time until the materials were used end. The mixture after that was put into the ball mixer and mixed for 10 minutes with the aid of ceramic balls. Finally, putting the mixture onto the steel mold and pressed under 15 MPa for 3 hours at 80^0 C. After curing, the mold was gradually cooled to room temperature, while applied pressure was kept constant. The post-cure process was conducted at 100^0 C in 3 hours. Because of difficulty in processing caused by higher viscosity with shorter fiber length, the same of fiber volume fraction for composites was impossible, therefore, in this research the volume fraction of fiber for 1, 3 and 25 mm composites was 25, 35 and 40%, respectively. For the sake of comparison, the strength/fiber volume of each composite was used in latter sections. The SEM pictures validate distribution of sGF in middle layers is more superior in this method than that of VARTM (see Fig. 3-3).

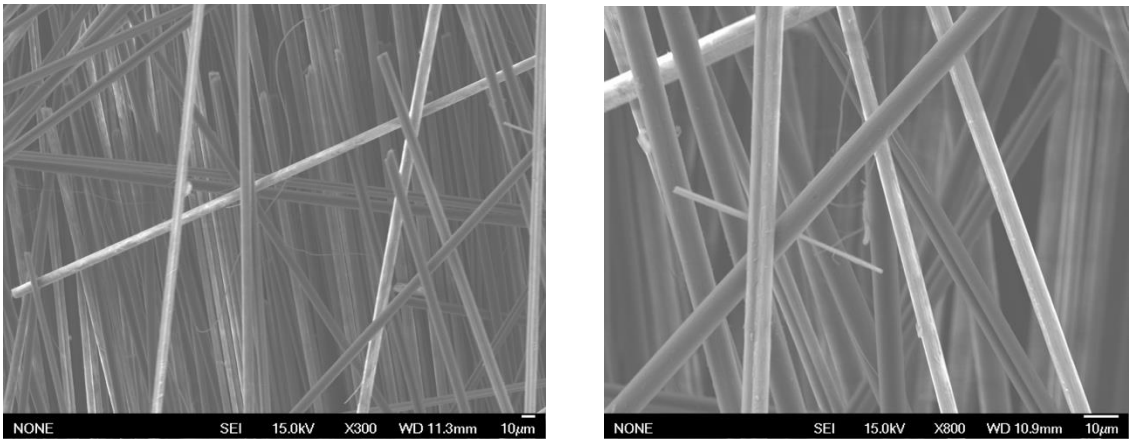

(a) at magnification of 300 times (b) at magnification of 800 times

Fig. 3-3. The sGF distribution in middle layers of 0.3 wt% modified composite sample after burning.

3.2.3. Evaluation of adhesion between single fiber and matrix

The micro droplet test was conducted to evaluate the interfacial shear strength of single fiber with matrix. The geometry of sample is shown in the Fig. 3-4. The condition for curing and post curing is the same with that of composite sample.

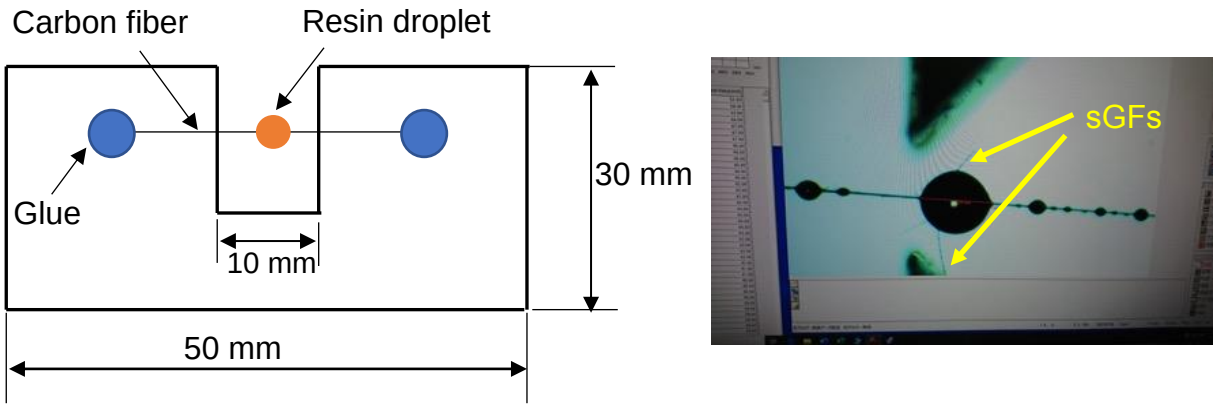

Fig. 3-4. The paper frame with single carbon fiber for the micro droplet test (left scheme) and the image of resin droplet under a microscope observation (right image).

The sample with single fiber in matrix also was prepared and tested under the tensile testing equipment (made by AMSEL laboratory) designed to pull both ends of the specimen slowly apart (Fig. 3-5). The segmentation of single fiber was observed by the microscope until full fragmentation occurs (as can be seen in the upper left corner of Fig. 3-5).

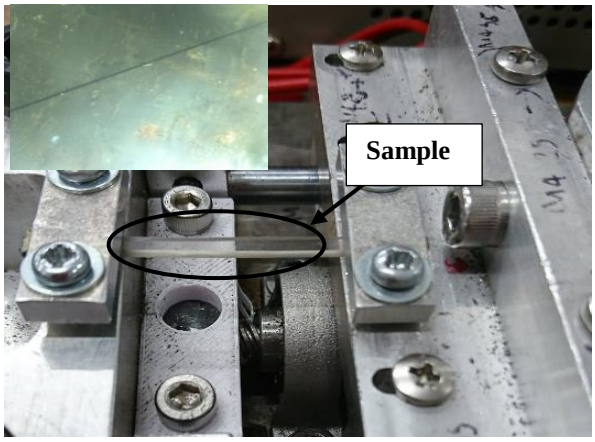

Fig. 3-5. The specimen in the test apparatus and observed fragmentation of single fiber under polarized microscope (small image in the upper left corner).

3.2.4. Density and void content of composites

To determine density and void content in composites, pieces of samples with foreknown dimensions (for calculating measured density) was dried until un-changed weight and ignited in the muffle furnace at 550 ^{0}C for 5 hours. The left after burning was considered as carbon fiber and used for calculating the theoretical density of composite. The void content was calculated following the standard of ASTM D 2734 – 94 as mentioned in the below equation:

$$V = 100(T_d - M_d)/T_d \quad (1)$$

Where:

V = Void content, volume %,

T_d = Theoretical composite density, and

M_d = Measured composite density.

3.2.5. Static mechanical characteristics of composites

Three point bending test was conducted followed the ASTM D 790–03 . The size of specimen was 100x15x2.5 mm^3. The cross head speed was controlled to be 2 mm/min with the support length of 80 mm. At least five specimens were used for each kind of sample.

The samples for tensile test were prepared following the ASTM D638 with dimensions 200x25x2.5 mm^3. The gage length was 100 mm and the speed of testing was control to be 1 mm/min. At least five specimens were used for each kind of sample.

The Izod impact test was performed using the pendulum testing device according to the standard JIS 7062 with the specimen dimensions were 65x10x4.5 mm^3. The test conducted when the hammer impact onto the flatten surface of specimen. At least 10 specimens were used for each sample group.

3.2.6. Measuring strain distribution of model specimen

To observe the strain distribution around the carbon fiber tip of CF, a model composite was prepared. CF in 25 mm long was embedded into VE, cured at 80^0 C for 3 hours then post cured at 100^0 C in the same time. Pre cracks with crack length approximate 1.5 mm was prepared by diamond cutter at both sides then natural cracks introduced by slicing razor at the pre-crack root before testing. The sample surface was painted by white and black paints to create a speckle pattern for digital image correlation analysis (Fig. 3-6). Sample size was 40x20x0.5 mm. The tensile load was applied to the model specimen at a constant cross head speed of 1 mm/min.

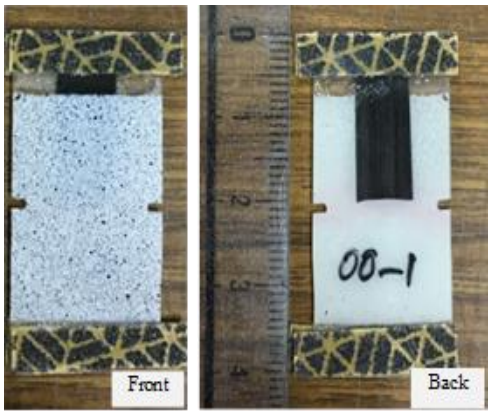

Fig. 3-6. Image of model specimen with speckle pattern from black and white paint for measuring strain distribution.

3.2.7. Fatigue test of composite

The tension-tension fatigue test was conducted on the hydraulic testing machine under load controlled condition – the Servo Pulser 100 kN of Shimazdu (see Fig. 3-7). The cyclic sinusoidal load with 5 Hz of frequency and stress ratio was 0.1 was applied. In this study, the test was truncated automatically when the cycles exceed the maximum cycles of 10^6 cycles. The maximum applied stress was set to be 50% for 1 and 3 mm composite while that of 25 mm composite is 45%, 55%, 60% and 70% of the average ultimate tensile strength. The sample size was the same with that of tensile coupons.

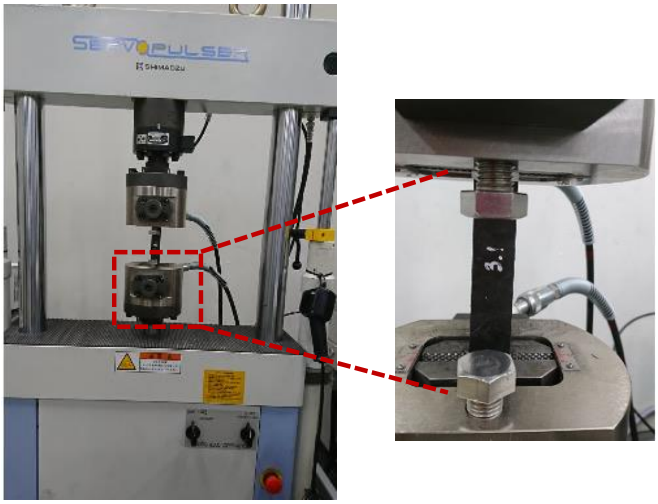

Fig. 3-7. The image of specimen under testing on the Servo Pulser 100 kN (Shimazdu).

3.3. Results and Discussions

3.3.1. Added sGF in resin and composite

The SEM pictures confirm that the sGF is well dispersed in the matrix by the conventional mixing technique as mentioned in the section 2.2 though the original fiber is in agglomeration form. Submicron filaments is separated from each other and distributed regularly without curviness of fiber (see Fig. 3-8).

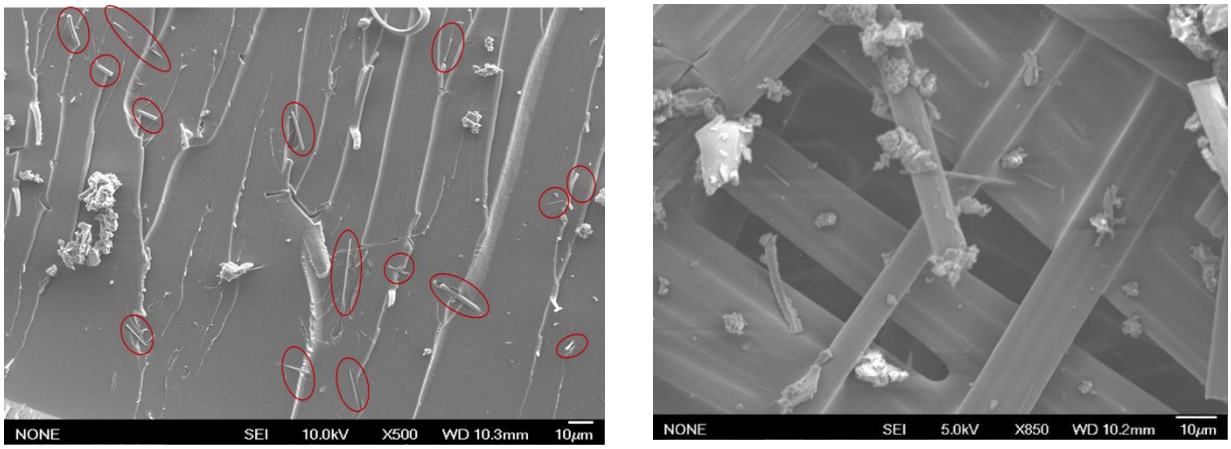

(a) sGF in neat resin (b) sGF in composite

Fig. 3-8. Distribution of 0.6% sGF in the VE matrix and in 3mm composite.

3.3.2. The adhesion fiber and matrix

As can be seen from the Table 3.1, the interfacial shear strength (IFSS) of modified sample is almost similar to that of un-modified resin. The length of fiber segments also

does not considerably change. This result indicates the adhesion between fiber and matrix is not affected by the addition of submicron glass fiber. The SEM of fracture surface of composite after tensile test also shows the adhesion between fiber and matrix is almost the same regardless the addition of glass fibers (see Fig. 3-9).

Table 3.1. The length of fiber segment after full fragmentation and the IFSS between fiber and matrix.

	Segmentation length of fiber (μm)	IFSS (MPa)
0.0 wt%	499.14 (402.24)	20.076 (3.43)
0.3 wt%	752.8 (186.7)	20.93 (3.72)
0.6 wt%	574.37 (211.12)	20.17 (4.23)

() parentheses contain standard deviation values of tested data.

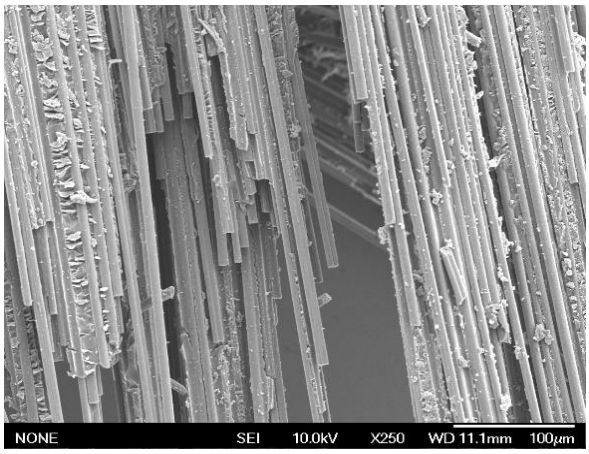

(a) 0.0 wt% sGF

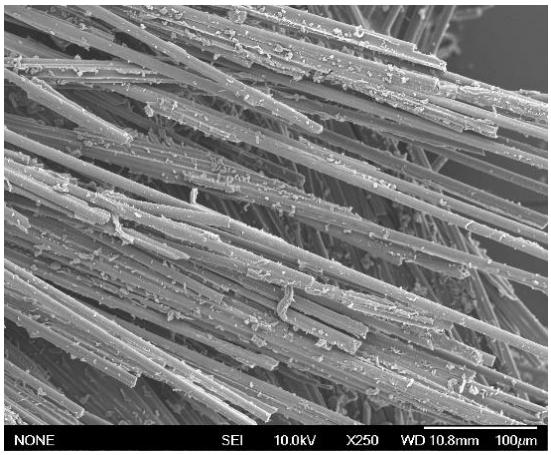

(b) 0.3 wt% sGF

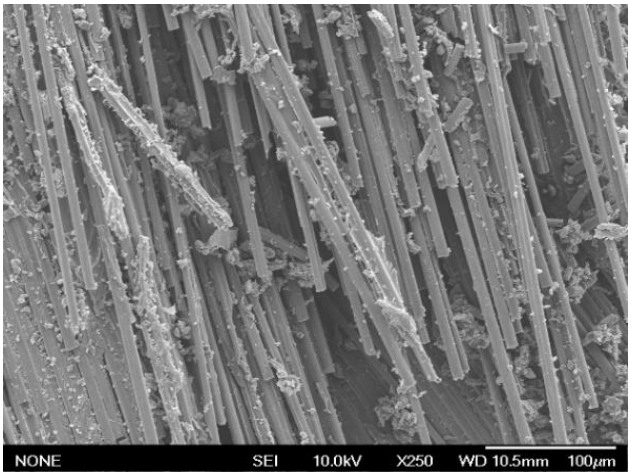

(c) 0.6 wt% sGF

Fig. 3-9. SEM images of fracture surface of 25 mm composites after tensile test.

3.3.3. Density, void content and lost weight of composite

The Table 3.2 shows the density, void content and lost weight of composites. In the component of vinyl ester resin, styrene is both dilution and curing – agent element. Though styrene has the boiling point approximately of 145 ^{0}C but the melting point as well as the vapor pressure are around -31 ^{0}C and 6.40 mm Hg at 25 °C, respectively [27], facilitate vaporization even at room temperature. Because of lower viscosity, the vaporization happens more strongly, leads to the higher lost weight after curing in unmodified composite. As mentioned by Chang.W.C, et al [25], the weight loss results in bulk shrinkage and the formation of porous voids within the composites. Mixing glass fiber into resin also brings air into filled-system. Therefore, the void contents in composites were not considerably different.

Table 3.2. The density, void content and lost weight of composites.

	Composite	Density (g/cm^3)	Void content (Volume %)	Lost weight (%)
1mm	0.0 wt%	1.2315	3.7891	
	0.3wt%	1.2373	3.3359	-
	0.6 wt%	1.2412	3.0313	
3mm	0.0 wt%	1.3277	2.3025	
	0.3wt%	1.3471	1.8263	-
	0.6 wt%	1.3472	1.3814	
25mm	0.0 wt%	1.3562	3.8178	4.3
	0.3 wt%	1.3734	2.5928	2.6
	0.6 wt%	1.3683	2.9556	2.6

3.3.4. Static mechanical characteristics of composite

Bending strength

Mechanical performance of short fiber composite often varies in a large range because of experimental scatter causes difficulties in predicting effect of modifiers on

filled-system [5]. Values in parentheses manifest large standard deviation of tested data of mechanical properties of composites (see Table 3.3, 3.4, 3.5). Table 3.3 and Fig.3-10 show the change of flexural strength of composites with respect to CF length corresponding to sGF content. The flexural strength of composites increased with the increase of CF length as mentioned by Thomason [28]. However, the significant improvement of bending strength only happened when the fiber length changes from 1 mm to 3 mm. In the other words, the bending strength per fiber volume fraction of 3 mm fiber length and 25 mm fiber length composite is almost the same. Observing from the view point of sGF content, the flexural strength only improved by sGF addition when carbon fiber length is pretty short (1 mm). Comparing with the neat resin, reinforcing VE by 1 mm carbon fiber increased the flexural brittleness, resulted in the slight decrease of the bending strength of resin. Therefore, the improvement of bending strength in 1 mm fiber composite might be explained from the view point of fiber aspect ratio. The aspect ratio of carbon fiber was 143, 429 and 3572 for 1 mm, 3 mm and 25 mm fiber length, respectively. Collating these values with those of glass fiber (Fig 2.5 – Chapter 2) suggests that the aspect ratio of glass fiber is approximate with that of 1 mm carbon fiber and much lower compared with that of 3 mm and 25 mm fiber length. Consequently, adding glass fiber into VE is only effective in the case of composite reinforced by 1mm carbon fiber length. Base on calculating from the equation 1-1 (Chapter 1) and the IFSS value from Table 3.1, the critical length of carbon fiber is around 1.3 mm to 1.5 mm. On the other hand, below the mentioned fiber length, the mechanical strength of composite is low. This explains the remarkable increase of bending strength when fiber length rose from 1 mm to 3 mm but remained the unchanged with 25 mm.

Table 3.3 The flexural strengths of composites and neat resin.

	Bending strength, MPa		
Composite	1mm	3mm	25mm
0.0 wt%	119.3 (8.76)	329.1 (14.73)	396.83 (57.5)
0.3 wt%	132.36 (18.3)	317.27 (38.74)	392.01 (75.83)
0.6 wt%	149.93 (16.03)	336.91 (40.57)	391.35 (90.53)
Neat resin		127.77 (1.18)	

() - parentheses contain standard deviation values of tested data.

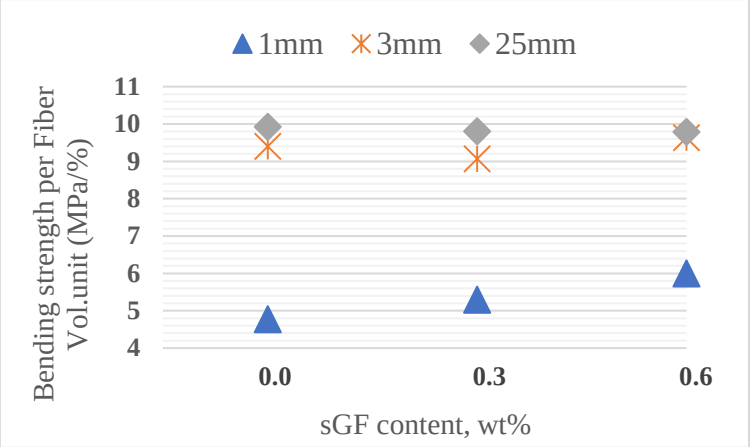

Fig. 3-10. The bending strength of composites with respect to CF length and sGF addition content.

Fig. 3-11, 3-12, 3-13 show the typical bending stress-bending strain diagram of composites made from 1, 3 and 25 mm of CF, respectively. Regardless of the difference of CF length and sGF content, the bending stress linearly increased until fracture with most of specimens. Test results also showed that the flexural modulus of composites were almost the same even if the sGF was added with the exception of 1 mm composite presented the marginal increase. Images of fractured region of 1 and 25 mm composites after testing were taken by a digital microscope shown in the Fig. 3-13. In 1mm composite, the cracks appeared in thickness direction. By contrast, cracks propagated in longitudinal (inter-laminar) direction in 25 mm composite. These results suggest that cracks form and propagate at CF ends in 1 mm composite but along the fiber in longer fiber composite.

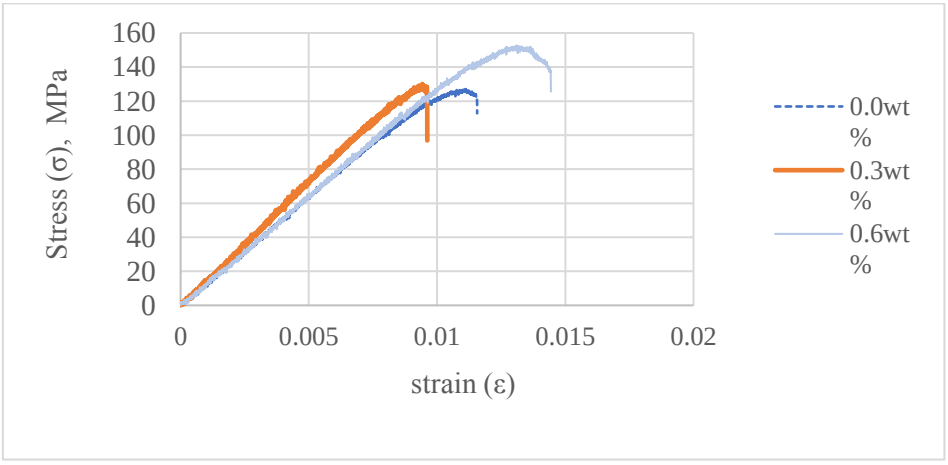

Fig. 3-11. The representative stress-strain curves of 1mm composites.

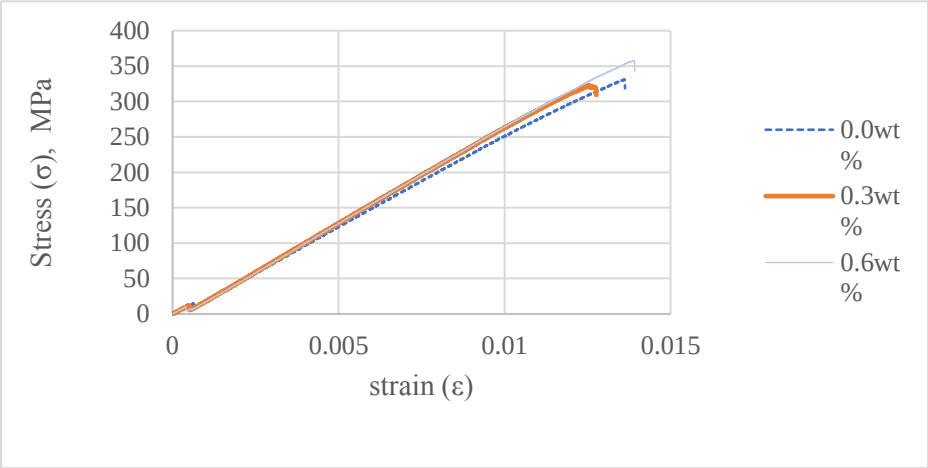

Fig. 3-12. The representative stress-strain curves of 3mm composites.

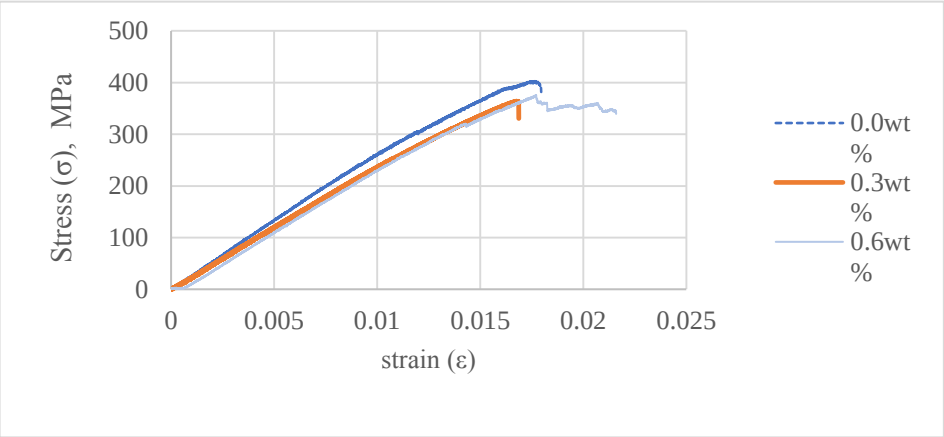

Fig. 3-13. The representative stress-strain curves of 25 mm composites

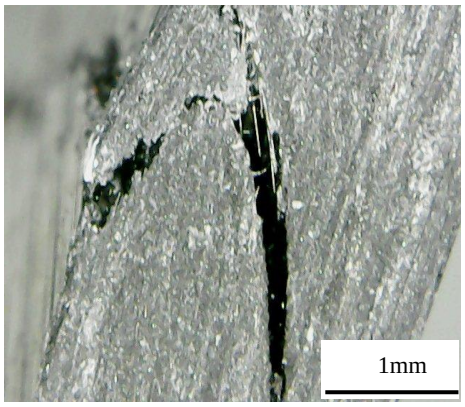

(a) 1mm fiber unmodified composite

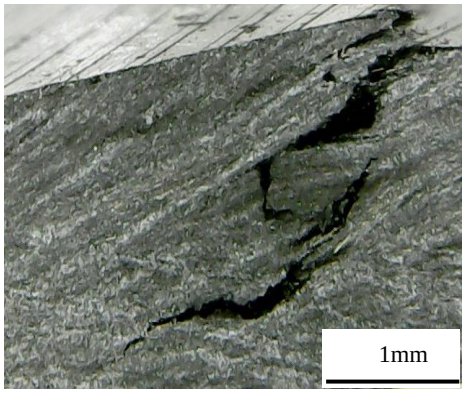

(b) 1mm fiber modified composite

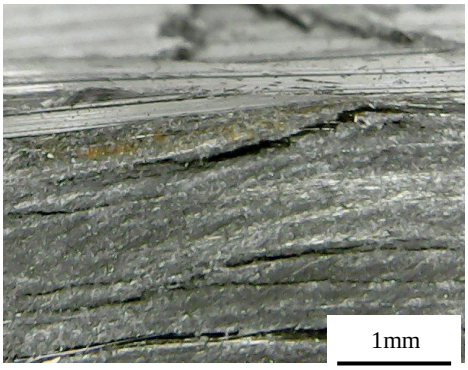

(c) 25 mm fiber unmodified composite

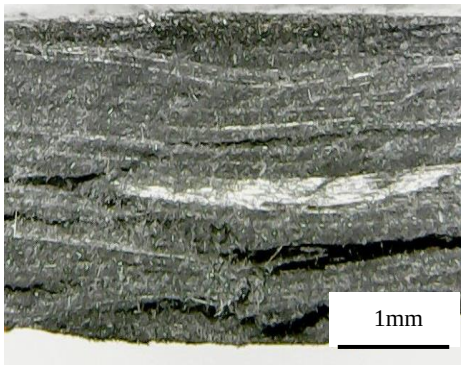

(d) 25 mm fiber modified composite

Fig. 3-14. Fracture on the edges of composites unmodified and modified with 0.6 wt% of sGF after bending test.

Table 3.4. The tensile strength of composites and neat resin.

	Tensile strength, MPa		
Composite	1mm	3mm	25mm
0.0 wt%	46.28 (2.5)	196.96 (13.67)	208.98 (35.29)
0.3 wt%	53.53 (4.83)	168.59 (36.69)	215.96 (22.46)
0.6 wt%	47.7 (4.76)	173.66 (25.71)	224.74 (27.31)
Neat resin		80*	

* Data from the supplier, () - parentheses contain standard deviation values of tested data.

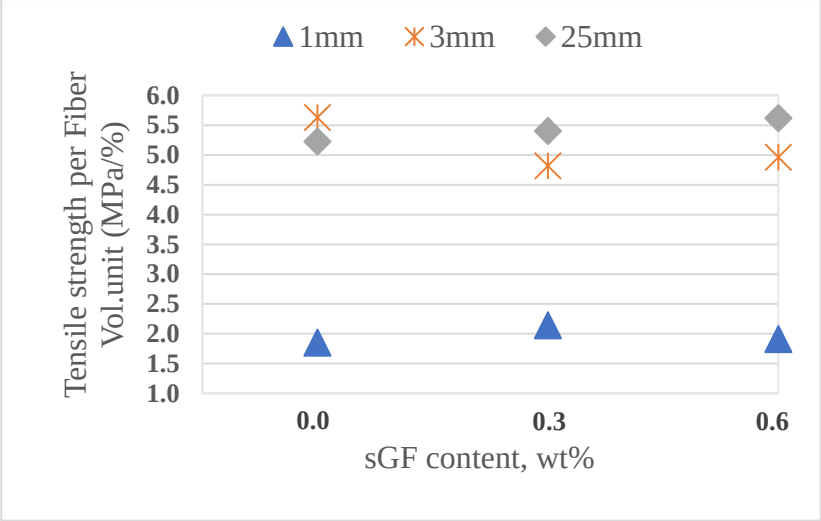

Fig. 3-15. The tensile strength of composites with respect to CF length and added sGF content.

Tensile strength

The same tendency with the flexural strength can be noticed in the tensile strength (Table 3.4 and Fig. 3-15). In the same volume fraction of fiber, 3 mm fiber composite and 25 mm fiber composite had similar tensile performance. Table 3.5 compares flexural and tensile strength of un-modified composites at continual range of carbon fiber length (i.e. 1 mm, 2 mm, 3 mm and 25 mm) and reveals the same result as pointed in the discussion section of bending strength.

Adding CF 1 mm into matrix at 25% fiber volume fraction significantly reduced the tensile strength of resin. The tensile strength of this composite falls to approximately 63% compared to that of neat resin. The longitudinal tensile strength of composite materials is determined mostly by the strength and volume content of the fibre reinforcement [29], therefore the decrease of ultimate tensile strength in 1 mm fiber composite was due to fiber length below critical length.

Table 3.5. Mechanical performance of un-modified composites at different lengths of carbon fiber.

Composite	Bending strength/Fiber Vol. (MPa/%)	Tensile strength/Fiber Vol. (MPa/%)
1mm	4.772	1.852
2mm	8.603	2.922
3mm	9.403	5.627
25mm	9.92	5.224

The impact resistance of composites

Fig.3-16 and Table 3.6 show the Izod impact resistance of neat resin and composites. The impact resistance of 1 mm fiber composite also declined in comparison with that of neat matrix. This result is suitable with that of bending and tensile strength. Nevertheless, the impact resistance performance of composites improved proportionally with the increase of fiber length at the same fiber volume fraction. Glass fiber modification did not affect energy absorption ability of composites. Actually, the impact resistance of resin considerably decreased by sGF modification (see section 2.3.2 – Chapter 2). On the other hand, the negative effect of glass fiber on impact resistance of composite was neglected for all fiber lengths. The mechanism for this phenomenon should be further studied in next research.

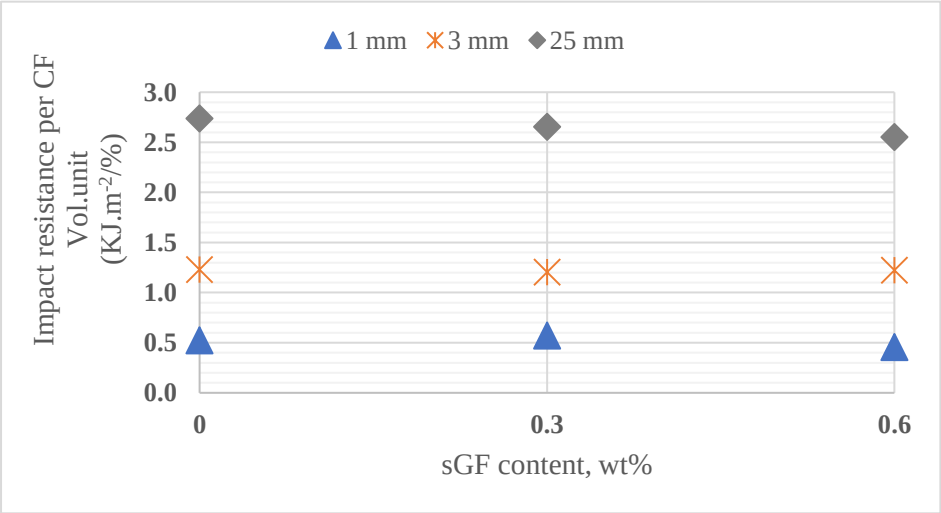

Fig. 3-16. Izod impact resistance of composites.

Table 3.6. The Izod impact resistance of composites and neat resin.

	Impact resistance (KJ/m^2)		
Composite	1mm	3mm	25mm
0.0 wt%	13.14 (1.68)	43.14 (5.6)	109.59 (11.58)
0.3 wt%	14.36 (6.38)	42.26 (5.68)	106.324 (8.85)
0.6 wt%	11.43 (4.07)	42.92 (5.41)	102.19 (9.62)
Neat resin		28.25 (7.99)	

() - parentheses contain standard deviation values of tested data.

Fig.3-17 shows the edge cracks of specimens after impact test. The crack formation in these cases was similar to that of the bending strength. Cracks propagated as in the zig-zag form in 25 mm composite but much straighter in 1 mm composite suggested about crack propagation model is dependent on fiber length.

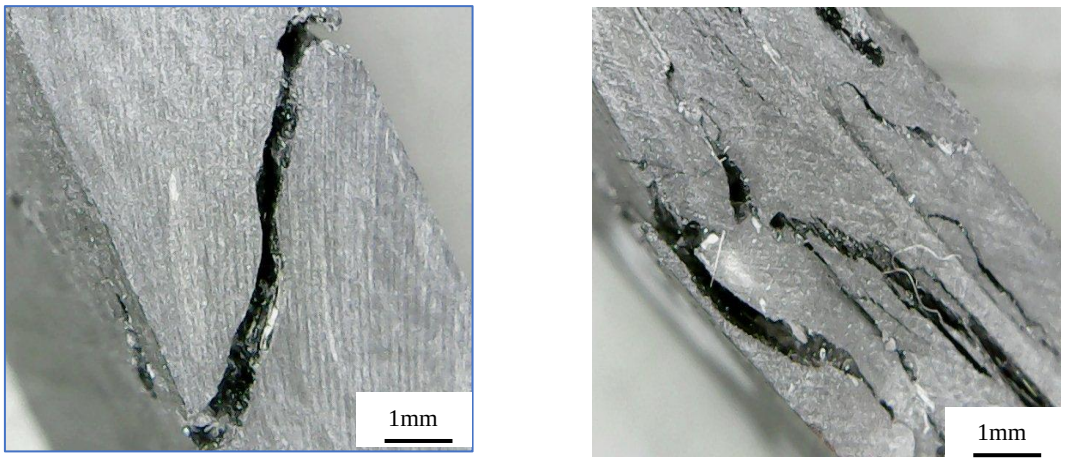

(a) (b)

Fig. 3-17. Edge fracture state of: (a) 1mm composite, (b) 25mm composite.

3.3.5. Strain distribution around carbon fiber tip

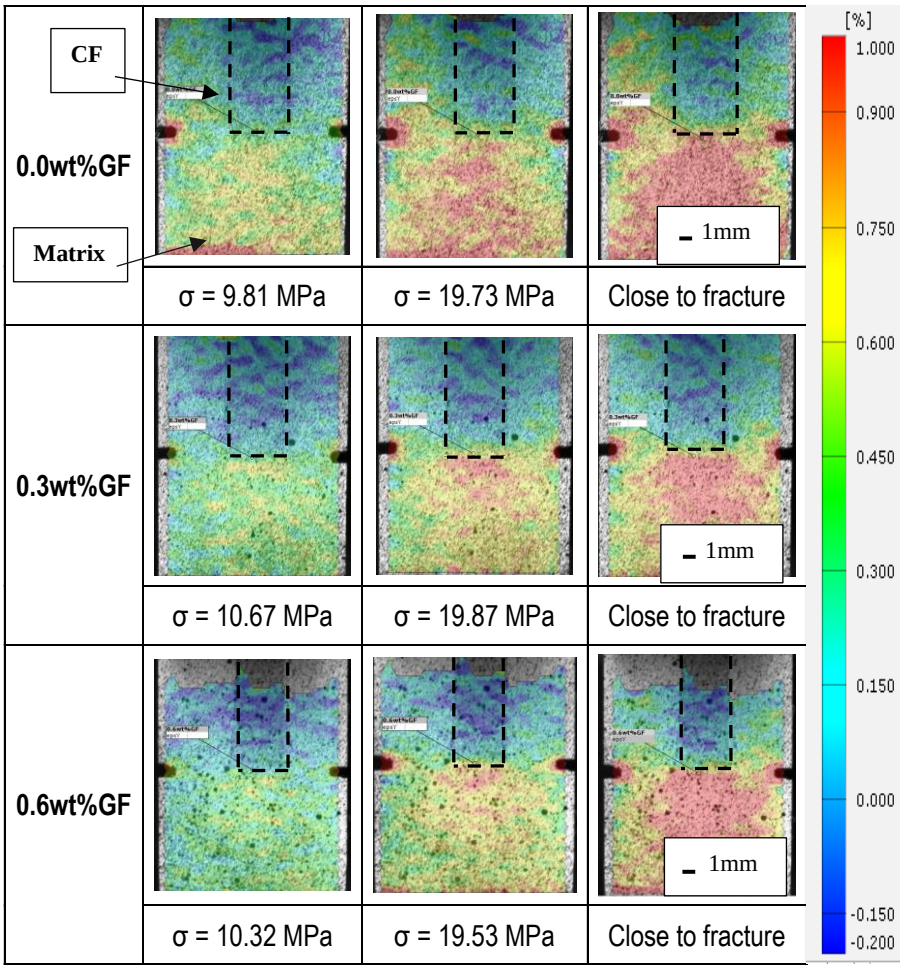

Fig. 3-18. Strain distribution of composite models consisted of single fiber bundle and unmodified/modified VE.

Fig. 3-18 shows the strain distribution along longitudinal direction of model composites under same level of tensile load. In this figure, the position of embedded carbon fiber bundle is illustrated in black dash lines. Test results indicated that the strain around carbon fiber bundle tip and pre crack increases with the increase of applied stress level. However, when matrix was modified with sGF, the strain concentration was suppressed. These results suggest that the existing of added sGF is helpful to avoid stress concentration at carbon fiber tip.

3.3.6. Effect of sGF addition on the fatigue life of composite

The fatigue test was conducted at 50 % maximum tensile strength with 1 mm and 3 mm composite. In the case of 25 mm composite, different stresses were chosen i.e 100, 120, 132, 154 MPa correspond with 45%, 55%, 60% and 70% of ultimate tensile strength (220 MPa) to ensure the consistency of result. Figure 3-19 to 3-21 show the number of cycle to failure composites with respect to fiber length. For all cases of fiber length, the fatigue life has noticeably extended with the addition of sGF. The improvement of number cycle to failure is proportional to the content of glass fiber in matrix regardless the fiber length. At the low stress levels (45 and 50%), all specimens modified by 0.6 wt% sGF survive over one million cycles. Besides, as can be seen from the Fig. 3-21, increasing loading test, the fatigue life of un-modified composite rapidly attenuated while that of modified composite showed the gradual decline. At high stress level of 70%, fatigue resistance ability of un-modified nearly disappears. To more clarify mechanism of fatigue improvement, SEM observation was carried out with fracture surfaces of un-modified and modified sample after test. On both of surfaces, it can be seen some air-voids where concentrates stress leads to early failure as well as large scatter of composite mechanical performance. In modified composite, some air-voids contain a lot of glass fibers (see Fig. 3-22). Macro matrix cracks also was found on surfaces, however the extension of macrocracks in the case of un-modified composite is much larger than that of the modified. Besides, the brittle failure feature in un-modified composite also was observed clearly with glassy surface and cleavage. By contrast, the broken surface of the modified shows debris of matrix left, indicates high dissipation of energy due to toughened-matrix (Fig. 3-23, 3-24).

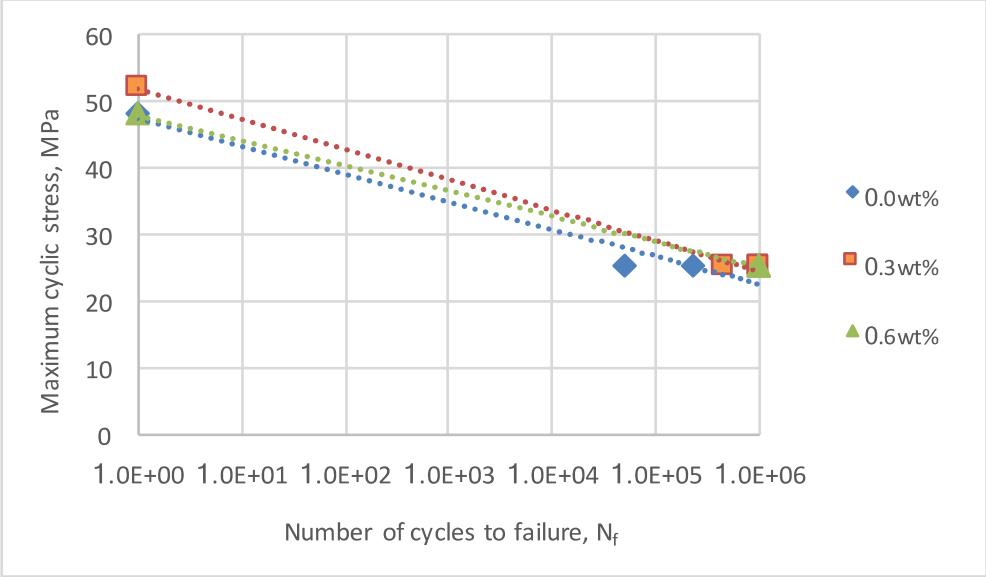

Fig. 3-19. The number of cycles to failure of composite reinforced by 1mm carbon fiber length.

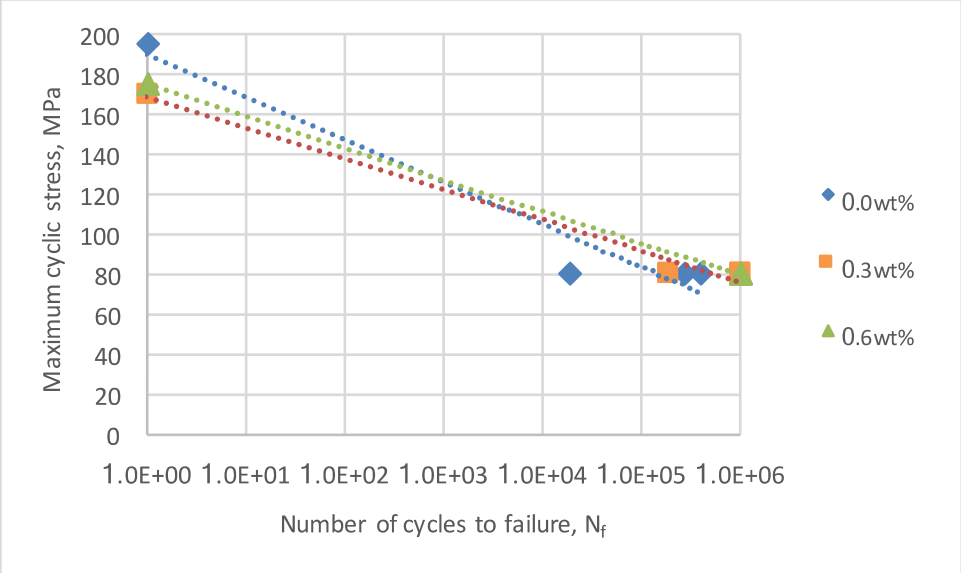

Fig. 3-20. The number of cycles to failure of composite reinforced by 3 mm carbon fiber length.

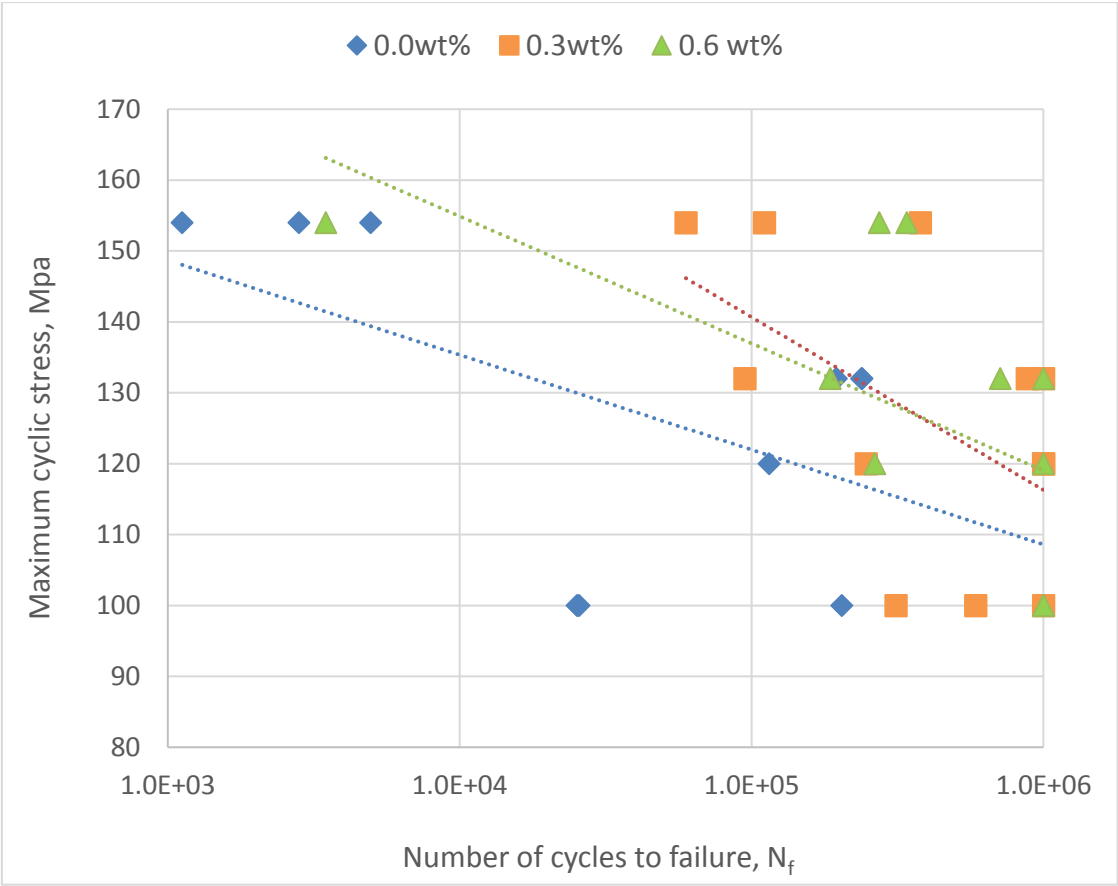

Fig. 3-21. The number of cycles to failure of composite reinforced by 25 mm carbon fiber length.

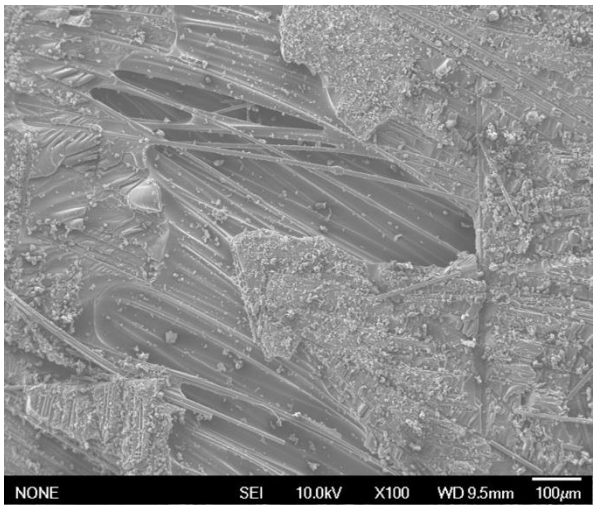

(a) un-modified composite

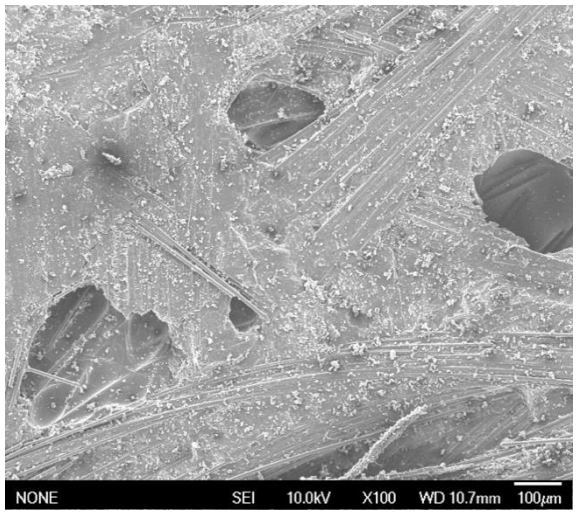

(b) modified-composite

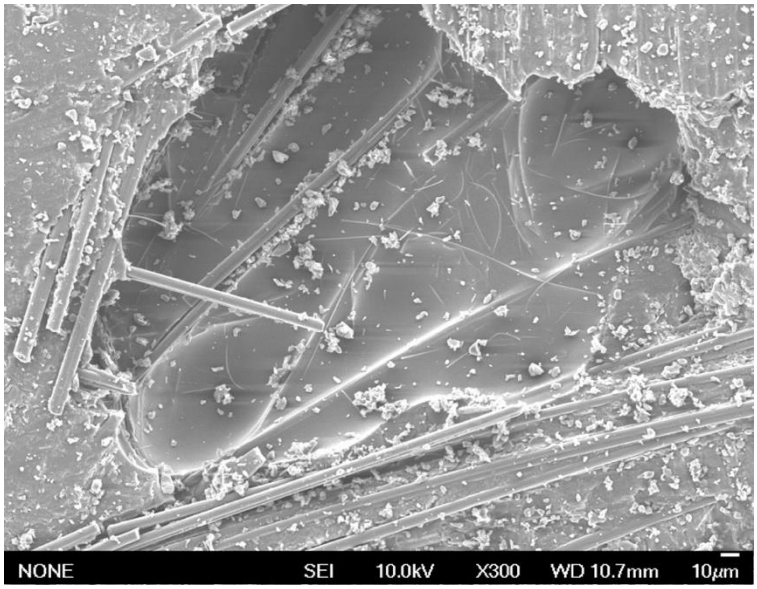

(c) Void-defect with glass

Fig. 3-22. Fracture surface of composites with air-voids.

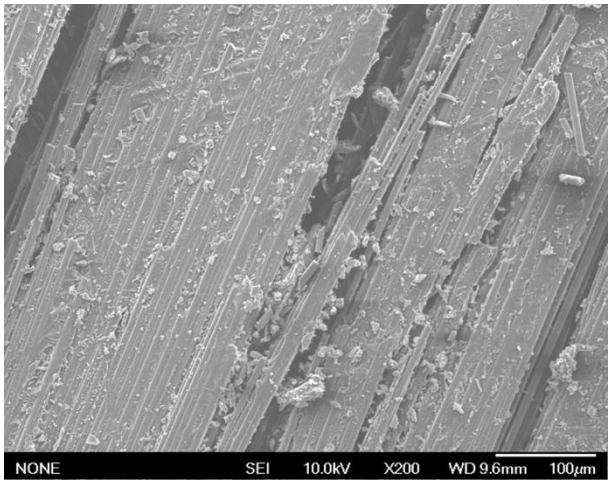

(a) Matrix cracks in unmodified composite

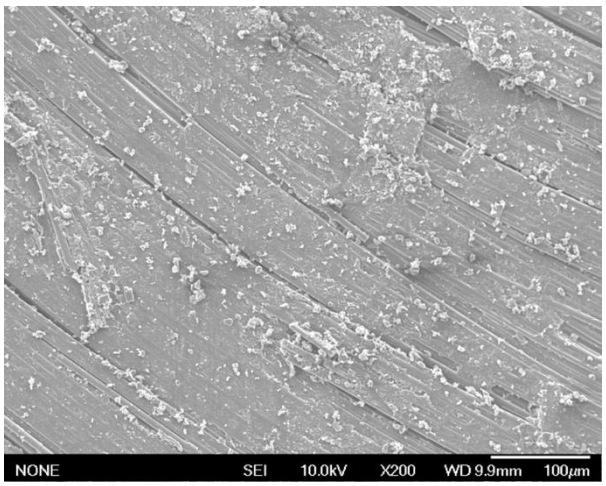

(b) Macro cracks in 0.6 wt% modified

Fig. 3-23. Macro cracks on the fracture surface after the fatigue test.

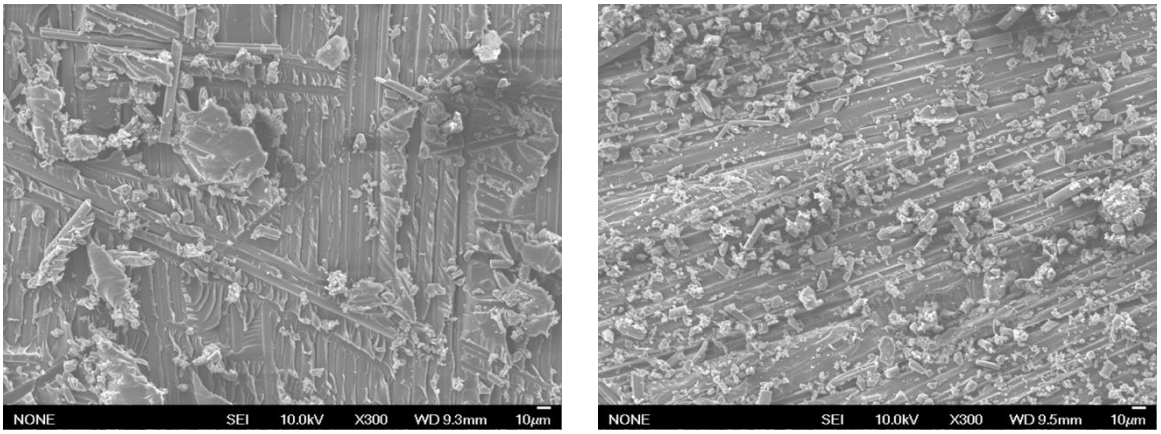

(a) Brittle failure of matrix in un- (b) Failure with more debris of matrix in 0.6 wt%

Fig. 3-24. Matrix failure on fracture surface of composites after fatigue test.

The strain distribution test suggests that sGF prevents the concentration of stress at carbon fiber tips as a result, delaying the propagation of micro cracks inside matrix. As pointed out in the chapter 2, the number of cycle to failure in the test of compact tension test of modified resin also remarkably improved thanks to the addition of glass fiber [30]. Therefore, the enlargement of fatigue life in composites was due to the presence of sGF dissipates energy for deflecting and delaying the propagation of micro cracks (see Fig. 3-25).

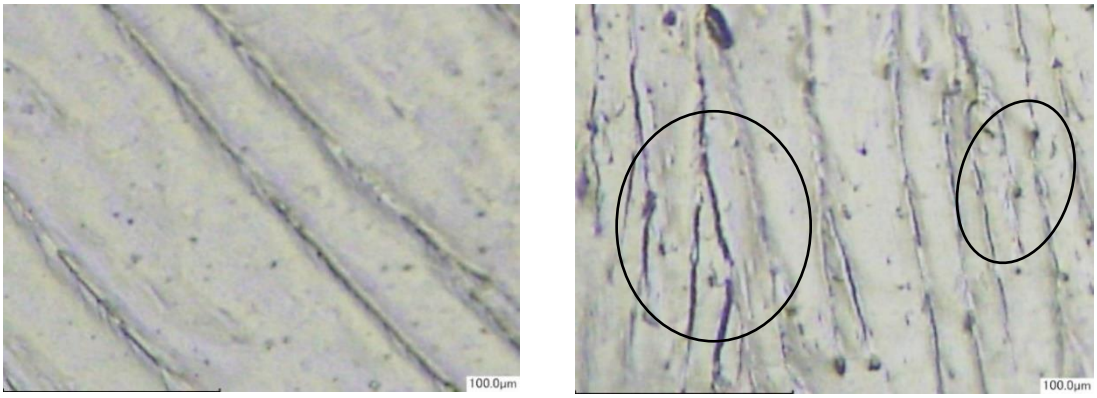

(a) unmodified-resin (b) 0.6 wt% sGF modified resin

Fig. 3-25. The laser microscope images of unmodified and modified resin specimens after compact tension test show the deflection of micro cracks [30].

Failure under static loading condition occured at very high rate compared to that of cyclic loading. Therefore, the delaying effect of crack propagation of sGF could be hidden or skipped under static condition since sGF particles did not have enough time for

absorbing partly failure energy. In other words, this suggests that sGF play important role in improving strength of composite under the cyclic loading applications.

3.4. Conclusions

Mechanical properties of short carbon fiber composite modified by submicron glass fiber were investigated under static and cyclic loading conditions. The SEM pictures showed the sGF was well dispersed in VE matrix by the conventional mixing used the homogenizer at speed of 5000 rpm in 30 minutes. The glass fibers were separated from each other and without waviness. The mechanical performance of composites increased with the increase of fiber length and showed the significant improvement when fiber length rose from 1 mm up to 3 mm. However, the bending and tensile strength of 3 mm fiber composite and 25 mm fiber composite were nearly the same in the view of the same volume fraction. These can be explained base on calculating from the equation 1-1 (Chapter 1) and the IFSS value from Table 3.1: the critical length of carbon fiber is around 1.3 mm to 1.5 mm. On the other hand, below the mentioned fiber length, the mechanical strength of composite is low.

Regarding to sGF modification, the effect of glass fiber addition can be observed in the case of pretty short fiber (1 mm). The aspect ratio of carbon fiber was 143, 429 and 3572 for 1 mm, 3 mm and 25 mm fiber length, respectively. Collating these values with those of glass fiber (Fig 2.5 – Chapter 2) suggests that the aspect ratio of glass fiber is approximate with that of 1 mm carbon fiber and much lower compared with that of 3 mm and 25 mm fiber length. Consequently, adding glass fiber into VE is only effective in the case of composite reinforced by 1mm carbon fiber length.

For all cases of fiber length, the fatigue life of composite remarkably improved with the addition of sGF. The improvement of number cycle to failure was proportional to the content of glass fiber in matrix regardless the fiber length. At the low stress levels (45 and 50%), all specimens modified by 0.6 wt% sGF survived over one million cycles. Besides, as can be seen from the Fig. 3-20, increasing loading test, the fatigue life of un-modified composite rapidly attenuated while that of modified composite showed the gradual decline. At high stress level of 70%, fatigue resistance ability of un-modified nearly disappeared. The strain distribution test with model specimens suggests that sGF delays the propagation of micro cracks resulting in the more energy dissipation and finally, the improvement of the fatigue life of modified composites.

References

[1] Koniuszewska, A.G., Kaczmar, J.W. 2016. Application of polymer based composite materials in transportation. *Progress in Rubber, Plastics and Recycling Technology*; 32, pp. 1-24.

[2] Cantor, K.M., Watts, P. Plastics Processing. 2016. In: Kutz M (ed) *Applied Plastics Engineering Handbook*. 2nd ed. New York: William Andrew, pp.195-203.

[3] Park, S.J., Seo, M.K. 2011. Composite characterization. *Interface Science and Technology*; 18, pp. 631-738.

[4] Ibrahim, I.D., et al. 2015. The use of polypropylene in bamboo fibre composite and their mechanical properties – A review. *Journal of Reinforced Plastics and Composite*; 34, pp.1347-1356.

[5] Kardos, J. 2009. Critical issues in achieving desirable mechanical properties for short fiber composites. *Pure and Applied Chemistry*; 57, pp. 1651-1657.

[6] Zhang, H., Zhang, Z., Klaus, F. 2007. Effect of fiber length on the wear resistance of short carbon fiber reinforced epoxy composites. *Composites Science and Technology*; 67, pp. 222-230.

[7] Fei, L., et al. 2015. Enhanced mechanical properties of short carbon fiber reinforced polyethersulfone composites by graphene oxide coating. *Polymer*; 59, pp. 155-165.

[8] Sarasini, F., Santulli., C. 2013. Vinyl ester resins as a matrix material in advanced fibre-reinforced polymer (FRP) composites. In: Bai J (ed) *Advanced FRP composites for structural applications.* Cambridge: Woodhead Publishing Limited, pp.69-86.

[9] Lee, H., et al. 2017. Fabrication of carbon fiber SMC composites with vinyl ester resin and effect of carbon fiber content on mechanical properties. *Carbon Letters*; 22, pp. 101-104.

[10] Alateyah, A.I., Dhakal, H.N., Zhang, Z.Y. 2013. Mechanical and thermal properties characterisation of vinyl ester matrix nanocomposites based on layered silicate. *World Academy of Science, Engineering and Technology International Journal of Mechanical and Mechatronics Engineering*; 7, pp. 1770-1777.

[11] Chandramohan, A., et al. 2013. Synthesis and characterization of bismaleimide modified vinyl ester monomer-unsaturated polyester intercross linked hybrid matrices. *Polymers and Polymer Composites*; 21, pp. 233-242.

[12] Jeon, Y.P., et al. 2013. Carbon Fibers. In: Somiya S (ed) *Handbook of Advanced Ceramics.* 2nd ed. Cambridge*:* Academic Press, pp.143-154.

[13] Yunus, R.B., et al. 2011. Mechanical properties of carbon fiber-reinforced polypropylene composites. *Key Engineering Materials*; 471-472, pp. 652-657.

[14] Jin, L., et al. 2016. Improvement of interfacial strength and thermal stability of carbon fiber composites by directly grafting unique particles: functionalized mesoporous silicas. *RSC Adv.*, 6, pp. 80485-80492.

[15] Ryohei, F., Kazuya. O., Toru., F. 2016. Improvement of fatigue life and prevention of internal crack initiation of chopped carbon fiber reinforced plastics modified with micro glass fibers. In: *SPIE Smart Structures and Material Systems + Nondestructive Evaluation and Health Monitoring*, Nevada, United States, 20 March-24 March 2016, paper no. 98000U, pp. Nevada: SPIE.

[16] Vautard, F., Xu, L., Drza, L.T. 2009. Carbon Fiber—Vinyl Ester Interfacial Adhesion Improvement by the Use of an Epoxy Coating. In: Daniel IM, Gdoutos EE, Rajapakse YDS (eds) *Major accomplishments in composite materials and sandwich structures*. Heidelberg: Springer Publisher, pp.27-50.

[17] Domun, N., et al. 2015. Improving the fracture toughness and the strength of epoxy using nanomaterials – a review of the current status. *Nanoscale*, 7, pp. 10294-10329.

[18] Dorigato, A., Morandi, S., Pegoretti, A. 2012. Effect of nanoclay addition on the fiber/matrix adhesion in epoxy/glass composites. *Journal of Composite Materials*; 46, pp. 1439–1451.

[19] Quaresimin, M., Varley, R. 2008. Understanding the effect of nano-modifier addition upon the properties of fibre reinforced laminates. *Composites Science and Technology*; 68, pp. 718-726.

[20] Norifumi, T., Kazuya, O., Toru F. 2008. Improvement of Fatigue Strength and Impact Properties of Plain-Woven CFRP Modified with Micro Fibrillated Cellulose. *Advanced Materials Research*; 47-50, pp. 133-136.

[21] Yuan, X., Suong, H.V. 2008. Mechanical properties of carbon fiber reinforced epoxy/clay nanocomposites. *Composites Science and Technology*; 68, pp. 854-861.

[22] Fawaz, J., Mittal, V. 2014. Polymer Nanotube Nanocomposites: A Review of Synthesis Methods, Properties and Applications. In: Mittal V (ed) *Polymer Nanotubes*

*Nanocomposites: Synthesis, Properties and Application*s. Massachusetts: Scrivener Publishing LLC, pp.1-44.

[23] Yalan, L. 2007. *The development of sub-micro filler enhanced polymer composite*. PhD Thesis, Nottingham Trent University, UK.

[24] National Research Council. 1996. *New Materials for Next-Generation Commercial Transports*. Washington, DC: The National Academies Press. https://doi.org/10.17226/5070.

[25] Chang, W.C., et al. 1994. Effects of processing methods and parameters on the mechanical properties and microstructure of carbon/carbon composites. *Journal of materials science* 29(22), pp. 5859 - 5867. https://doi.org/10.1007/BF00366868

[26] Song, X. 2003. *Vacuum Assisted Resin Transfer Molding (VARTM): Model Development and Verification.* PhD Thesis, Virginia Polytechnic Institute and State University, US.

[27] https://pubchem.ncbi.nlm.nih.gov/compound/Styrene. U.S. National Library of Medicine National Center for Biotechnology Information

[28] Thomason, J.L., Vlug, M.A. 1996. Influence of fibre length and concentration on the properties of glass fibre-reinforced polypropylene: 1. Tensile and flexural modulus. *Composites Part A: Applied Science and Manufacturing*, 27, pp. 477-484.

[29] Mouritz, A.P. 2012. Fibre–polymer composites for aerospace structures and engines. In Mouritz AP (ed) *Introduction to Aerospace Materials.* 1st ed. Cambridge: Woodhead Publishing Limited, pp. 338-393.

Chapter 4

Impact tolerance of short carbon fiber reinforced vinyl ester composite modified by submicron glass fiber

4.1. Introduction

Composite material is more and more widely applied in many areas of social life such as aerospace, automotive, defence and wind power industries due to their high strength/stiffness to weight ratio and advantageous mechanical properties as compared to metals. However, susceptibility to impact damage which can occur in either handling or service serious threat to the composite structures since low-velocity impact (LVI) loading can creates invisible internal damage, and significantly reduce their mechanical performance. Failure mechanisms happen under impact event may involve indentation, matrix cracking, fibre matrix debonding, delamination, inter-laminar failure and eventually fibre breakage for higher impact energies. In many situations, the level of impact at which visible damage is formed is much higher than the level at which substantial loss of residual properties occurs. Thus, the study of impact response of composites has become an area of great concern in the composite communities [1-4]. To improve impact tolerance of composite, methods have proposed to reinforcement and matrix such as changing fiber architecture, improving adhesion fiber/matrix and toughening matrix [5-7]. Improving matrix toughness not only leads to increase of impact damage resistance but also post-impact compression damage tolerance performance. Various techniques have been conducted for improving fracture toughness of matrix such as modifying with rubber, rigid inorganic fillers (carbon nanotube, nanoclay, nanosilica) [5, 8-11]. Failure modes can be occurred in a laminate composite and difference in composites with or without toughener can be seen in the Figure 4-1.

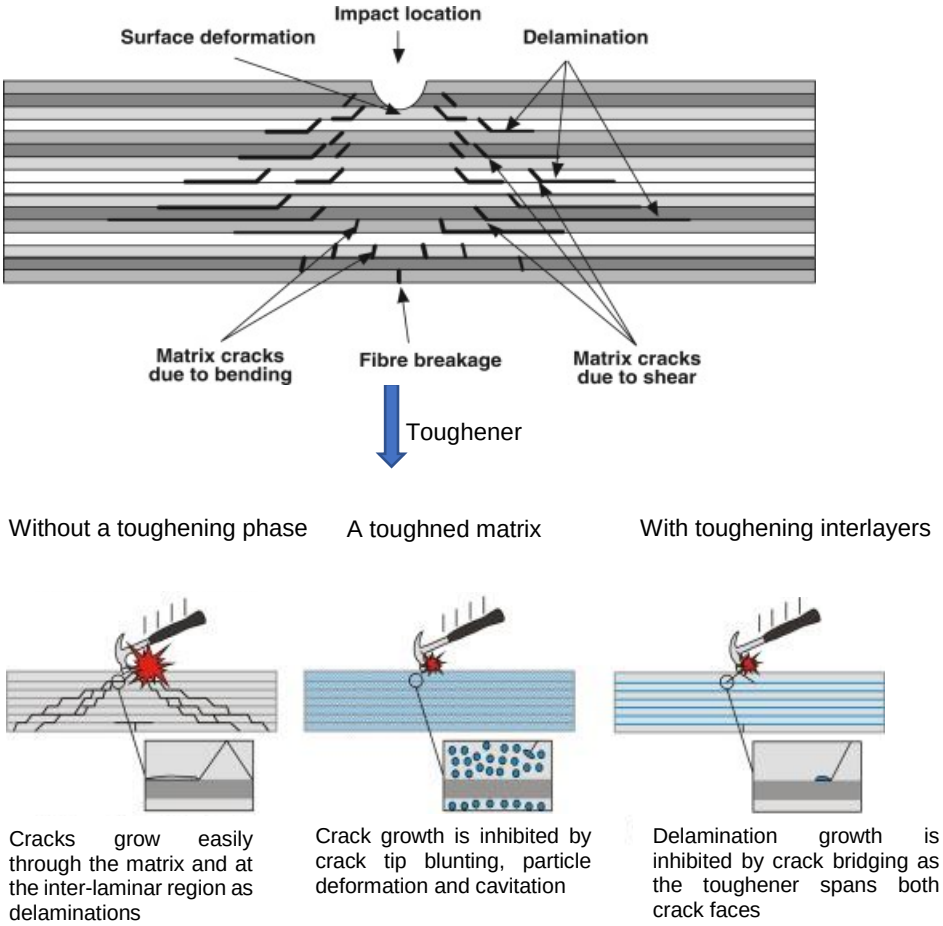

Fig. 4-1. Failures under impact event and difference in modified composites and un-modified composite thanks to presence of toughener [12,13].

To define the damage resistance of composites after an impact event, a compression after impact (CAI) test is frequently used since even not visible induced damage still causes significantly reduce a residual strength, especially residual compressive strength [14-19]. The CAI strength is dependent on the position geometry and the extent of damage induced during impact. During the post-impact test, the damage present in the laminate will lead to different failure modes. However, damage characterisation in CFRP is by no means easy, in particular because the mode of failure depends on the material and geometry, so that different compressive failure modes, such as microbuckling, kinking, delamination, debonding and fibre failure may occur in the composite laminates [4, 20]. As aforementioned in the previous chapter, adding submicron glass fiber to VE significantly increase the fracture toughness of resin. Therefore, sGF modification was expected to improve impact resistance of composite and so, increase compressive residual

strength of composite. The object of this chapter is to validate effect of this modification on the CAI strength after drop weight impact test.

4.2. Material and Methods

4.2.1. Materials

Materials, content of sGF and procession of manufacturing composite were the same with those in the chapter 3. The sample is in rectangular shape with the dimension of 100x60x4 mm^3. Carbon fiber in this research was used at 25 mm length and 50% in weight in composite. The image of a representative specimen is shown in the Fig. 4-2.

The Fig. 4-2. The representative image of sample for impact test.

4.2.2. Drop weight impact test

The constituent of the impact device is shown in the Fig. 4-3. The impactor has the weight of 1.099 kg while the impact mass is 9.395 kg. The striker tip of the impactor is in the hemispherical shape with the diameter of 10mm. The sample was clamped by a system with an inner hole diameter of 40 mm, and impacted at the centre. The impact event is triggered by the laser system. The rebound catcher system was enabled to stop the impactor during its second descent. For the sake of comparison, two level of impact energy of 10 J and 15 J was chosen. The testing condition corresponds with each level of energy is shown in the Table 4-1.

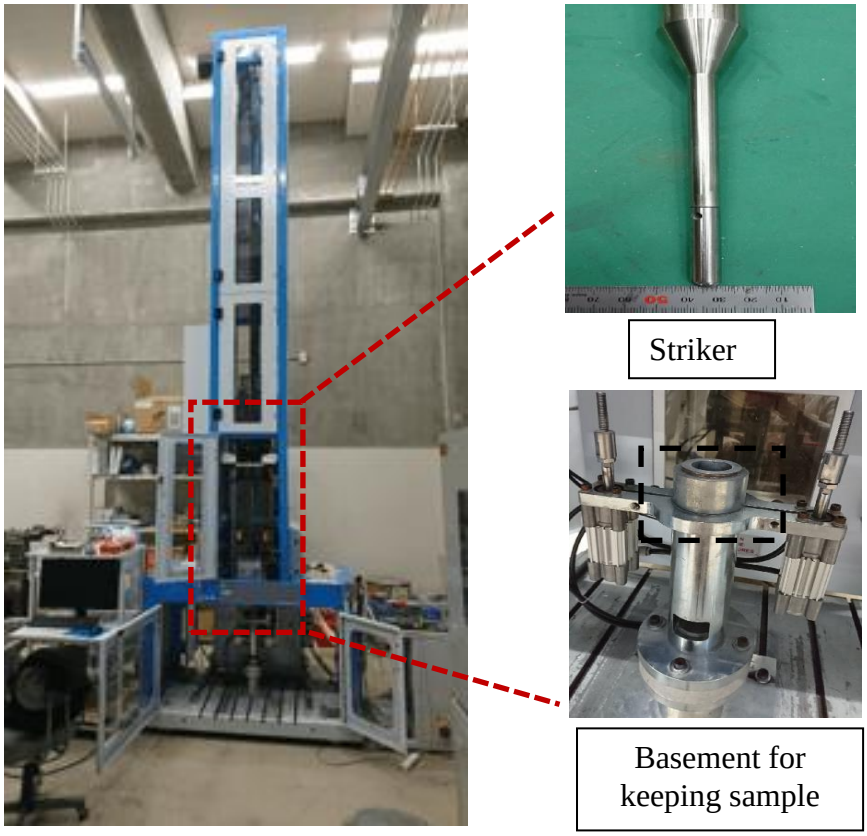

(a) Device for the drop weight impact test.

(b) The element of clamping sample of the impact device.

The Fig. 4-3. The drop weight impact device.

Table 4-1. The impact testing condition.

Energy J	Height (m)	Velocity (m/s)
10	0.109	1.46
15	0.163	1.79

4.2.3. The compressive test

The compression test was conducted for the sample with/without impact test to determine the compression after impact (CAI) strength as well as original compressive strength of composites. The image of the rig is shown in the Fig. 4-4.

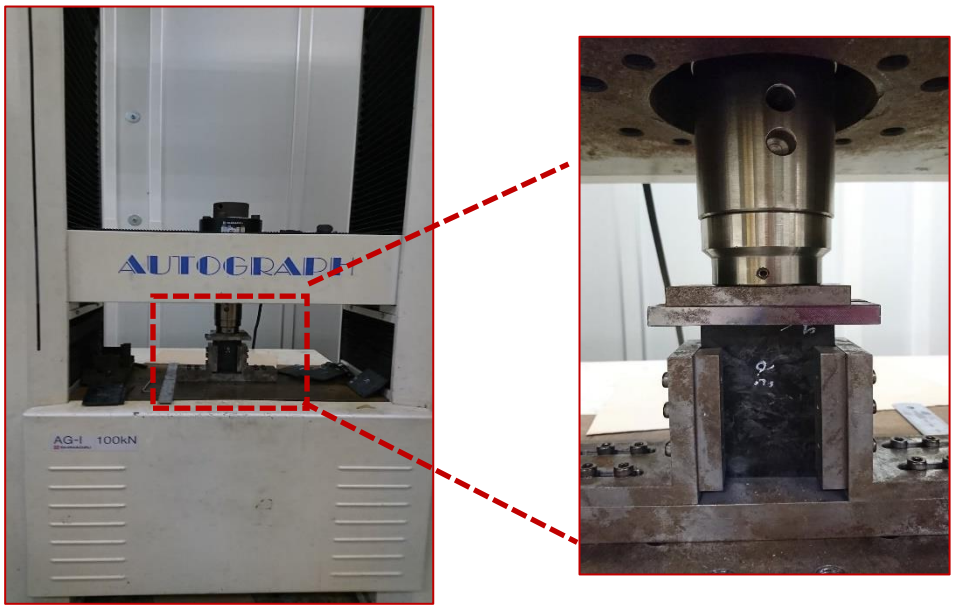

Fig. 4-4. The images of compressive testing.

The testing speed was 1 mm/minute and carried out on the Instron 100 kN (Shimazdu). At least 7 samples were tested for each condition.

4.2.4. Inspection sample after testing

To evaluate the state of internal damage after impact test, the inspection was carried out on the ultrasonic C-scan equipment Omni Scan SX (Olympus) as well as the CT scan equipment (see Fig. 4-5). The specimen was sunk in the water environment.

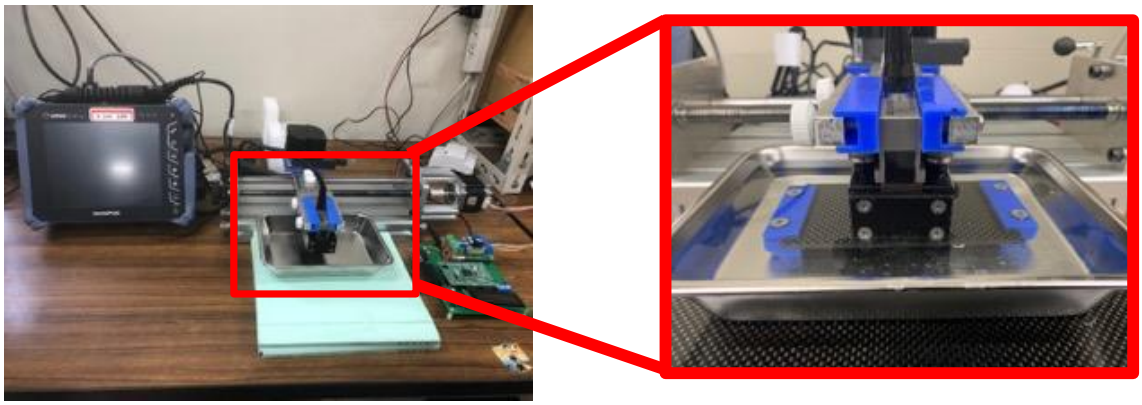

The Omni Scan SX for ultrasonic inspection

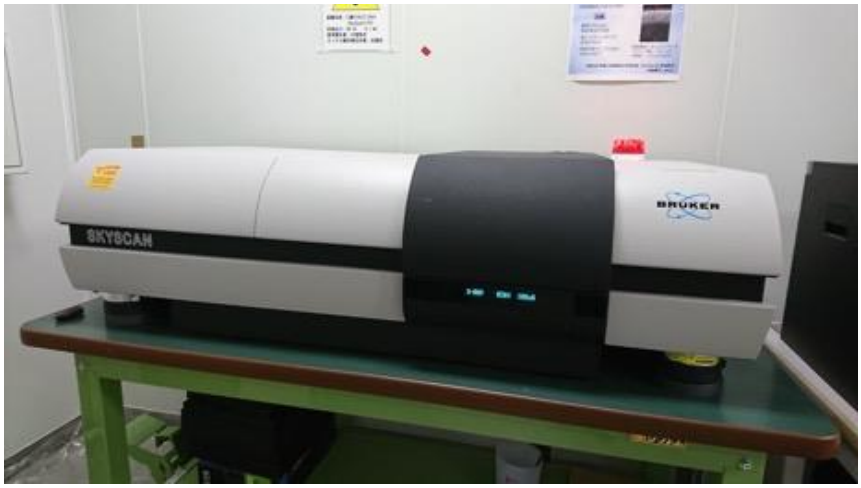

The X ray CT scan (Skyscan MicroCT - Brucker)

Fig. 4-5. The actual images of the ultrasonic equipment and the Xray CT scan.

4.3. Results and Discussions

4.3.1. The compressive strength of composite

The Table 4-2 shows the compressive strength of composite. It can be seen that the compressive performance of composite is unchanged with the addition of submicron glass fiber. As mentioned in previous chapter, the scatter of data is big for all composites. It well-known that the compressive strength is always lower than tensile strength in composite. In some cases, the difference is pretty large. For example, the compressive strengths of unidirectional carbon fibre epoxy laminates are often less than 60% of their tensile strengths while [21]. However, in this research, the ratio of compression and tensile strength is high, varies around 0.85 (see Fig. 4-6) with all content of the modifier.

Table 4-2. Compressive strength of composites.

sGF content	Compressive strength, MPa	Void content, % (volume)
0.0 wt%	185.10 (38.86)	2.1
0.3 wt%	191.77 (22.66)	2.68
0.6 wt%	183.912 (24.31)	3.25

() - parentheses contain standard deviation values of tested data.

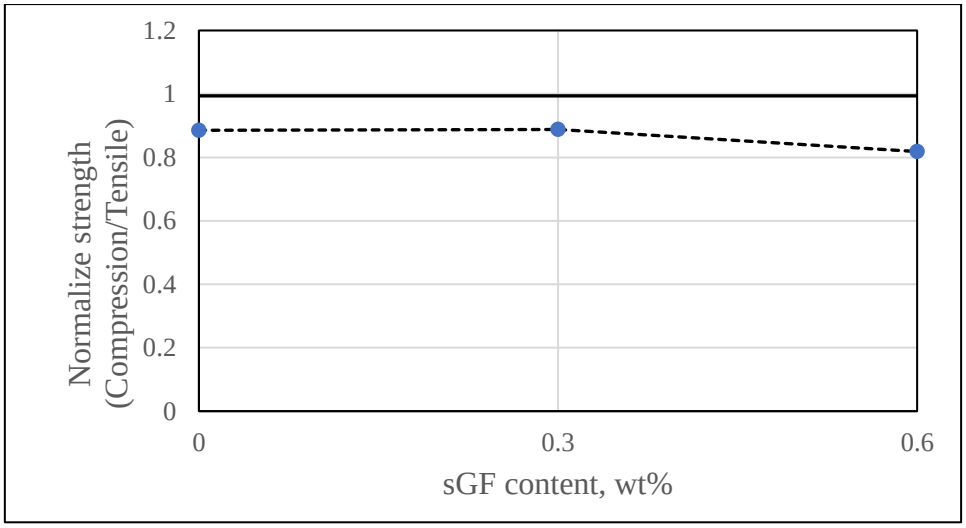

Fig. 4-6. The ratio of compressive to tensile strength in short carbon fiber composite.

This can be explained by random orientation of fiber, leads to the mechanical characteristics are quasi-isotropic in above composites, hence the difference between tensile and compressive performance is narrowed. Not as expected, failure did not only occur at centre-region of specimen but also near wide-edge and at edges regardless sGF content (see Fig. 4-7). Therefore, weakest region in some specimens is not located at centre region where compressive stress reaches maximum during the test, suggests about some defects inside them. Small images in upper right corners show failure modes, includes buckling and delamination with delaminated cracks are clearly observed. Obviously, failure is nearer centre region of specimen are more serious with more buckling phenomenon, consequently a higher compressive strength can be achieved.

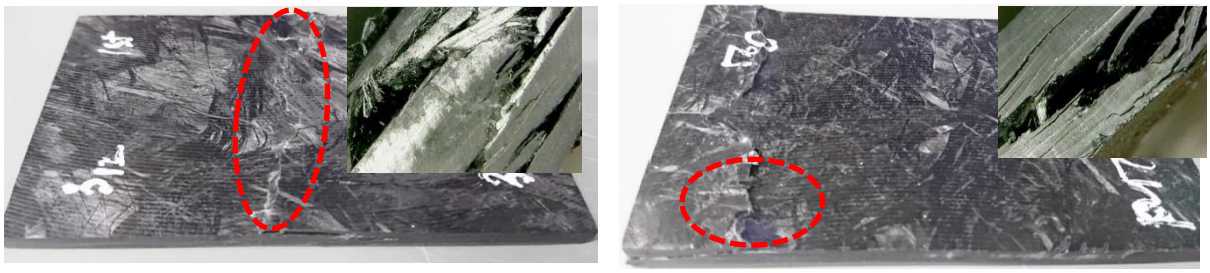

(a) Failure at centred-region (b) Failure near wide-edge

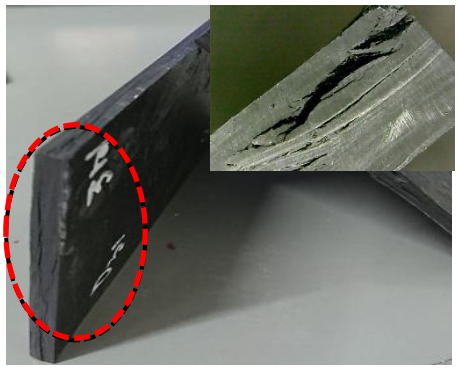

(c) Failure at edges

Fig. 4-7. Failure under compressive load of specimens.

4.3.2. Impact tolerance of composite

The impact test was conducted at 10 J and 15 J. Both these energy levels have not yet caused perforation of specimens. The inspection shows there is the increasing of the delamination under impact loading in modified composite, this growth can be more clearly observed after a higher energy imparted. (see Fig. 4-8 and Fig.4-9). This suggest about the increase of absorbed energy in un-modified composite.

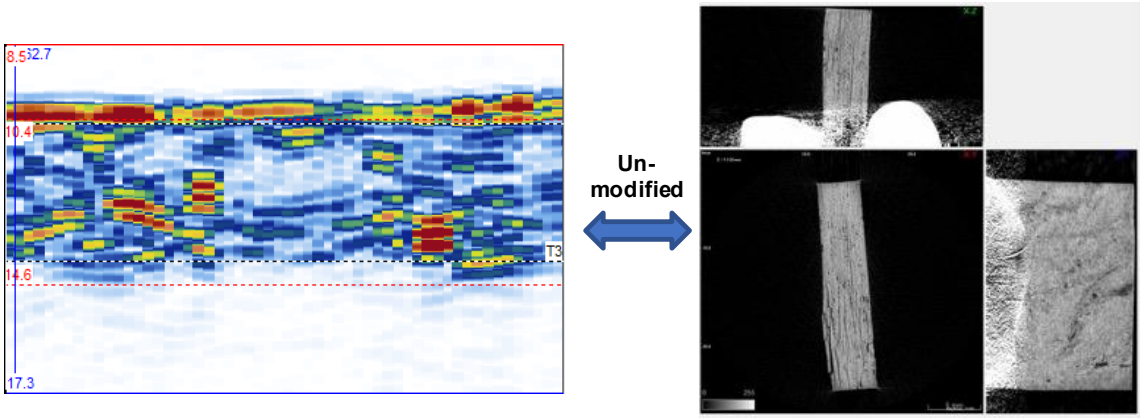

(a) un-modified composite after 10 J energy impact.

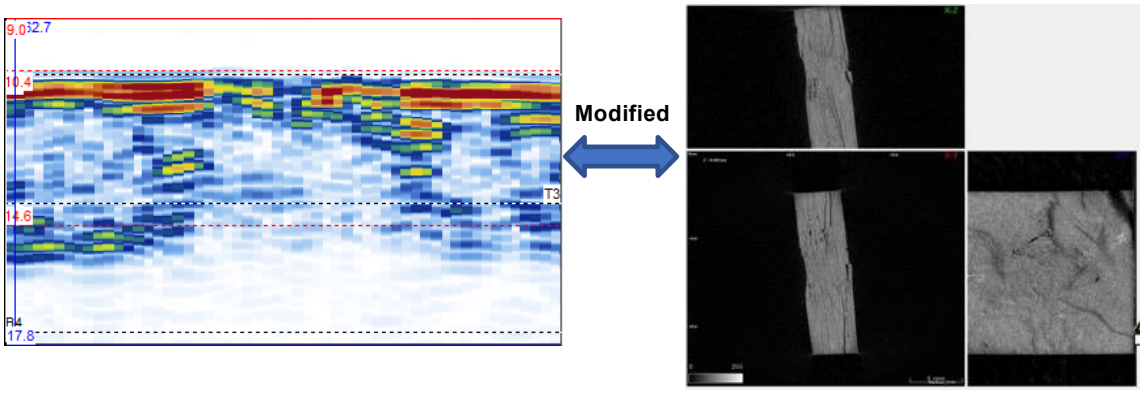

(b) modified composite after 10 J energy impact.

Figure. 4-8. The ultrasonic C-scan images and CT-scan images of composite after impact event of 10 J energy.

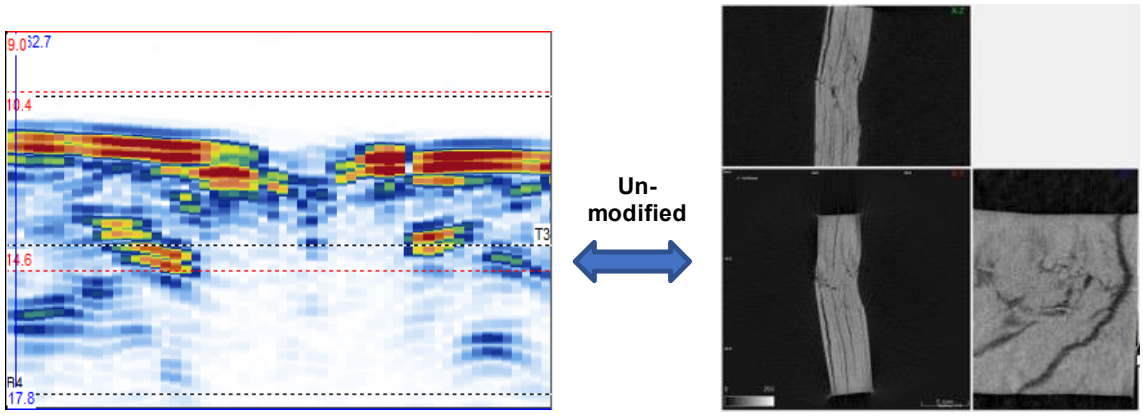

(a) un-modified composite after 15 J energy impact.

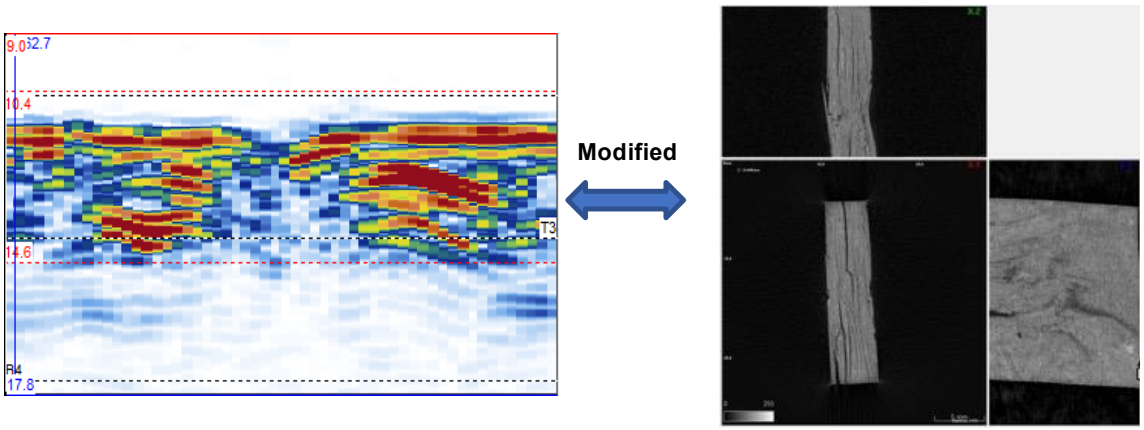

(b) modified composite after 15 J energy impact.

Figure. 4-9. The ultrasonic C-scan images and CT-scan images of composite after impact event of 15 J energy.

Table 4-3. Impact characteristics of composites under 15 J impact energy.

sGF content	Fmax, kN	Impact Energy, J	Puncture Energy, J	Absorbed Energy, J	Puncture deflection, mm
0.0 wt%	5.99 (0.58)	14.9 (0.04)	14.52 (0.38)	12.62 (0.45)	3.66 (0.02)
0.3 wt%	6.29 (0.1)	14.94 (0.00)	13.93 (0.17)	11.92 (0.06)	3.4 (0.12)
0.6 wt%	6.21 (0.3)	14.84 (0.11)	13.76 (0.65)	12.02 (0.45)	3.52 (0.21_

() - parentheses contain standard deviation values of tested data.

Table 4-4. Impact characteristics of composites under 10 J impact energy.

sGF content	Fmax, kN	Impact Energy, J	Puncture Energy, J	Absorbed Energy, J	Puncture deflection, mm
0.0 wt%	6.06 (0.37)	10.03 (0.08)	9.49 (0.48)	7.47 (0.56)	2.66 (0.1)
0.3 wt%	6.14 (0.3) (	10.03 (0.07)	9.26 (0.36)	7.32 (0.37)	2.6 (0.13)
0.6 wt%	5.79 (0.29)	9.99 (0.07)	9.33 (0.3)	7.23 (0.3)	2.67 (0.17)

() - parentheses contain standard deviation values of tested data.

As can be seen from Table 4-3 and 4-4 along with the Fig. 4-8, Fig. 4-9, the behaviour of composites under impact loading is similar for both of energy level. For both cases, puncture energy and absorbed energy marginally decreased with the increase of submicron glass fiber content addition while the value of Fmax minimally rose in modified samples. Besides, as can be seen from Figures of 4-10 and 4-11, the strong fluctuation of force when the crack propagated shows that the matrix failure was serious. The plots of force-displacement also hint that at the fluctuation amplitude of force in unmodified samples were higher than that in modified composites, suggests about increasing toughness in modified matrices. Fig. 4-12 indicates an increase of absorbed energy in composites: higher energy imparted, more absorption, and a decrease of energy dissipated ability with the addition of glass fiber into composite. A puncture deflection or maximum penetration was also a bit lower with modified composite in the case of 15 J (Fig. 4-13). However, these changes are pretty minimal.

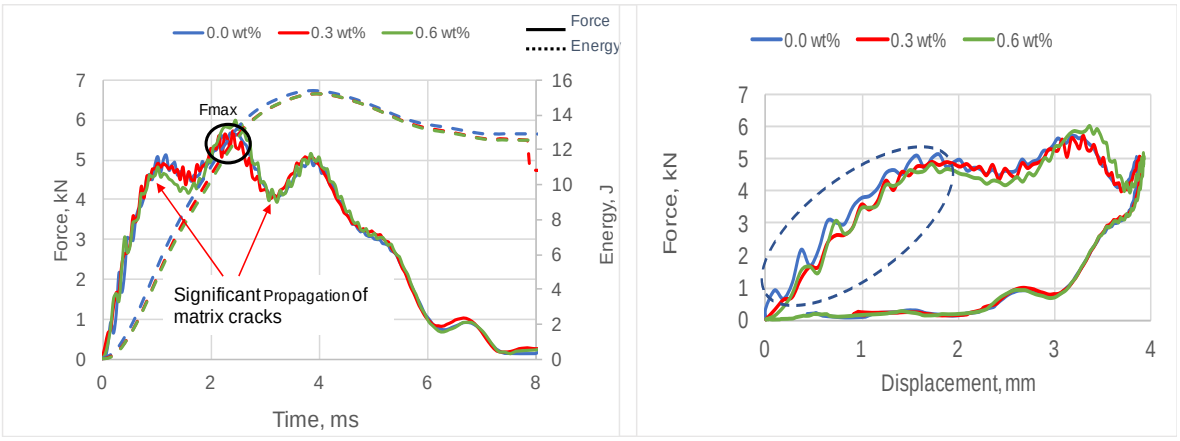

(a)

(b)

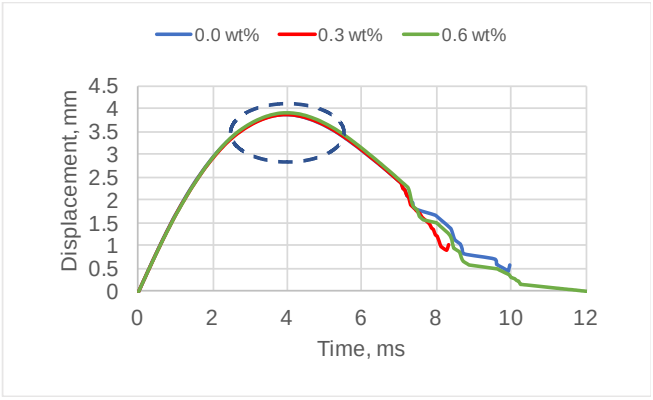

(c)

Fig. 4-10. The plots of force - time, energy - time curve (a), force - displacement (b) and displacement – time (c) of composites under 15 J impact.

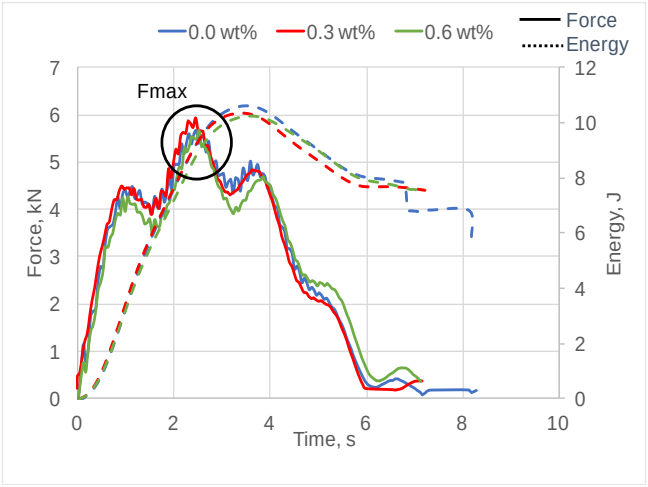

(a)

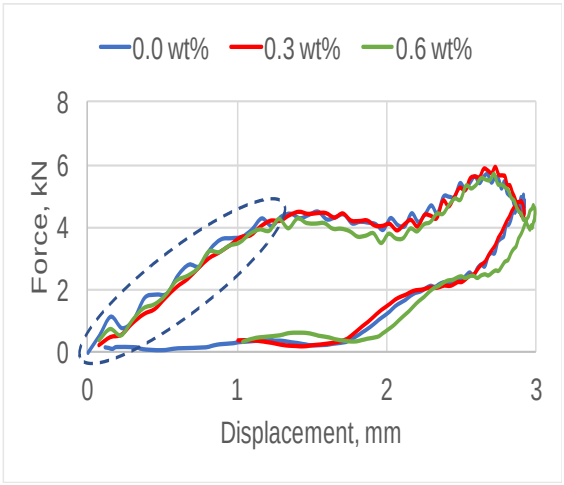

(b)

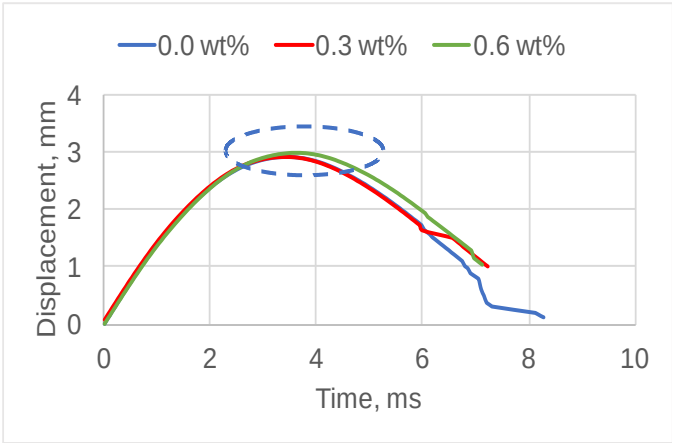

(c)

Fig. 4-11. The plots of force - time, energy - time curve (a), force - displacement (b) and displacement – time (c) of composites under 10 J impact.

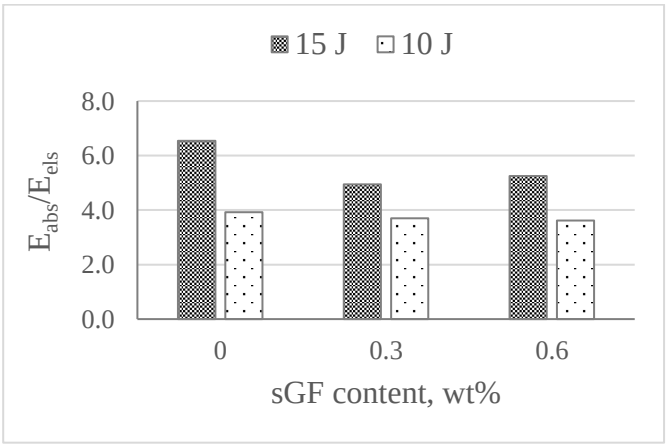

Fig. 4-12. The ratio of absorbed energy and elastic energy at impact energy of 10 J and 15 J.

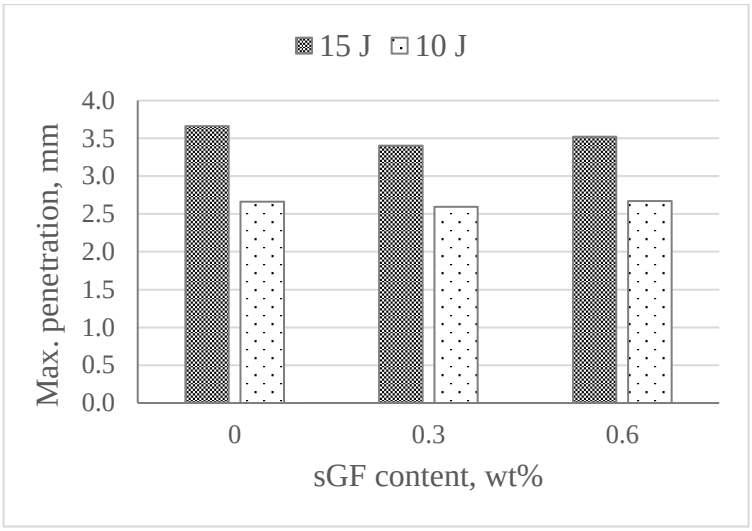

Fig. 4-13. The maximum penetration during the impact event.

Fig. 4-14 and 4-15 show the compressive strength of composite before and after impact test. Although fore mentioned about the slight decrease of absorbed energies in modified composites, but the compressive strength of composites after impact test is unchanged with the addition of submicron glass fiber. This might be the change in absorbed energy is marginal with the addition of sGF. These results are good agreement with the Izod impact resistance of resin when this value declined by sGF adding.

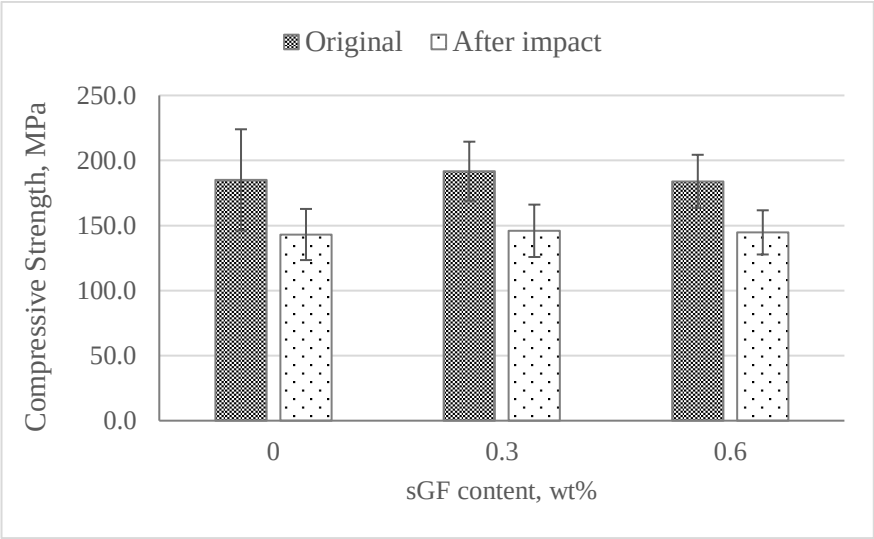

Fig. 4-14. The compression strength of composites before and after impact test at 15 J.

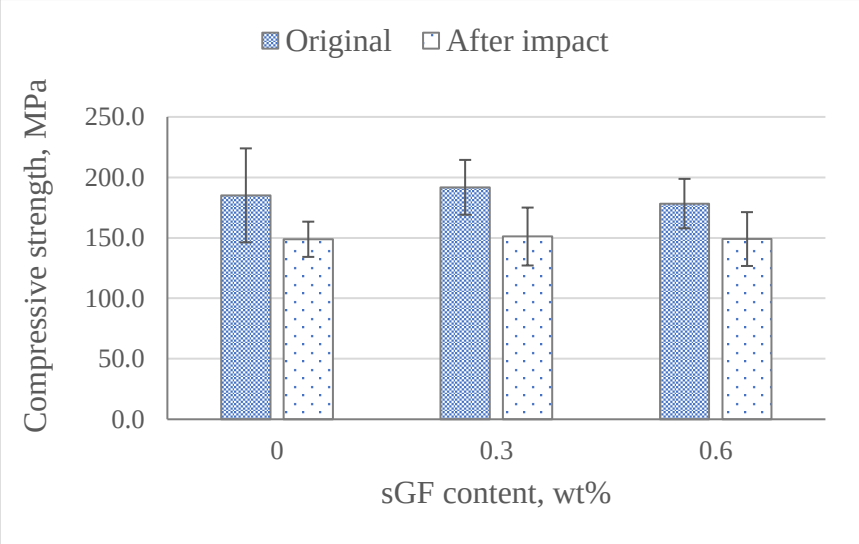

Fig. 4-15. The compression strength of composite before and after impact test at 10 J.

Compared to the compressive test for original specimens (before impacting), most of specimens broken at centre region during the CAI test This indicates that weakest region moved from defect positions to impacted positions. We tried the impact test at two other energies were 6 J and 8 J. Observing by naked-eyes showed that under compression load, most of 6 J specimens fractured at position far from impacted position while at 8 J, around half of them fractured across this area (see Fig. 4-16). Comparing about the damage statement, it is pointed out that 10 J starts leading to serious failures in composites (Fig. 4-17 – images taken at edge while 6J imparted specimen did not show failure at this position).

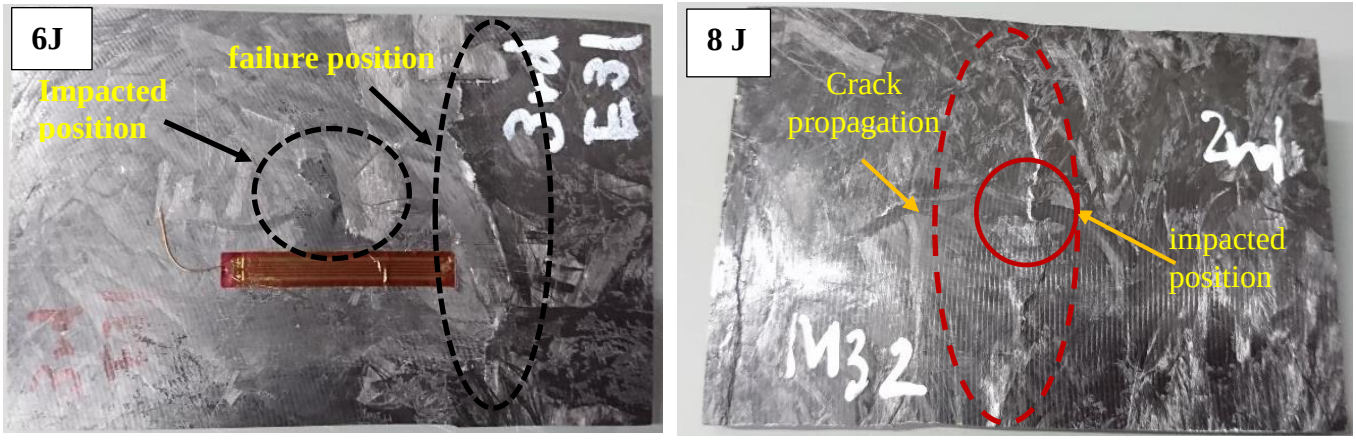

Fig. 4-16. The failure of specimens after CAI test (post-impact at 6J and 8J).

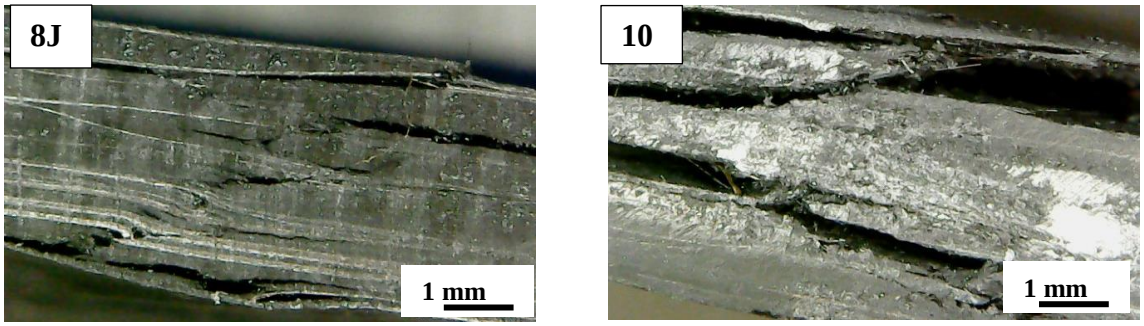

(a) (b)

Fig. 4-17. Digital microscope images of specimens after CAI test (a) 8 J post impacted and (b) 10 J post impacted.

In spite of starting of serious damage under 10 J impact energy, the residual compression strength of composites imparted by impact energy of 15 J also did not considerably decline compared to that of the former energy (see Table 4-5). The value of samples impacted by 15 J energy even reach approximately 96% that of samples were sustained the energy of 10 J.

Table 4-5. The residual compression strength of composites at impact level of 10 J and 15 J.

sGF content	10 J	15 J
0.0 wt%	148.82 (19.66)	143.09 (14.57)
0.3 wt%	151.08 (20.13)	145.93 (23.94)
0.6 wt%	149.00 (16.97)	144.72 (22.25)

() - parentheses contain standard deviation values of tested data.

4.4. Conclusions

The drop weight impact test was carried out at two levels of impact energy 10 J and 15 J. Although adding sGF into matrix significantly improve fracture toughness of resin, but not as expected, the original compression strength as well as the residual compressive strength after impacted did not change with sGF modification. Inspection was conducted after impact event showed the increasing of delamination area in modified composite, suggest the decrease of the absorbed energy in these samples. However, calculation indicated that the change of absorption energy is pretty minimal, therefore, the CAI strength of composite was not affected by the addition of glass fiber modifier. Besides, the ratio between the original compression strength to the tensile strength is pretty high, around the value of 0.85. The quasi-isotropic characteristic of random orientation fiber

composite is considered as main reason contributes to retain strength of composite under compressive load. Although the level of 10 J starts leading to serious damage in composite with the evidences of failure in post-impact specimens happens at centre region instead of at other defect positions but there is not significant change in the CAI of specimens sustained the energy level of 15 J compared to that of 10 J.

References

[1] Jang, B. Z. 1988. Impact Resistance and Energy Absorption Mechanisms in Hybrid Composites. *Composites Science and Technology* 34, pp. 305-335

[2] Zhou, G. 1996. Effect of impact damage on residual compressive strength of glass-fibre reinforced polyester (GFRP) laminates. *Composite Structure* 35, pp. 171-181.

[3] Sha, S.Z.H., et al. 2019. Impact resistance and damage tolerance of fiber reinforced composites: A Review. *Composite Structures*, 217, pp. 100-121.

[4] Freitas, M., Reis, L. 1998. Failure mechanisms on composite specimens subjected compression after impact. *Composite Structures*, 42, pp. 365-373

[5] Kausar, A. 2017. Role of Thermosetting Polymer in Structural Composite. *American Journal of Polymer Science & Engineering*, 5, pp. 1-12.

[6] Walker, L., Sohn, M.S., Hu, X.Z. 2002. *Composites Part A: Applied Science and Manufacturing*, 33(6), pp. 893-902.

[7] Jogi, S.A., et al. 2017. Evaluation of Impact Strength of Epoxy Based Hybrid Composites Reinforced with E-Glass/Kevlar 49. *Mehran University Research Journal of Engineering & Technology*, 36(4), pp. 1009-1016.

[8] Krushnamurty, K., et al. 2015. Effect of nanoclay on the toughness of epoxy and mechanical, impact properties of E-glass-epoxy composites. *Advanced Materials Letters*, 6(8), pp. 670-755.

[9] Liu, S., Fan, X., He, C. 2016. Improving the Fracture Toughness of Epoxy with Nanosilica-Rubber Core-Shell Nanoparticles. *Composites Science and Technology*, 125(23), pp. 132-140.

[10] Dadfar, M.R., Ghadami, F. 2013. Effect of rubber modification on fracture toughness properties of glass reinforced hot cured epoxy composites. *Materials and Design*, 47, pp. 16–20.

[11] Cha, J., et al. 2017. Improvement of modulus, strength and fracture toughness of CNT/Epoxy nanocomposites through the functionalization of carbon nanotubes. *Composites Part B: Engineering*, 129(15), pp. 169-179.

[12] Emile, S. G. 2009. Defects and damage and their role in the failure of polymer composites. In: Emile, S. G (ed). *Failure analysis and fractography of polymer composites* Volume 7, pp. 356-440. Publisher: Woodhead Publishing.

[13] Nash, N.H., Young, T.M., McGrail, P.T., Stanley, W.F. 2015. Inclusion of a thermoplastic phase to improve impact and post-impact performances of carbon fibre reinforced thermosetting composites — A review. *Materials & Design*, 85, pp. 582-597.
[14] Liu, H., Falzon, B.G., Tan, W. 2017. Predicting the Compression-After-Impact (CAI) strength of damage-tolerant hybrid unidirectional/woven carbon-fibre reinforced composite laminates. *Composites Part A: Applied Science and Manufacturing*, 105, pp. 189-202
[15] Lopresto, V., Papa, I., Langella, A. 2017. Residual strength evaluation after impact tests in extreme temperature conditions. New equipment for CAI tests. *Composites Part B: Engineering*, 127, pp. 44-52
[16] Duus, P. 2016. Residual Strength of Composite Hulls after Impact. Master Thesis. Norwegian University of Science and Technology.
[17] Koo, J.M., Choi, J.H., Seok, C.S. 2014. Prediction of Residual Strength after Impact of CFRP Composite Structures. *International Journal of Precision Engineering and Manufacturing*, 15(7), pp. 1323-1329.
[18] Petit, S., Bouvet, C., Bergerot, A., Barrau, J-J. 2007. *Composites Science and Technology*, 67(15–16), pp. 3286-3299 DOI: 10.1007/s12541-014-0472-0.
[19] Abir, M.R., Tay, T.E., Ridha, M., Lee, H. 2017. On the relationship between failure mechanism and Compression After Impact(CAI) strength in composites. *Composite Structures*, 182C, pp. 242-250. DOI: 10.1016/j.compstruct.2017.09.038.
[20] Arumugam, V., Sidharth, A., Santulli, C. 2014. Failure modes characterization of impacted carbon fibre reinforced plastics laminates under compression loading using acoustic emission. Journal of Composite Materials, 48(28), pp. 3457–3468.
[21] Budiansky, B., Fleck, N.A. 1993. I. Mrch. P/tw. S&l.7 Vol. 41, No. I, pp. 183-11

Chapter 5. Final Remarks and Proposal

This chapter briefly recalls remarkable results achieved from this research.

The submicron glass fiber was well dispersed into vinyl ester resin by the conventional mixing methods with the speed of 5000 rpm in 30 minutes. The length of glass fiber after mixing was confirmed by means of SEM observation showed the aspect ratio of this modifier changes in a wide range. Adding glass fiber in to VE did not improve the Izod impact resistance as well as bending strength of resin but significant increase the fracture toughness. The K_{Ic} value of fracture toughness proportionally increase with the content of sGF in resin. Dynamic mechanical analysis indicated the slight increase of elastic behavior and the decrease of damping property in sMC. Crack growth rate of notch specimens of modified resin under tensile cyclic load also considerably degraded. The observation of SEM and lazer microscope shows evidence of improving fatigue life in modified matrix is due to deflecting micro-cracks and delaying the propagation of cracks as well as partly dissipating crack growth energy for de-bonding fibers from matrix.

Composite was prepared for static and tension-tension fatigue test at different carbon fiber length and sGF content. Results showed that mechanical performance of composites increased with the increase of fiber length and showed the significant improvement when fiber length changed from 1 mm up to 3 mm. However, the bending and tensile strength of 3 mm and 25 mm were nearly the same in the view of the same volume fraction. These can be explained base on calculating from the equation 1-1 (Chapter 1) and the IFSS value from Table 3.1: the critical length of carbon fiber is around 1.3 mm to 1.5 mm. On the other hand, below the mentioned fiber length, the mechanical strength of composite is low. Regarding to sGF modification, the effect of glass fiber addition can be observed in the case of pretty short fiber (1 mm). The aspect ratio of carbon fiber was 143, 429 and 3572 for 1 mm, 3 mm and 25 mm fiber length, respectively. Collating these values with those of glass fiber (Fig 2.5 – Chapter 2) suggests that the aspect ratio of glass fiber is approximate with that of 1 mm carbon fiber and much lower compared with that of 3 mm and 25 mm fiber length. Consequently, adding glass fiber into VE is only effective in the case of composite reinforced by 1mm carbon fiber length. Besides, though glass fiber modification declined impact resistance of neat resin but this negative effect was neglected in composite system. The mechanism for this compensation

should be further studied in next research. In contrast to the static strength, for all cases of fiber length, the fatigue life of composite remarkably improved with the addition of sGF. The improvement of number cycle to failure was proportional to the content of glass fiber in matrix regardless the fiber length. At the low stress levels (45 and 50%), all specimens modified by 0.6 wt% sGF survived over one million cycles. Besides, increasing loading test, the fatigue life of un-modified composite rapidly attenuated while that of modified composite showed the gradual decline. At high stress level of 70%, fatigue resistance ability of un-modified nearly disappears. The strain distribution test with model specimens suggests that sGF delays the propagation of micro cracks resulting in the more energy dissipation and finally, the improvement of the fatigue life of modified composites.

The drop weight impact test was carried out at two levels of impact energy 10 J and 15 J. Although adding sGF into matrix remarkbly improved fracture toughness of resin, but not as expected, the original compression strength as well as the residual compressive strength after impacted did not change with sGF modification. The delamination area in modified composite was observed from ultrasonic S-scan inspection increased, suggests about the decline of absorbed energy in this system. However, the calculation from impact test shows absorbed energies are not significantly different. This explains the unchanged of the residual compressive strength of composites by adding glass fiber. The ratio between the original compression strength to the tensile strength was pretty high, around the value of 0.85. The quasi-isotropic characteristic of random orientation fiber composite is considered as main reason contributes to retain strength of composite under compressive load. Besides, the level of 10 J started leading to serious damage in composite with the evidences of failure in post-impact specimens happens at centre region instead of at other defect positions. In spite of that, the residual compression strength of composites imparted by impact energy of 15 J also did not considerably decline compared to that of the former energy, reached around 96% the value CAI of specimens impacted by 10 J energy.

From the above remarks, the author would like to show some proposals for the future works as below:

1. Because the low contents (0.3 wt% and 0.6 wt%) of glass fiber were used in this research, therefore its effect was not significant in modified-resins. Increasing content of submicron glass fiber could achieve more positive results for resin system.

2. In the Chapter 2, three kinds of fiber were used: 1 mm, 3 mm and 25 mm in composites at different weight fractions. The static strengths of 1 mm fiber composite also improved with the addition of glass fiber. This improvement could be the similarity in aspect ratio of glass fiber and carbon fiber. In the opinion of author, increasing aspect ratio of the modifier in 3 mm and 25 mm composite could lead to the increasing of mechanical properties in these composites. The technique for distributing glass fiber into resin without decreasing fiber length should be further discussed.

3. This research also pointed out that the adhesion between glass fiber and resin was poor. Improving this interfacial shear strength by using coupling agents as silica could increase properties for modified resin as well as modified composite.

5. The scatter of data in this research were large. Some methods can be proposed such as using additives, using Weibull distribution function should be used for further investigations.

Acknowledgement

First and foremost, I would like to express my sincere gratitude to my advisor Prof. Kazuya Okubo for the continuous support of my PhD study and related research, for his patience, motivation, and immense knowledge. He is always nice and free to let me explore research on my own but ready to give me right instructions to go on right way. Please kindly let me say sincerely thankful words to Assoc.Prof. Kiyotaka Obunai who teaches me a lot of knowledge about failure mechanisms in composite material, for his patience and assistance for instructing me about using new equipment and testing methods. Without his valuable advices, I could not complete this research on time. I also would like to express grateful to my former Prof. Toru Fujii who gave me the opportunity to learn and study in AMSEL laboratory, has led me to the new but interesting challenge of the research work. I am very grateful to Prof. Nguyen Thanh Liem (Polymer Center, Hanoi City, Vietnam) for his encouragement to try to doctoral degree. Special thanks to Dr Hironori Nishida who helped me to practice and correct my presentation for the Conference ICCM 22. I greatly appreciate his support and discussion for doing the impact test in Hiroshima Prefectural Technology Research Institute. I thank Ms. Fujimoto (Secretary of Prof. Okubo), Ms. Hasegawa (Secretary of Assoc. Prof. Obunai) as well as officers in Department of Mechanical and Systems Engineering, who is always willing to help me when I have any difficulty relates to administrative procedures. I also would like to thank Ms Toda, who is in charge of SEM room, is usually promptly respond to all my queries about analysis equipment. I would like to thank my fellow labmates for their friendly, support and warmness who gave me during the last three years. I also would like to thank Ms. Dung (former master), Mr. Okimura (master student, the member in my research group), Mr. Ueda (master student), Mr. Miyakita (former master student) for their friendship as well as support during my research. I also thank to Ms. Marta Perez (master student) for her correcting of my journal paper; we have a nice friendship and the consideration between each other.

I would like to acknowledge Yoshida Foundation Scholarship for supporting finance for not only me but also my family to help me focus on the research.

Last but not the least, I would like to thank my family: my parents, my older brothers for their always support, love and belief on me, especially my wonderful husband

(Bui Van Vinh) and lovely daughters (Bui Nguyen Ha My and Bui Nguyen My Linh) who is always beside me every moment of the life. Without their love and encouragement, I could not fulfil this study.